

***The Environmental Fluid Dynamics Code  
Theory and Computation  
Volume 2: Sediment and Contaminant  
Transport and Fate***

Tetra Tech, Inc.  
10306 Eaton Place  
Suite 340  
Fairfax, VA 22030

June 2007

## Preface

This document comprises the second volume of the theoretical and computational documentation for the Environmental Fluid Dynamics Code (EFDC). The material in this volume was previously distributed as:

Tetra Tech, 2002: EFDC Technical Memorandum: Theoretical and Computational Aspects of Sediment and Contaminant Transport in the EFDC Model. Fairfax, VA.

## Acknowledgements

The Environmental Fluid Dynamics Code (EFDC) is a public domain, open source, surface water modeling system, which includes hydrodynamic, sediment and contaminant, and water quality modules fully integrated in a single source code implementation. EFDC has been applied to over 100 water bodies including rivers, lakes, reservoirs, wetlands, estuaries, and coastal ocean regions in support of environmental assessment and management and regulatory requirements.

EFDC was originally developed at the Virginia Institute of Marine Science (VIMS) and School of Marine Science of The College of William and Mary, by Dr. John M. Hamrick beginning in 1988. This activity was supported by the Commonwealth of Virginia through a special legislative research initiative. Dr. Robert Byrne, the late Dr. Bruce Neilson, and Dr. Albert Kuo of VIMS are acknowledged for their efforts in supporting the original development activity. Subsequent support for EFDC development at VIMS was provided by the U.S. Environmental Protection Agency and the National Oceanic and Atmospheric Administration's Sea Grant Program. The contributions of VIMS staff and former students including Mr. Gamble Sisson, Dr. Zaohqing Yang, Dr. Keyong Park, Dr. Jian Shen, and Dr. Sarah Rennie are gratefully acknowledged.

Tetra Tech, Inc. (Tt) became the first commercial user of EFDC in the early 1990's and upon Dr. Hamrick's joining Tetra Tech in 1996, the primary location for the continued development of EFDC. Tetra Tech has provided considerable internal research and development support for EFDC over the past 10 years and Mr. James Pagenkopf, Dr. Mohamed Lahlou, and Dr. Leslie Shoemaker are gratefully acknowledged for this. Mr. Michael Morton of Tetra Tech is particularly recognized for his many contributions to EFDC development and applications. The efforts Tetra Tech colleagues including Dr. Jeff Ji, Dr. Hugo Rodriguez, Mr. Steven Davie, Mr. Brain Watson, Dr. Ruiz Zou, Dr. Sen Bai, Dr. Yuri Pils, Mr. Peter von Lowe, Mr. Will Anderson, and Dr. Silong Lu are also recognized. Their wide-ranging applications of EFDC have contributed to the robustness of the model and lead to many enhancements.

Primary external support of both EFDC development and maintenance and applications at Tetra Tech over the past 10 years has been generously provided by the U. S. Environmental Protection Agency including the Office of Science and Technology, the Office of Research and Development and Regions 1 and 4. In particular, Dr. Earl Hayter (ORD), Mr. James Greenfield (R4), Mr. Tim Wool (R4) and Ms. Susan Svirsky (R1) are recognized for their contributions in managing both EFDC developmental and application work assignments.

The ongoing evolution of the EFDC model has to a great extent been application driven and it is appropriate to thank Tetra Tech's many clients who have funded EFDC applications over the past 10 years. The benefits of ongoing interaction with a diverse group of EFDC users in the academic, governmental, and private sectors are also acknowledged.

## Table of Contents

Preface	2
Acknowledgements	3
Contents	4
List of Figures	5
1. Introduction	6
2. Summary of Hydrodynamic and Generic Transport Formulations	7
3. Solution of the Sediment Transport Equation	13
4. Hydrodynamic and Sediment Boundary Layers	16
5. Sediment Bed Mass Conservation and Geomechanics	39
6. Noncohesive Sediment Settling, Deposition and Resuspension	56
7. Cohesive Sediment Settling, Deposition and Resuspension	68
8. Sorptive Contaminant Transport	75
9. References	91

## List of Figures

		Page
5.1	Specific Weight Normalized Effective Stress Versus Void Ratio	54
5.2	Compress Length Scale, $(g\rho_w)^{-1}(d\sigma_e/d\varepsilon)$ , Versus Void Ratio.	54
5.3	Hydraulic Conductivity Versus Void Ratio	55
5.4	Hydraulic Conductivity/(1 + Void Ratio) Versus Void Ratio	55
6.1	Critical Shield's shear velocity and settling velocity as a function of sediment grain size	67

## 1. Introduction

This report summarizes theoretical and computational aspects of the sediment and sorptive contaminant transport formulations used in the EFDC model. Theoretical and computational aspects for the basic EFDC hydrodynamic and generic transport model components are presented in Hamrick (1992). Theoretical and computational aspects of the EFDC water quality-eutrophication model component are presented in Park *et al.* (1995). The paper by Hamrick and Wu (1997) also summarized computational aspects of the hydrodynamic, generic transport and water quality-eutrophication components of the EFDC model. The EFDC model has been extensively applied to estuaries (Fredricks and Hamrick, 1996; Shen and Kuo, 1999; Shen *et al.*, 1999; Ji *et al.*, 2001), lakes (Jin *et al.*, 2000; 2002), reservoirs (Hamrick and Mills, 2000), rivers (Ji *et al.*, 2002), and wetlands (Moustafa and Hamrick, 2000). The model has also been used for a number of fundamental process studies (Hamrick, 1994; Kuo *et al.*, 1996; Yang *et al.*, 2000).

This report is organized as follows. Chapter 2 summarizes the hydrodynamic and generic transport formulations used in EFDC. Chapter 3 summarizes the solution of the transport equation for suspended cohesive and noncohesive sediment. A discussion of near bed boundary layer processes relevant to sediment transport is presented in Chapter 4. Sediment bed mass conservation and methods for representation of the bed's geomechanical properties are discussed in Chapter 5. Chapters 6 and 7 summarize noncohesive and cohesive sediment settling, deposition and resuspension process representations. The final chapter, Chapter 9, documents the EFDC model's sorptive contaminant transport and fate formulations.

## 2. Summary of Hydrodynamic and Generic Transport Formulations

This section summarizes the hydrodynamic and transport equations used by the EFDC model. Reference is made to Hamrick (1992), Hamrick and Wu (1997) and Tetra Tech (2007a) for details of the computational procedure. This section does however describe modifications to the solution procedure when the model operates in a geomorphologic mode.

The EFDC model's hydrodynamic component is based on the three-dimensional hydrostatic equations formulated in curvilinear-orthogonal horizontal coordinates and a sigma or stretched vertical coordinate. The momentum equations are:

$$\begin{aligned} & \partial_t (m_x m_y H u) + \partial_x (m_y H u u) + \partial_y (m_x H v u) + \partial_z (m_x m_y w u) - f_e m_x m_y H v \\ & = -m_y H \partial_x (p + p_{atm} + \phi) + m_y (\partial_x z_b^* + z \partial_x H) \partial_z p + \partial_z \left( m_x m_y \frac{A_v}{H} \partial_z u \right) \\ & + \partial_x \left( \frac{m_y}{m_x} H A_H \partial_x u \right) + \partial_y \left( \frac{m_x}{m_y} H A_H \partial_y u \right) - m_x m_y c_p D_p (u^2 + v^2)^{1/2} u \end{aligned} \quad (2.1)$$

$$\begin{aligned} & \partial_t (m_x m_y H v) + \partial_x (m_y H u v) + \partial_y (m_x H v v) + \partial_z (m_x m_y w v) + f_e m_x m_y H u \\ & = -m_x H \partial_y (p + p_{atm} + \phi) + m_x (\partial_y z_b^* + z \partial_y H) \partial_z p + \partial_z \left( m_x m_y \frac{A_v}{H} \partial_z v \right) \\ & + \partial_x \left( \frac{m_y}{m_x} H A_H \partial_x v \right) + \partial_y \left( \frac{m_x}{m_y} H A_H \partial_y v \right) - m_x m_y c_p D_p (u^2 + v^2)^{1/2} v \end{aligned} \quad (2.2)$$

$$m_x m_y f_e = m_x m_y f - u \partial_y m_x + v \partial_x m_y \quad (2.3)$$

$$(\tau_{xz}, \tau_{yz}) = A_v H^{-1} \partial_z (u, v) \quad (2.4)$$

where  $u$  and  $v$  are the horizontal velocity components in the dimensionless curvilinear-orthogonal horizontal coordinates  $x$  and  $y$ , respectively. The scale factors of the horizontal coordinates are  $m_x$  and  $m_y$ . The vertical velocity in the stretched vertical coordinate  $z$  is  $w$ . The physical vertical coordinates of the free surface and bottom bed are  $z_s^*$  and  $z_b^*$  respectively. The total water column depth is  $H$ , and  $\phi$  is the free surface potential which is equal to  $gz_s^*$ . The effective Coriolis acceleration  $f_e$  incorporates the curvature acceleration terms, with the Coriolis parameter,  $f$ , according to (2.3). The  $Q$  terms in (2.1) and (2.2) represents optional horizontal momentum diffusion terms. The vertical turbulent viscosity  $A_v$  relates the shear stresses to the vertical shear of the horizontal velocity components by (4.4). The kinematic atmospheric pressure, referenced

to water density, is  $p_{atm}$ , while the excess hydrostatic pressure in the water column is given by:

$$\partial_z p = -gHb = -gH(\rho - \rho_o)\rho_o^{-1} \quad (2.5)$$

where  $\rho$  and  $\rho_o$  are the actual and reference water densities and  $b$  is the buoyancy. The horizontal turbulent stress on the last lines of (2.1) and (2.2), with  $A_H$  being the horizontal turbulent viscosity, are typically retained when the advective acceleration are represented by central differences. The last terms in (2.1) and (2.2) represent vegetation resistance where  $c_p$  is a resistance coefficient and  $D_p$  is the dimensionless projected vegetation area normal to the flow per unit horizontal area.

The three-dimensional continuity equation in the stretched vertical and curvilinear-orthogonal horizontal coordinate system is:

$$\partial_t(m_x m_y H) + \partial_x(m_y H u) + \partial_y(m_x H v) + \partial_z(m_x m_y w) = Q_H + \delta(0)(Q_{SS} + Q_{SW}) \quad (2.6)$$

with  $Q_H$  representing volume sources and sinks including rainfall, evaporation, and lateral inflows and outflows having negligible momentum fluxes. The terms  $Q_{SS}$  and  $Q_{SW}$  are the net volumetric fluxes of sediment and water between the bed and water column, defined as positive from the bed to the water column, when the model operates in a geomorphologic mode. The delta function,  $\delta(0)$  indicates these fluxes enter the bottom layer of the water column. Integration of (2.6) over the depth gives

$$\partial_t(m_x m_y H) + \partial_x(m_y H \bar{u}) + \partial_y(m_x H \bar{v}) = \bar{Q}_H + Q_{SS} + Q_{SW} \quad (2.7)$$

In the geomorphologic mode, the water column continuity equation is coupled to a bulk volume conservation equation for the sediment bed.

$$\partial_t(m_x m_y B) = Q_{GW} - Q_{SS} - Q_{SW} \quad (2.8)$$

where  $B$  is the total thickness of the resolved sediment bed and  $Q_{GW}$  is the volumetric ambient groundwater inflow at the bottom of the sediment bed. The bed surface elevation is defined by

$$\eta = B + z_{bb}^* \quad (2.9)$$

Where  $z_{bb}^*$  is the time invariant elevation at the bottom of the sediment bed. Using (2.9), equation (2.8) can be written as

$$\partial_t(m_x m_y \eta) = Q_{GW} - Q_{SS} - Q_{SW} \quad (2.10)$$

Adding (2.7) and (2.10) gives

$$\partial_t (m_x m_y \zeta) + \partial_x (m_y H \bar{u}) + \partial_y (m_x H \bar{v}) = \bar{Q}_H + Q_{GW} \quad (2.11)$$

where the water surface elevation,  $\zeta$ , is defined by

$$\zeta = z_s^* = H + \eta \quad (2.12)$$

The EFDC model solves the external mode continuity equation (2.11) using a two-step procedure. The first step corresponding to the standard implicit external mode hydrodynamic solution is

$$\begin{aligned} (m_x m_y \zeta)^* - (m_x m_y \zeta)^n + \frac{\theta}{2} \partial_x (m_y H \bar{u})^{n+1} + \frac{\theta}{2} \partial_x (m_y H \bar{u})^n \\ + \frac{\theta}{2} \partial_y (m_x H \bar{v})^{n+1} + \frac{\theta}{2} \partial_y (m_x H \bar{v})^n = \theta \bar{Q}_H^{n+1/2} \end{aligned} \quad (2.13)$$

where  $\theta$  is the time step between  $n$  and  $n+1$ . The intermediate time level notation,  $n+1/2$ , denotes an average between the two time levels. The second step is taken after the bed volumetric continuity equation is updated to time level  $n+1$  and is

$$(m_x m_y \zeta)^{n+1} - (m_x m_y \zeta)^* = \theta \bar{Q}_G^{n+1/2} \quad (2.14)$$

Combining (2.13) and (2.14) gives the equivalent full step.

$$\begin{aligned} (m_x m_y \zeta)^{n+1} - (m_x m_y \zeta)^n + \frac{\theta}{2} \partial_x (m_y H \bar{u})^{n+1} + \frac{\theta}{2} \partial_x (m_y H \bar{u})^n \\ + \frac{\theta}{2} \partial_y (m_x H \bar{v})^{n+1} + \frac{\theta}{2} \partial_y (m_x H \bar{v})^n = \theta \bar{Q}_H^{n+1/2} + \theta \bar{Q}_G^{n+1/2} \end{aligned} \quad (2.15)$$

The water column depth is then updated by

$$H^{n+1} = \zeta^{n+1} - \eta^{n+1} \quad (2.16)$$

prior to the next hydrodynamic time step.

The EFDC model includes the ability to simulate drying and wetting of shallow areas. Drying and wetting is iteratively determined during the implicit solution of equation (2.13) after the time discrete depth average horizontal momentum equations have been inserted to form an elliptic equation for the water surface elevation. The solution procedure is as follows. A preliminary solution for the water surface elevation is determined by solving (2.13) with all horizontal grid interior horizontal cell faces open. The resulting cell center water depth in each cell is then compared to a small dry depth  $H_{dry}$ . If the depth is greater than the dry depth, the cell is defined as wet. If the depth is

less than the dry depth and less than the depth at the previous time step, the cell is defined as wet and its four flow faces are blocked. If the depth is less than the dry depth, but greater than the depth at the previous time step, the direction of flow on each cell face is checked and faces having outflow are block. Following this checking and blocking, (2.13) is solved again, followed by the same checking procedure. This iteration is repeated until wet or dry status of each cell does not change from that of the subsequent iteration. Typically two or three iterations are required. This implementation of drying and wetting is fully mass conservative and does not produce negative water column depths.

The generic transport equation for a dissolved or suspended material having a mass per unit volume concentration  $C$ , is

$$\begin{aligned} & \partial_t (m_x m_y H C) + \partial_x (m_y H u C) + \partial_y (m_x H v C) + \partial_z (m_x m_y w C) - \partial_z (m_x m_y w_{sc} C) \\ & = \partial_x \left( \frac{m_y}{m_x} H K_H \partial_x C \right) + \partial_y \left( \frac{m_x}{m_y} H K_H \partial_y C \right) + \partial_z \left( m_x m_y \frac{K_v}{H} \partial_z C \right) + Q_c \end{aligned} \quad (2.17)$$

where  $K_v$  and  $K_H$  are the vertical and horizontal turbulent diffusion coefficients, respectively,  $w_{sc}$  is a positive settling velocity,  $C$  represents a suspended material, and  $Q_c$  represents external sources and sinks and reactive internal sources and sinks.

The solution of the momentum equations, (2.1) and (2.2) and the transport equation (2.17), requires the specification of the vertical turbulent viscosity,  $A_v$ , and diffusivity,  $K_v$ . To provide the vertical turbulent viscosity and diffusivity, the second moment turbulence closure model developed by Mellor and Yamada (1982) (MY) and modified by Galperin *et al.* (1988) and Blumberg *et al.* (1988) is used. The MY model relates the vertical turbulent viscosity and diffusivity to the turbulent intensity,  $q$ , a turbulent length scale,  $l$ , and a turbulent intensity and length scaled based Richardson number,  $R_q$ , by:

$$\begin{aligned} A_v &= \phi_A A_o q l \\ \phi_A &= \frac{(1 + R_1^{-1} R_q)}{(1 + R_2^{-1} R_q)(1 + R_3^{-1} R_q)} \\ A_o &= A_1 \left( 1 - 3C_1 - \frac{6A_1}{B_1} \right) = \frac{1}{B_1^{1/3}} \\ R_1^{-1} &= 3A_2 \frac{(B_2 - 3A_2) \left( 1 - \frac{6A_1}{B_1} \right) - 3C_1 (B_2 + 6A_1)}{\left( 1 - 3C_1 - \frac{6A_1}{B_1} \right)} \\ R_2^{-1} &= 9A_1 A_2 \\ R_3^{-1} &= 3A_2 (6A_1 + B_2 (1 - C_3)) \end{aligned} \quad (2.18)$$

$$K_v = \phi_K K_o q l$$

$$\phi_K = \frac{1}{(1 + R_3^{-1} R_q)} \quad (2.19)$$

$$K_o = A_2 \left( 1 - \frac{6A_1}{B_1} \right)$$

$$R_q = -\frac{gH\partial_z b}{q^2} \frac{l^2}{H^2} \quad (2.20)$$

where the so-called stability functions,  $\phi_A$  and  $\phi_K$ , account for reduced and enhanced vertical mixing or transport in stable and unstable vertically density stratified environments, respectively. Mellor and Yamada (1982) specify the constants  $A_1$ ,  $B_1$ ,  $C_1$ ,  $A_2$ , and  $B_2$  as 0.92, 16.6, 0.08, 0.74, and 10.1, respectively.

The turbulent intensity and the turbulent length scale are determined by the transport equations:

$$\begin{aligned} & \partial_t (m_x m_y H q^2) + \partial_x (m_y H u q^2) + \partial_y (m_x H v q^2) + \partial_z (m_x m_y w q^2) \\ & = \partial_z \left( m_x m_y \frac{A_q}{H} \partial_z q^2 \right) - 2m_x m_y \frac{H q^3}{B_1 l} \\ & + 2m_x m_y \left( \frac{A_v}{H} ((\partial_z u)^2 + (\partial_z v)^2) + \eta_p c_p D_p (u^2 + v^2)^{3/2} + g K_v \partial_z b \right) + Q_q \end{aligned} \quad (2.21)$$

$$\begin{aligned} & \partial_t (m_x m_y H q^2 l) + \partial_x (m_y H u q^2 l) + \partial_y (m_x H v q^2 l) + \partial_z (m_x m_y w q^2 l) \\ & = \partial_z \left( m_x m_y \frac{A_{ql}}{H} \partial_z (q^2 l) \right) - m_x m_y E_2 \frac{H l q^3}{l B_1} \left( 1 + E_4 \left( \frac{l}{\kappa H z} \right)^2 + E_5 \left( \frac{l}{\kappa H (1-z)} \right)^2 \right) \\ & + m_x m_y l \left( E_1 \frac{A_v}{H} ((\partial_z u)^2 + (\partial_z v)^2) + E_3 g K_v \partial_z b + E_1 \eta_p c_p D_p (u^2 + v^2)^{3/2} \right) + Q_l \end{aligned} \quad (2.22)$$

where  $(E_1, E_2, E_3, E_4, E_5) = (1.8, 1.0, 1.8, 1.33, 0.25)$ . The second term on the last line of each equation represents net turbulent energy production by vegetation drag where  $\eta_p$  is a production efficiency factor having a value less than one. The terms  $Q_q$  and  $Q_l$  may represent additional source-sink terms such as subgrid scale horizontal turbulent diffusion. The vertical diffusivity,  $A_q$ , is set to  $0.2ql$  following Mellor and Yamada (1982). For stable stratification, Galperin *et al.* (1988) suggest limiting the length scale such that the square root of  $R_q$  is less than 0.52. When horizontal turbulent viscosity and diffusivity are included in the momentum and transport equations, they are determined independently using Smagorinsky's (1963) subgrid scale closure formulation.

Vertical boundary conditions for the solution of the momentum equations are based on the specification of the kinematic shear stresses, equation (2.4), at the bed and the free surface. At the free surface, the  $x$  and  $y$  components of the stress are specified by the water surface wind stress

$$(\tau_{xz}, \tau_{yz}) = (\tau_{sx}, \tau_{sy}) = c_s \sqrt{U_w^2 + V_w^2} (U_w, V_w) \quad (2.23)$$

where  $U_w$  and  $V_w$  are the  $x$  and  $y$  components of the wind velocity at 10 meters above the water surface. The wind stress coefficient is given by:

$$c_s = 0.001 \frac{\rho_a}{\rho_w} \left( 0.8 + 0.065 \sqrt{U_w^2 + V_w^2} \right) \quad (2.24)$$

for the wind velocity components in meters per second, with  $\rho_a$  and  $\rho_w$  denoting air and water densities, respectively. At the bed, the stress components are related to the near bed or bottom layer velocity components by the quadratic resistance formulation

$$(\tau_{xz}, \tau_{yz}) = (\tau_{bx}, \tau_{by}) = c_b \sqrt{u_1^2 + v_1^2} (u_1, v_1) \quad (2.25)$$

where the  $I$  subscript denotes bottom layer values. Under the assumption that the near bottom velocity profile is logarithmic at any instant of time, the bottom stress coefficient is given by

$$c_b = \left( \frac{\kappa}{\ln(\Delta_I / 2z_o)} \right)^2 \quad (2.26)$$

where  $\kappa$  is the von Karman constant,  $\Delta_I$  is the dimensionless thickness of the bottom layer, and  $z_o = z_o^* / H$  is the dimensionless roughness height. Vertical boundary conditions for the turbulent kinetic energy and length scale equations are:

$$q^2 = B_1^{2/3} |\tau_s| \quad : \quad z = 1 \quad (2.27)$$

$$q^2 = B_1^{2/3} |\tau_b| \quad : \quad z = 0 \quad (2.28)$$

$$l = 0 \quad : \quad z = 0, 1 \quad (2.29)$$

where the absolute values indicate the magnitude of the enclosed vector quantity. Equation (2.28) can become inappropriate under a number of conditions associated with either or both high near bottom sediment concentrations and high frequency surface wave activity. The quantification of sediment and wave effects on the bottom stress is discussed in Chapter 4.

### 3. Solution of the Sediment Transport Equation

This section describes the solution of the transport equations for suspended sediment. The general procedure follows that for the salinity transport equation, which uses a high order upwind difference solution scheme for the advective terms, described in Hamrick (1992) and Tetra Tech (2007a). Although the advection scheme is designed to minimize numerical diffusion, a small amount of horizontal diffusion remains inherent in the scheme. Due the small inherent numerical diffusion, the physical horizontal diffusion terms in (2.17) are omitted as to give:

$$\begin{aligned} \partial_t (m_x m_y H S_j) + \partial_x (m_y H u S_j) + \partial_y (m_x H v S_j) + \partial_z (m_x m_y w S_j) \\ - \partial_z (m_x m_y w_{sj} S_j) = \partial_z \left( m_x m_y \frac{K_V}{H} \partial_z S_j \right) + Q_{sj}^E + Q_{sj}^I \end{aligned} \quad (3.1)$$

where  $S_j$  represents the concentration of the  $j$ th sediment class and the source-sink term has been split into an external part, which would include point and nonpoint source loads, and internal part which could include reactive decay of organic sediments or the exchange of mass between sediment classes if floc formation and destruction were simulated. Vertical boundary conditions for (3.1) are:

$$\begin{aligned} -\frac{K_V}{H} \partial_z S_j - w_{sj} S_j = J_{jo} : z \approx 0 \\ -\frac{K_V}{H} \partial_z S_j - w_{sj} S_j = 0 : z = 1 \end{aligned} \quad (3.2)$$

where  $J_{jo}$  is the net water column-bed exchange flux defined as positive into the water column.

The numerical solution of (3.1) utilizes a fractional step procedure. The first step advances the concentration due to advection and external sources and sinks having corresponding volume fluxes by

$$\begin{aligned} H^{n+1} S^* = H^n S^n + \frac{\theta}{m_x m_y} (Q_{sj}^E)^{n+1/2} \\ - \frac{\theta}{m_x m_y} \left( \partial_x (m_y (Hu)^{n+1/2} S^n) + \partial_y (m_x (Hv)^{n+1/2} S^n) + \partial_z (m_x m_y w^{n+1/2} S^n) \right) \end{aligned} \quad (3.3)$$

where  $n$  and  $n+1$  denote the old and new time levels and  $*$  denotes the intermediate fractional step results. The portion of the source and sink term, associated with volumetric sources and sinks is included in the advective step for consistency with the continuity constraint. This source-sink term, as well as the advective field  $(u, v, w)$ , is defined as intermediate in time between the old and new time levels consistent with the

temporal discretization of the continuity equation. Note that the sediment class subscripts have been dropped for clarity. The advection step uses the anti-diffusive MPDATA scheme (Smolarkiewicz and Clark, 1986) with optional flux corrected transport (Smolarkiewicz and Grabowski, 1990).

The second fractional step or settling step is given by

$$S^{**} = S^* + \frac{\theta}{H^{n+1}} \partial_z (w_s S^{**}) \quad (3.4)$$

which is solved by a fully implicit upwind difference scheme

$$\begin{aligned} S_{kc}^{**} &= S_{kc}^* - \frac{\theta}{\Delta_z H^{n+1}} (w_s S^{**})_{kc} \\ S_k^{**} &= S_k^* + \frac{\theta}{\Delta_1 H^{n+1}} (w_s S^{**})_{k+1} - \frac{\theta}{\Delta_z H^{n+1}} (w_s S^{**})_k \quad : \quad 2 \leq k \leq kc-1 \\ S_1^{**} &= S_1^* + \frac{\theta}{\Delta_z H^{n+1}} (w_s S^{**})_2 \end{aligned} \quad (3.5)$$

marching downward from the top layer. The implicit solution includes an optional anti-diffusion correction across internal water column layer interfaces.

The third fractional step accounts for water column-bed exchange by resuspension and deposition

$$S_1^{***} = S_1^{**} + \frac{\theta}{\Delta_z H^{n+1}} L_o J_o^{***} \quad (3.6)$$

Where  $L_o$  is a flux limiter such that only the current top layer of the bed can be completely resuspended in single time step. The representation of the water column bed exchange by a distinct fractional step is equivalent to a splitting of the bottom boundary condition (3.2) such that the bed flux is imposed intermediate between settling and vertical diffusion. For resuspension and deposition of suspended noncohesive sediment, the bed flux is given by

$$J_o^{***} = \frac{w_s}{\nu} (\mu S_{eq} - S_1^{***}) \quad (3.7)$$

which will be further discussed in Chapters 4 and 6. Inserting (3.7) into (3.6) gives

$$\left( 1 + \frac{\theta L_o w_s}{\Delta_z H^{n+1} \nu} \right) S_1^{***} = S_1^{**} + \frac{\theta L_o w_s}{\Delta_z H^{n+1} \nu} \mu S_{eq} \quad (3.8)$$

For cohesive sediment resuspension, the bed flux is specified as a function of the bed stress and bed geomechanical properties. For cohesive sediment deposition, the bed flux is typically given by

$$J_o^{***} = -P_d w_s S_1^{***} \quad (3.9)$$

where  $P_d$  is a probability of deposition which will be further discussed in Chapter 7. Inserting (3.9) into (3.6) gives

$$\left( 1 + \frac{\theta P_d w_s}{\Delta_z H^{n+1}} \right) S_1^{***} = S_1^{**} \quad (3.10)$$

The remaining step is an implicit vertical turbulent diffusion step corresponding

$$S^{n+1} = S^{***} + \theta \partial_z \left( \left( \frac{K_V}{H^2} \right)^{n+1} \partial_z S^{n+1} \right) \quad (3.11)$$

with zero diffusive fluxes at the bed and water surface.

## 4. Hydrodynamic and Sediment Boundary Layers

Both two-dimensional and three-dimensional applications of the EFDC model require parameterization of near bed boundary layer processes. In the absence of high frequency surface gravity waves and when sediment transport is not being simulated, this parameterization is made through the bottom friction coefficient, (2.26) and the bottom turbulence intensity boundary conditions (2.28). The presence of high frequency surface gravity waves and near bed gradients of suspended sediment requires additional parameterization since the sediment and wave boundary layers cannot be directly resolved by typical vertical grid resolution. Approximate parameterizations of hydrodynamic and sediment boundary layer appropriate for representing the bottom stress and the water column-bed exchange of sediment under conditions including ambient flow, high frequency surface waves and high near bed suspended sediment gradients can be derived from simplified forms of the momentum and sediment transport equations and the turbulent kinetic energy equation.

### 4.1 Boundary Layer Equations

First consider the horizontally homogeneous momentum equation written in vector form

$$\partial_t \mathbf{u} = -\nabla(p + g\zeta) + H^{-1} \partial_z (A_v \partial_z \mathbf{u}) \quad (4.1)$$

The horizontal velocity, pressure and water surface elevation can be decomposed into components associated with the current or mean flow and the high frequency surface gravity wave motion

$$\begin{aligned} \mathbf{u} &= \mathbf{u}_c + \mathbf{u}_w \\ p &= p_w \\ \zeta &= \zeta_c + \zeta_w \end{aligned} \quad (4.2)$$

where the current pressure in excess of hydrostatic pressure has been set to zero. Assuming the current is steady with respect to the time scale of the wave motion and inserting (4.2) into (4.1) gives

$$\partial_t \mathbf{u}_w = -\nabla p_w - g \nabla (\zeta_w + \zeta_c) + H^{-1} \partial_z (A_v \partial_z (\mathbf{u}_w + \mathbf{u}_c)) \quad (4.3)$$

On non-geophysical scales where the bottom current boundary layers does not exhibit Ekman effects, equation (4.3) can be vectorially split into components aligned with the wave and current directions

$$\begin{aligned} & \partial_t u_w + \nabla_w (p_w + g\zeta_w) - \partial_z \left( \frac{A_v}{H^2} \partial_z u_w \right) \\ & + \cos(\psi_c - \psi_w) \left( g \nabla_c \zeta_c - \partial_z \left( \frac{A_v}{H^2} \partial_z u_c \right) \right) = 0 \end{aligned} \quad (4.4)$$

$$\begin{aligned} & \cos(\psi_c - \psi_w) \left( \partial_t u_w + \nabla_w (p_w + g\zeta_w) - \partial_z \left( \frac{A_v}{H^2} \partial_z u_w \right) \right) \\ & + \left( g \nabla_c \zeta_c - \partial_z \left( \frac{A_v}{H^2} \partial_z u_c \right) \right) = 0 \end{aligned} \quad (4.5)$$

where  $\psi_c$  and  $\psi_w$  are the directions of the current and wave propagation, respectively, and for simplicity in notation  $u_w$  and  $u_c$  are the wave and current velocities in these two directions. Subtracting the wave period average of (4.4) from (4.4) gives an equation for the wave motion

$$\begin{aligned} & \partial_t u_w + \nabla_w (p_w + g\zeta_w) - \partial_z \left( \frac{A_v}{H^2} \partial_z u_w - \left\langle \frac{A_v}{H^2} \partial_z u_w \right\rangle \right) \\ & - \cos(\psi_c - \psi_w) \partial_z \left( \frac{(A_v - \langle A_v \rangle)}{H^2} \partial_z u_c \right) = 0 \end{aligned} \quad (4.6)$$

Averaging (4.5) over the wave period gives an equation for the mean current

$$g \nabla_c \zeta_c - \partial_z \left( \frac{\langle A_v \rangle}{H^2} \partial_z u_c \right) - \cos(\psi_c - \psi_w) \partial_z \left( \left\langle \frac{A_v}{H^2} \partial_z u_w \right\rangle \right) = 0 \quad (4.7)$$

Wave-current boundary layer models formulated for use with numerical circulation models typically neglect variations in the vertical turbulent viscosity at the wave time scale (Styles and Glenn, 2000) allowing (4.6) and (4.7) to be reduced to

$$\partial_t u_w + \nabla_w (p_w + g\zeta_w) - \partial_z \left( \frac{A_v}{H^2} \partial_z u_w \right) = 0 \quad (4.8)$$

$$g \nabla_c \zeta_c - \partial_z \left( \frac{A_v}{H^2} \partial_z u_c \right) = 0 \quad (4.9)$$

Above the wave boundary layer, the wave velocity field is inviscid and (4.8) reduces to

$$\partial_t u_{w\infty} + \nabla_w (p_w + g\zeta_w) = 0 \quad (4.10)$$

which is subtracted from (4.8) to give the wave boundary layer equation

$$\partial_t u_w - \partial_z \left( \frac{A_v}{H^2} \partial_z u_w \right) = \partial_t u_{w\infty} \quad (4.11)$$

The boundary conditions for (4.11) are

$$\frac{A_v}{H} \partial_z u_w = \tau_{wb} \quad (4.12)$$

or

$$u_w = 0$$

As  $z$  goes to the roughness height  $z_o$ , and

$$u_w \rightarrow u_{w\infty} \quad (4.13)$$

as  $z$  becomes large.

Integrating of (4.9) over the bottom hydrodynamic model layer and subtracting the results from (4.9) gives the current boundary layer equation

$$\partial_z \left( \frac{A_v}{H} \partial_z u_c \right) = \frac{(\tau_{cl} - \tau_{cb})}{\Delta_l} \quad (4.14)$$

where the  $cl$  and  $cb$  subscripts denote the shear stresses at the top and bottom of the bottom grid layer. Integration of (4.14) gives

$$\frac{A_v}{H} \partial_z u_c = \tau_{cb} + (\tau_{cl} - \tau_{cb}) \frac{z}{\Delta_l} \quad (4.15)$$

where  $\Delta_l$  is the dimensionless thickness of the bottom grid layer. For small  $z$  near the bed, (4.15) is approximated as a constant stress layer

$$\frac{A_v}{H} \partial_z u_c = \tau_{cb} \quad (4.16)$$

The boundary condition for (4.16) is

$$u_c = 0 \quad (4.17)$$

as  $z$  goes to the roughness height  $z_o$ . In the bottom hydrodynamic layer the integral condition

$$\int_0^{\Delta_1} u_c dz = \Delta_1 u_1 \quad (4.17)$$

is imposed where  $u_1$  is the current velocity in the bottom grid layer.

The sediment boundary layer equation can be derived from the horizontally homogeneous approximation to the sediment transport equation (3.1).

$$\partial_t (HS) - \partial_z \left( w_s S + \frac{K_V}{H} \partial_z S \right) = 0 \quad (4.18)$$

Integrating (4.18) over the bottom hydrodynamic layer gives

$$\partial_t (HS_1) = \frac{J_{sb} - J_{s1}}{\Delta_1} \quad (4.19)$$

where  $S_1$  is the bottom layer sediment concentration and  $J_{sb}$  and  $J_{s1}$  are the sediment fluxes at the bed and the top of the bottom grid layer. Subtracting (4.19) from (4.18) gives

$$\partial_t (HS - HS_1) - \partial_z \left( w_s S + \frac{K_V}{H} \partial_z S \right) = \frac{J_{s1} - J_{sb}}{\Delta_1} \quad (4.20)$$

Assuming that the temporal derivative in (4.20) is small and can be neglected, (4.20) is integrated to give

$$-w_s S - \frac{K_V}{H} \partial_z S = J_{sb} + (J_{s1} - J_{sb}) \frac{z}{\Delta_1} \quad (4.21)$$

For small  $z$  near the bed, (4.21) is approximated as a constant flux layer

$$-w_s S - \frac{K_V}{H} \partial_z S = J_{sb} \left( 1 - \frac{z}{\Delta_1} \right) \quad (4.21x)$$

$$-w_s S - \frac{K_V}{H} \partial_z S = J_{sb} \quad (4.22)$$

The bottom boundary condition for (4.22) is

$$S = S_r \quad (4.23)$$

as  $z$  goes to the dimensionless sediment reference height  $z_r$ , which can be the roughness height. In the bottom hydrodynamic layer the integral condition

$$\int_0^{\Delta_1} S dz = \Delta_1 S_1 \quad (4.24)$$

is imposed.

The near bed wave, current and sediment boundary layer equations (4.11, 4.16, and 4.22) require specification of the near bed forms of the vertical turbulent viscosity and diffusion coefficients. Near the bed, the turbulent kinetic energy equation (2.21) can be approximated by its equilibrium form

$$\frac{q^3}{B_1 l} = \frac{A_v}{H^2} \left( (\partial_z u)^2 + (\partial_z v)^2 \right) + g \frac{K_v}{H} \partial_z b \quad (4.25)$$

where the vegetation term has been dropped since the horizontal velocity components approach zero. Introducing the definitions of  $A_v$  and  $K_v$  given by (2.18) and (2.19) and solving for the turbulent intensity gives

$$q^2 = \left( \frac{B_1 A_o \phi_A}{1 + B_1 K_o \phi_K R_q} \right) \left( \frac{l^2}{H^2} \right) \left( (\partial_z u)^2 + (\partial_z v)^2 \right) \quad (4.26)$$

Equation (4.25) can be also be written in terms of the shear stresses after multiplying by  $A_v$ , inserting the definitions of  $A_v$  and  $K_v$  given by (2.18) and (2.19), and using (2.20), to give

$$q^2 = \left( \frac{B_1}{A_o \phi_A} \right)^{1/2} \left( 1 + B_1 K_o \phi_K R_q \right)^{-1/2} \left( \tau_{xz}^2 + \tau_{yz}^2 \right)^{1/2} \quad (4.27)$$

When (4.27) is evaluated at the bed, the results

$$q_b^2 = \left( \frac{B_1}{A_o \phi_A} \right)^{1/2} \left( 1 + B_1 K_o \phi_K R_q \right)^{-1/2} \left( \tau_{bx}^2 + \tau_{by}^2 \right)^{1/2} \quad (4.28)$$

is equivalent to (2.28) under neutral conditions where  $R_q$  is equal to zero. High near bed sediment concentrations and associated vertical gradients can result in nonzero values of  $R_q$  immediately above the bed.

The buoyancy gradient near the bed is primarily due to gradients in suspended sediment concentration with the effect of sediment on density given by

$$\rho = \sum_j \left( \left( 1 - \frac{S_j}{\rho_{sj}} \right) \rho_w + \left( \frac{S_j}{\rho_{sj}} \right) \rho_{sj} \right) \quad (4.29)$$

where  $S_j$  is the mass concentration of sediment class  $j$  per unit volume of the water-sediment mixture. The buoyancy is expressed in terms of the sediment concentration using

$$b = \frac{\rho - \rho_w}{\rho_w} = \sum_j \left( \frac{\rho_{sj} - \rho_w}{\rho_w} \right) \left( \frac{S_j}{\rho_{sj}} \right) = \sum_j \alpha_j S_j \quad (4.30)$$

which can be used to evaluate the buoyancy gradients.

When high frequency surface waves are present, the velocity components in (4.25) and (4.26) and the shear stress components in (4.26) and (4.27) can be decomposed into

$$u = u_c \cos \psi_c + u_w \cos \psi_w \quad (4.31)$$

$$v = u_c \sin \psi_c + u_w \sin \psi_w$$

$$\tau_{xz} = \tau_{cz} \cos \psi_c + \tau_{wz} \cos \psi_w \quad (4.32)$$

$$\tau_{yz} = \tau_{cz} \sin \psi_c + \tau_{wz} \sin \psi_w$$

where  $u_c$  and  $u_w$  are the current and wave velocities and  $\tau_c$  and  $\tau_w$  are the current and wave shear stress magnitudes, each aligned with the current and wave directions denoted by  $\psi_c$  and  $\psi_w$ . Using (4.31) and (4.32), the shear and bed stress terms can be written as

$$\left( (\partial_z u)^2 + (\partial_z v)^2 \right) = (\partial_z u_c)^2 + (\partial_z u_w)^2 + 2 \cos(\psi_c - \psi_w) \partial_z u_c \partial_z u_w \quad (4.33)$$

$$\left( \tau_{xz}^2 + \tau_{yz}^2 \right) = \tau_{cz}^2 + \tau_{wz}^2 + 2 \cos(\psi_c - \psi_w) \tau_{cz} \tau_{wz} \quad (4.34)$$

Assuming the wave velocity and shear stress to be periodic

$$u_w = u_{wm} \sin(\omega t) \quad (4.35)$$

$$\tau_{wz} = \tau_{wzm} \sin(\omega t)$$

$$\psi_w = \psi_{wm} \operatorname{sgn}(\sin(\omega t))$$

the wave period averages of (4.31) and (4.32) are

$$\left\langle (\partial_z u)^2 + (\partial_z v)^2 \right\rangle = (\partial_z u_c)^2 + \frac{1}{2} (\partial_z u_{wm})^2 + \frac{4}{\pi} \cos(\psi_c - \psi_{wm}) \partial_z u_c \partial_z u_{wm} \quad (4.36)$$

$$\langle \tau_{cz}^2 + \tau_{wz}^2 \rangle = \tau_{cz}^2 + \frac{1}{2} \tau_{wzm}^2 + \frac{4}{\pi} \cos(\psi_c - \psi_{wm}) \tau_{cb} \tau_{wzm} \quad (4.37)$$

Analytical solutions of the wave, current and sediment boundary layer equations (4.11, 4.16, and 4.22), as exemplified most recently by Styles and Glenn (2000), typically assume tractable forms of the vertical turbulent viscosity and diffusivity inside the wave-current and the current boundary layers. The following sections discuss boundary layer parameterization for neutral and stratified boundary layers in absences and presences of waves.

## 4.2 Neutral Current and Sediment Boundary Layers

For neutral conditions, the turbulent intensity (4.27) and the vertical turbulent exchange coefficients (2.18) and (2.19) can be written as

$$q^2 = B_1^{2/3} (\tau_{xz}^2 + \tau_{yz}^2)^{1/2} \quad (4.38)$$

$$A_v^n = A_o q l = (\tau_{xz}^2 + \tau_{yz}^2)^{1/4} l \quad (4.39)$$

$$K_v^n = K_o q l = \frac{K_o}{A_o} (\tau_{xz}^2 + \tau_{yz}^2)^{1/4} l \quad (4.40)$$

For three-dimensional, multiple vertical layer applications equation (4.16) becomes

$$\frac{l}{H} \partial_z u_c = \sqrt{\tau_{cb}} \quad (4.41)$$

Letting  $l/H = \kappa z$ , and using (4.17) gives the logarithmic profile

$$u_c = \frac{\sqrt{\tau_{cb}}}{\kappa} \ln \left( \frac{z}{z_o} \right) \quad (4.42)$$

Applying the integral condition (4.17) over the bottom layer gives

$$\begin{aligned} \tau_{cb} &= c_b |u_1| u_1 \\ c_b &= \left( \frac{\kappa}{\ln(\Delta_1 / 2z_o)} \right)^2 \end{aligned} \quad (4.43)$$

For two-dimensional depth average applications (4.15) becomes

$$\frac{l}{H} \partial_z u_c = \sqrt{\tau_{cb}} \sqrt{1-z} \quad (4.44)$$

For consistency with the subsequent solution of the sediment boundary layer equation, the length scale is chosen as

$$\frac{l}{H} = \frac{\kappa z}{\sqrt{1-z}} \quad (4.45)$$

With the solution of (4.44) becoming

$$u_c = \frac{\sqrt{\tau_{cb}}}{\kappa} \left( \ln \left( \frac{z}{z_o} \right) - (z - z_o) \right) \quad (4.46)$$

Applying the integral constraint (4.14) to (4.46) gives

$$\begin{aligned} \tau_{cb} &= c_b |u_1| u_1 \\ c_b &= \left( \frac{\kappa}{\ln(1/2z_o)} \right)^2 \end{aligned} \quad (4.47)$$

For three-dimensional multiple layer, applications, the sediment boundary layer equation (4.22) can be written as

$$\frac{z}{R} \partial_z S + S = -\frac{J_{sb}}{w_s} \quad (4.48)$$

where

$$R = \frac{A_o}{K_o} \frac{w_s}{\kappa \sqrt{\tau_{cb}}} \quad (4.49)$$

is the Rouse parameter. The solution of (4.48) is

$$S = -\frac{J_{sb}}{w_s} + \frac{C}{z^R} \quad (4.50)$$

For noncohesive sediment, the constant of integration is evaluated using

$$S = S_{eq} \quad : \quad z = z_{eq} \quad \text{and} \quad J_{sb} = 0 \quad (4.51)$$

that sets the near bed sediment concentration to an equilibrium value,  $S_{eq}$ , defined just above the bed under no net flux condition. Using (4.51), equation (4.50) becomes

$$S = \left( \frac{z_{eq}}{z} \right)^R S_{eq} - \frac{J_{sb}}{w_s} \quad (4.52)$$

For non-equilibrium conditions, the net flux is given by evaluating (4.52) at the equilibrium level

$$J_{sb} = w_s (S_{eq} - S_{ne}) \quad (4.53)$$

where  $S_{ne}$  is the actual concentration at the reference equilibrium level. Equation (4.53) indicates that when the near bed sediment concentration is less than the equilibrium value a net flux from the bed into the water column occurs. Likewise when the concentration exceeds equilibrium, a net flux to the bed occurs. For the relationship (4.53) to be useful in a numerical model, the bed flux must be expressed in terms of the model layer mean concentration. For a three-dimensional application, (4.53) and the constraint (4.24) give

$$J_{sb} = w_s (S_{eqe} - S_1) \quad (4.54)$$

where

$$S_{eqe} = \frac{\ln(\Delta z_{eq}^{-1})}{(\Delta z_{eq}^{-1} - 1)} S_{eq} : R = 1 \quad (4.55)$$

$$S_{eqe} = \frac{\left( (\Delta z_{eq}^{-1})^{1-R} - 1 \right)}{(1-R)(\Delta z_{eq}^{-1} - 1)} S_{eq} : R \neq 1$$

defines an effective bottom layer mean equilibrium concentration in terms of the near bed equilibrium concentration. The corresponding quantities in the numerical solution bottom boundary condition (3.7) are

$$W_r S_r = w_s S_{eqe} \quad (4.56)$$

$$W_d = w_s$$

If the dimensionless equilibrium elevation,  $z_{eq}$  exceeds the dimensionless layer thickness, (4.54) and (4.55) can be modified to

$$J_{sb} = w_s (\bar{S}_{eqe} - \bar{S}) \quad (4.57)$$

$$\bar{S}_{eqe} = \frac{\ln(M \Delta z_{eq}^{-1})}{(M \Delta z_{eq}^{-1} - 1)} S_{eq} : R = 1 \quad (4.57)$$

$$\bar{S}_{eqe} = \frac{\left( (M \Delta z_{eq}^{-1})^{1-R} - 1 \right)}{(1-R)(M \Delta z_{eq}^{-1} - 1)} S_{eq} : R \neq 1 \quad (4.58)$$

where the over bars in (4.57) and (4.58) implying an average of the first  $M$  grid layers above the bed. When multiple sediment size classes are simulated, the equilibrium concentration,  $S_{eq}$ , in (4.55) and (4.58) are reduced from their uniform values by multiplying by the sediment class volume fractions at the bed surface.

For cohesive sediment resuspension, the flux is presumed known, and the constant of integration in (4.48) is determined by the integral constraint with the resulting sediment concentration distribution being

$$S = -\frac{J_{sb}}{w_s} + \frac{(1-R)(\Delta_1 - z_r)}{z^R (\Delta_1^{1-R} - z_r^{1-R})} \left( S_1 + \frac{J_{sb}}{w_s} \right) : R \neq 1 \quad (4.59)$$

$$S = -\frac{J_{sb}}{w_s} + \frac{(\Delta_1 - z_r)}{z \ln(\Delta_1 z_r^{-1})} \left( S_1 + \frac{J_{sb}}{w_s} \right) : R = 1$$

For cohesive sediment deposition, the bed flux is given by

$$J_{sb} = -P_d w_s S_r \quad (4.60)$$

where  $P_d$  is the probability of deposition. Evaluating (4.59) at the reference level, inserting into (4.60) and solving, gives the deposition flux in terms of the bottom layer concentration

$$J_{sb} = -\left( 1 - P_d + \frac{P_d (1-R)(\Delta_1 - z_r)}{z_r^R (\Delta_1^{1-R} - z_r^{1-R})} \right)^{-1} \left( \frac{(1-R)(\Delta_1 - z_r)}{z_r^R (\Delta_1^{1-R} - z_r^{1-R})} \right) P_d w_s S_1 : R \neq 1 \quad (4.61)$$

$$J_{sb} = -\left( 1 - P_d + \frac{P_d (\Delta_1 - z_r)}{z_r \ln(\Delta_1 z_r^{-1})} \right)^{-1} \left( \frac{(\Delta_1 - z_r)}{z_r \ln(\Delta_1 z_r^{-1})} \right) P_d w_s S_1 : R = 1$$

The sediment concentration profile under depositional conditions is also give by (4.59) using the flux from (4.61).

For depth average applications, the sediment boundary layer equation (4.21) can be written as

$$\frac{\sqrt{1-z}}{R} \frac{l}{\kappa H} \partial_z S + S = -\frac{J_{sb}}{w_s} (1-z) \quad (4.59)$$

A closed form solution is possible by choosing

$$\frac{l}{H} = \frac{\kappa z}{\sqrt{1-z}} \quad (4.60)$$

with (4.59) becoming

$$\partial_z S + \frac{R}{z} S = -\frac{J_{sb}}{w_s} \frac{R}{z} (1-z) \quad (4.61)$$

The solution of (4.61) is

$$S = -\left(1 - \frac{Rz}{(1+R)}\right) \frac{J_{sb}}{w_s} + \frac{C}{z^R} \quad (4.62)$$

Evaluating the constant of integration using (4.51) gives

$$S = \left(\frac{z_{eq}}{z}\right)^R S_{eq} - \left(1 - \frac{Rz}{(1+R)}\right) \frac{J_{sb}}{w_s} \quad (4.63)$$

For non-equilibrium conditions, the net flux is given by evaluating (4.63) at the equilibrium level

$$J_{sb} = w_s \left( \frac{(1+R)}{1+R(1-z_{eq})} \right) (S_{eq} - S_{ne}) \quad (4.64)$$

where  $S_{ne}$  is the actual concentration at the reference equilibrium level. Since  $z_{eq}$  is on the order of the sediment grain diameter divided by the depth of the water column, (4.64) is essentially equivalent to (4.54). To obtain an expression for the bed flux in terms of the depth average sediment concentration, equation (4.63) is integrated over the depth to give

$$J_{sb} = w_s \left( \frac{2(1+R)}{2+R(1-z_{eq})} \right) (\bar{S}_{eqe} - \bar{S}) \quad (4.65)$$

where

$$\bar{S}_{eqe} = \frac{\ln(z_{eq}^{-1})}{(z_{eq}^{-1} - 1)} S_{eq} : R = 1 \quad (4.66)$$

$$\bar{S}_{eqe} = \frac{(z_{eq}^{R-1} - 1)}{(1-R)(z_{eq}^{-1} - 1)} S_{eq} : R \neq 1$$

When multiple sediment size classes are simulated, the equilibrium concentration,  $S_{eq}$ , in (4.66) is reduced from its uniform value by multiplying by the sediment class volume fractions at the bed surface. The corresponding quantities in the numerical solution bottom boundary condition (3.7) are

$$W_r S_r = w_s \left( \frac{2(1+R)}{2+R(1-z_{eq})} \right) \bar{S}_{eqe} \quad (4.67)$$

$$W_d = \left( \frac{2(1+R)}{2+R(1-z_{eq})} \right) w_s$$

For cohesive sediment resuspension, the flux is presumed known, and the constant of integration in (4.62) is determined by the integral constraint with the resulting sediment concentration distribution being

$$S = \left( \left( 1 - \frac{R(\Delta_1 + z_r)}{2(1+R)} \right) \left( \frac{(\Delta_1 - z_r)(1-R)}{(\Delta_1)^{1-R} - (z_r)^{1-R}} \right) \frac{1}{z^R} - \left( 1 - \frac{Rz}{(1+R)} \right) \right) \frac{J_{sb}}{w_s} \quad (4.68)$$

$$+ \left( \frac{(\Delta_1 - z_r)(1-R)}{(\Delta_1)^{1-R} - (z_r)^{1-R}} \right) \frac{S_1}{z^R} : R \neq 1$$

$$S = \left( \frac{(\Delta_1 - z_r)}{z} \left( \ln \left( \frac{\Delta_1}{z_r} \right) \right)^{-1} \left( 1 - \frac{(\Delta_1 + z_r)}{4} \right) - \left( 1 - \frac{z}{2} \right) \right) \frac{J_{sb}}{w_s}$$

$$+ \frac{(\Delta_1 - z_r)}{z} \left( \ln \left( \frac{\Delta_1}{z_r} \right) \right)^{-1} (S_1) : R = 1$$

For cohesive sediment deposition, the bed flux is given by

$$J_{sb} = -P_d w_s S_r \quad (4.69)$$

where  $P_d$  is the probability of deposition. The depositional flux can be determined by evaluating (4.68) at the reference level, inserting the results into (4.69), and solving for the flux. The sediment concentration profile under depositional conditions is also give by (4.68) using the depositional flux.

### 4.3 Stratified Current and Sediment Boundary Layers

Analytical solutions for stratified current and sediment boundary layers are difficult to obtain unless tractable expressions are assumed for the near bed distribution of the vertical turbulent viscosity and diffusion coefficients. An alternative is a numerical solution of the boundary layer equations using a sub-grid embedded in the bottom hydrodynamic grid layer. The distribution of the vertical turbulent viscosity and diffusion coefficients is presumed known from the sub-grid layer solution at the previous time step using (4.26) or (4.27) to determine the turbulent intensity. The sub-grid layer solution proceeds by writing equation (4.16) in finite difference form as

$$u_c^{k+1} = u_c^k + \tau_{cb} \left( \frac{\delta_s H}{A_v} \right)^k \quad (4.70)$$

where  $k$  denotes the sub-grid layer and

$$\delta_s = \frac{(\Delta_1 - z_o)}{k_s} \quad (4.71)$$

is the thickness of the sub-grid layers with  $k_s$  being the number of sub-grid layers embedded in the bottom grid layer. The integral constraint (4.17) becomes

$$\sum_{k=1}^{k_s} u_c^k = k_s u_{c1} \quad (4.72)$$

where  $u_{c1}$  is the current velocity in the bottom grid layer. Solving the recursion (4.70) and substituting into (4.72) gives

$$u_c^1 + \frac{1}{k_s} \left( \sum_1^{k_s} (k_s - k) \left( \frac{\delta_s H}{A_v} \right)^k \right) \tau_{cb} = u_{c1} \quad (4.73)$$

The velocity profile in the bottom half of the near bed sub-grid layer is assumed to be logarithmic

$$u_c^1 = \frac{\sqrt{\tau_{cb}}}{\kappa} \ln \left( \frac{\delta_s}{2} \right) \quad (4.74)$$

Inserting (4.74) into (4.73) gives

$$u_c^1 \left( 1 + \frac{1}{k_s} \left( \sum_1^{k_s} (k_s - k) \left( \frac{\delta_s H}{A_v} \right)^k \right) \left( \frac{1}{\kappa} \ln \left( \frac{\delta_s}{2} \right) \right)^{-2} |u_c^1| \right) = u_{c1} \quad (4.75)$$

which can be solved iteratively for the current velocity in the bottom sub-grid layer when the distribution of the turbulent viscosity at the sub-grid interfaces is known. The recursion (4.70) can then be solved for the velocity in the remaining sub-grid layers.

The finite difference form of the sediment boundary layer equation (4.22) is

$$\left( \left( \frac{K_v}{\delta_s H} \right)^k - (1 - \lambda) w_s^k \right) S^k - \left( \left( \frac{K_v}{\delta_s H} \right)^k + \lambda w_s^k \right) S^{k+1} = J_{sb} \quad (4.76)$$

where  $\lambda$  equals 1 for upwind settling and 0.5 for central difference settling. The constraint equation is

$$\sum_{k=1}^{k_s} S^k = k_s S_1 \quad (4.77)$$

For noncohesive sediment transport, the sub-grid near bottom sediment concentration  $S^l$  is specified as a function of the bed stress and the bed composition. The sediment flux and primary bottom grid layer concentration,  $S_1$ , must then be determined. This is accomplished by introducing a dimensionless sediment variable

$$\psi^k = \frac{w_s^1 S^k}{J_{sb}} \quad (4.78)$$

Into (4.76) to give

$$\beta^k \psi^{k+1} - \gamma^k \psi^k = -1 \quad (4.79)$$

where

$$\beta^k = \left( \frac{K_v}{w_s^1 \delta_s H} \right)^k + \lambda \frac{w_s^k}{w_s^1} \quad (4.80)$$

$$\gamma^k = \left( \frac{K_v}{w_s^1 \delta_s H} \right)^k - (1 - \lambda) \frac{w_s^k}{w_s^1}$$

Since  $S^l$  is known, the first equation becomes

$$\beta^1 \psi^2 = \gamma^1 \psi^1 - 1 \quad (4.81)$$

and (4.78) now represents a closed system of  $k_s-1$  equations. The of solution of (4.79) can be written as

$$\psi^k = \tilde{\psi}^k + \hat{\psi}^k \quad (4.82)$$

which is the sum of the solutions of the two simpler linear systems

$$\beta^k \tilde{\psi}^{k+1} = \gamma^k \tilde{\psi}^k \quad (4.83)$$

$$\begin{aligned} \beta^1 \hat{\psi}^2 &= -1 \\ \beta^k \hat{\psi}^{k+1} &= \gamma^k \hat{\psi}^k - 1 \quad : \quad k \geq 2 \end{aligned} \quad (4.84)$$

The solution of (4.83) can be written as

$$\tilde{\psi}^{k+1} = \left( \prod_{k=1}^k \frac{\gamma^k}{\beta^k} \right) \psi^1 = \sigma^{k+1} \psi^1 \quad (4.85)$$

while (4.80) is solved numerically. The dimensionless form of the constraint (4.77) is

$$\psi_1 = \frac{1}{k_s} \sum_1^{k_s} \psi^k \quad (4.86)$$

and can be written as

$$\psi_1 = \mu \psi^1 - \nu \quad (4.87)$$

where

$$\begin{aligned} \mu &= \frac{1}{k_s} \sum_{k=1}^{k_s} \sigma^k \\ \sigma^k &= \begin{cases} 1 : k = 1 \\ \frac{\gamma^{k-1}}{\beta^{k-1}} \sigma^{k-1} : k \geq 2 \end{cases} \end{aligned} \quad (4.88)$$

$$\nu = -\frac{1}{k_s} \sum_{k=1}^{k_s} \hat{\psi}^k \quad (4.89)$$

Reverting to the original variables gives the bed flux

$$J_{sb} = \frac{w_s^1}{V} (\mu S^1 - S_1) \quad (4.90)$$

where  $\mu S^1$  can be interpreted as the equilibrium sediment concentration for the bottom layer of the primary vertical grid. The flux relationship (4.90) is used to determine the sediment concentration,  $S_1$  in the bottom grid layer, using

$$S_1 = S_1^{old} + \frac{\theta}{\Delta_1 H} J_{sb} \quad (4.91)$$

where  $\theta$  is the time step for integration of the primary grid equations. The flux is then evaluated and used to determine the vertical sediment concentration distribution in the sub-grid layers using

$$S^k = \sigma^k S^1 + \hat{\psi}^k \frac{J_{sb}}{w_s^1} \quad : \quad k \geq 2 \quad (4.92)$$

which follows from (4.76), (4.82), and (4.85). The sediment concentration is used to determine the buoyancy distribution in the sub-grid layers.

For cohesive sediment resuspension, the bed flux is known as a function of the bed stress and geomechanical bed properties. The sediment concentration in the bottom grid layer,  $S_1$ , can be determined using (4.91). The  $k_s$ -1 equations (4.76) supplemented by (4.77) then form a tri-diagonal system linear system, with a zero lower diagonal, supplemented by a full last row. The system is readily solved using the Sherman-Morrison formula (Press *et al.*, 1992) for the vertical distribution of sediment in the boundary layer sub-grid. For cohesive sediment deposition, the bed flux can be represented by

$$J_{Sbd} = -P_d w_s^1 S^1 \quad (4.93)$$

where  $P_d$  is the probability of deposition which depends on the bed stress and a critical depositional stress. Inserting (4.93) into (4.76) gives a system of  $k_s$ -1 equations which must be supplement the equation formed by introducing (4.93) and (4.91) into (4.74) or

$$\sum_{k=1}^{k_s} S^k + k_s \frac{\theta}{H \Delta_b} P_d w_s^1 S^1 = k_s S_1^{old} \quad (4.94)$$

The resulting system of linear equations is of tri-diagonal form, with a zero a zero lower diagonal, supplemented by a full first column and a full last row. The system is readily solved using the Sherman-Morrison formula (Press *et al.*, 1992) for the vertical distribution of sediment in the boundary layer sub-grid.

#### 4.4 Neutral Wave, Current, and Sediment Boundary Layers

Analytical solutions of the wave, current and sediment boundary layer equations (4.11, 4.16, and 4.22), as exemplified most recently by Styles and Glenn (2000), typically assume tractable forms of the vertical turbulent viscosity and diffusivity inside the wave-current and the current boundary layers. Closed form solutions, using special mathematical functions, are possible for the neutral case where the sediment concentrations are low enough to assume that the buoyancy is zero. An alternate approach is to extend the numerical sub-grid approach of the previous section to include a numerical solution for the wave boundary layer with the resulting formulation being applicable to both neutral and sediment stratified conditions. The sub-grid formulation for the wave boundary layer, which is applicable to both neutral and sediment stratified conditions will be presented in the following section, while this section presents a semi-analytical solution appropriate for neutral conditions.

For both the semi-analytical and sub-grid solution of the wave, current and sediment boundary layers, the turbulent viscosity and diffusion coefficients are assumed to be time invariant with (2.18) and (2.19) written in terms of the root mean square turbulent intensity

$$A_v = \phi_A A_o \sqrt{\langle q^2 \rangle} l \quad (4.95)$$

$$K_v = \phi_K K_o \sqrt{\langle q^2 \rangle} l \quad (4.96)$$

Equations (4.26) and (4.36) used to determine the mean square turbulent intensity

$$\langle q^2 \rangle = \left( \frac{B_1 A_o \phi_A}{1 + B_1 K_o \phi_K R_q} \right) \left( \frac{l^2}{H^2} \right) \left( \begin{array}{l} (\partial_z u_c)^2 + \frac{1}{2} (\partial_z u_{wm})^2 \\ + \frac{4}{\pi} \cos(\psi_c - \psi_{wm}) \partial_z u_c \partial_z u_{wm} \end{array} \right) \quad (4.97)$$

Converting the shears in (4.97) to stresses using (4.95) gives

$$\langle q^2 \rangle^2 = \left( \frac{B_1}{\phi_A A_o + B_1 \phi_A A_o \phi_K K_o R_q} \right) \left( \begin{array}{l} \left( \frac{A_v}{H} \partial_z u_c \right)^2 + \frac{1}{2} \left( \frac{A_v}{H} \partial_z u_{wm} \right)^2 \\ + \frac{4}{\pi} \cos(\psi_c - \psi_{wm}) \left( \frac{A_v}{H} \partial_z u_c \right) \left( \frac{A_v}{H} \partial_z u_{wm} \right) \end{array} \right) \quad (4.98)$$

which for neutral conditions reduces to

$$\langle q^2 \rangle^2 = B_1^{4/3} \left( \begin{aligned} & \left( \frac{A_v}{H} \partial_z u_c \right)^2 + \frac{1}{2} \left( \frac{A_v}{H} \partial_z u_{wm} \right)^2 \\ & + \frac{4}{\pi} \cos(\psi_c - \psi_{wm}) \left( \frac{A_v}{H} \partial_z u_c \right) \left( \frac{A_v}{H} \partial_z u_{wm} \right) \end{aligned} \right) \quad (4.99)$$

The neutral version of the Styles and Glenn (2000) wave current boundary layer formulation defines two regions for the turbulent intensity

$$\begin{aligned} \sqrt{\langle q^2 \rangle} = q_{wc} = B_1^{1/3} \left( \tau_{cb}^2 + \frac{1}{2} \tau_{wbm}^2 + \frac{4}{\pi} \cos(\psi_c - \psi_{wm}) \tau_{cb} \tau_{wbm} \right)^{1/4} & : 0 \leq z < \frac{q_{wc}}{q_w} \delta_{wc} \\ \sqrt{\langle q^2 \rangle} = q_c = B_1^{1/3} (\tau_{cb}^2)^{1/4} & : z \geq \frac{q_{wc}}{q_w} \delta_{wc} \end{aligned} \quad (4.100)$$

and three regions for the length scale

$$\begin{aligned} l = \kappa z H & : z_o \leq z < \delta_{wc} \\ l = \kappa \delta_w H & : \delta_{wc} \leq z < \frac{q_{wc}}{q_c} \delta_{wc} \\ l = \kappa z H & : z \geq \frac{q_{wc}}{q_c} \delta_{wc} \end{aligned} \quad (4.101)$$

where  $\delta_{wc}$  is a characteristic thickness of the wave-current boundary layer relative to the water column depth. The resulting turbulent viscosity distribution is

$$\begin{aligned} \frac{A_v^n}{H} = A_o q_{wc} \kappa z & : z_o \leq z < \delta_{wc} \\ \frac{A_v^n}{H} = A_o q_{wc} \kappa \delta_{wc} & : \delta_{wc} \leq z < \frac{q_{wc}}{q_c} \delta_{wc} \\ \frac{A_v^n}{H} = A_o q_c \kappa z & : z \geq \frac{q_{wc}}{q_c} \delta_{wc} \end{aligned} \quad (4.102)$$

with corresponding distributions for the vertical turbulent diffusivity.

Rather than solving the wave boundary layer velocity distribution using special mathematical functions and then approximating these functions by series expansions, the solution proceeds by introducing an approximate velocity distribution in the lower region

$$u = \text{Re} \left\{ U_{w1} \ln \left( \frac{z}{z_o} \right) \exp(i\omega t) + U_{w2} \left( \frac{z - z_o}{z_o} \right) \exp(i\omega t) \right\} : z_o \leq z \leq \delta_{wc} \quad (4.103)$$

and an exact distribution in the constant viscosity central region

$$u_w = u_{w\infty} + \text{Re} \left\{ U_{w3} \exp \left( -\beta \left( \frac{z - \delta_{wc}}{\delta_{wc}} \right) \right) \exp(i\omega t) \right\} : \delta_{wc} \leq z \quad (4.104)$$

where  $U_{w1}$ ,  $U_{w2}$ , and  $U_{w3}$  are complex constants and

$$\beta^2 = i \frac{\omega H \delta_{wc}}{A_o q_{wc} \kappa} \quad (4.105)$$

Since  $\beta$  is of order unity, the wave boundary layer scale is on the order of

$$\begin{aligned} \delta_{wc} &= O \left( \frac{A_o q_{wc} \kappa}{\omega H} \right) \\ \delta_{wc}^2 &= O \left( \frac{A_v}{\omega H^2} \right) \end{aligned} \quad (4.106)$$

The solution the lower region is obtained by a Galerkin procedure. Substitution of (4.103) into (4.11) gives a residual error:

$$E = i\omega \left( U_{w1} \ln \left( \frac{z}{z_o} \right) + U_{w2} \left( \frac{z - z_o}{z_o} \right) \right) - \partial_z \left( \frac{A_v}{H^2} \left( \frac{U_{w1}}{z} + \frac{U_{w2}}{z_o} \right) \right) - i\omega U_{w\infty} \quad (4.107)$$

The Galerkin weighted residual errors are then set to zero

$$\begin{aligned} \int_{z_o}^{\delta_{wc}} \ln \left( \frac{z}{z_o} \right) E dz &= 0 \\ \int_{z_o}^{\delta_{wc}} \left( \frac{z - z_o}{z_o} \right) E dz &= 0 \end{aligned} \quad (4.108)$$

Expanding (4.107) and integrating the vertical stress gradient by parts gives

$$\begin{aligned} \int_{z_o}^{\delta_{wc}} \left( i\omega \ln^2 \left( \frac{z}{z_o} \right) + \frac{A_v}{H^2} \frac{1}{z^2} \right) dz U_{w1} + \int_{z_o}^{\delta_{wc}} \left( i\omega \ln \left( \frac{z}{z_o} \right) \left( \frac{z - z_o}{z_o} \right) + \frac{A_v}{H^2} \frac{1}{z_o z} \right) dz U_{w2} \\ = i\omega \int_{z_o}^{\delta_{wc}} \ln \left( \frac{z}{z_o} \right) dz U_{w\infty} + \ln \left( \frac{\delta_{wc}}{z_o} \right) \left( \frac{A_v}{H^2} \partial_z U \right)_{z=\delta_{wc}} \end{aligned} \quad (4.109)$$

$$\begin{aligned}
 & \int_{z_o}^{\delta_{wc}} \left( i\omega \left( \frac{z-z_o}{z_o} \right) \ln \left( \frac{z}{z_o} \right) + \frac{A_v}{H^2} \frac{1}{z_o z} \right) dz U_{w1} + \int_{z_o}^{\delta_{wc}} \left( i\omega \left( \frac{z-z_o}{z_o} \right)^2 + \frac{A_v}{H^2} \frac{1}{z_o^2} \right) dz U_{w2} \\
 & = \int_{z_o}^{\delta_{wc}} i\omega \left( \frac{z-z_o}{z_o} \right) dz U_{w\infty} + \left( \frac{\delta_{wc}-z_o}{z_o} \right) \left( \frac{A_v}{H^2} \partial_z U_w \right)_{\delta_{wc}}
 \end{aligned} \tag{4.110}$$

Or

$$\begin{aligned}
 a_{11}U_{w1} + a_{12}U_{w2} &= b_1 \\
 a_{21}U_{w1} + a_{22}U_{w2} &= b_2
 \end{aligned} \tag{4.111}$$

Where

$$\begin{aligned}
 a_{11} &= \int_{z_o}^{\delta_{wc}} \left( \ln^2 \left( \frac{z}{z_o} \right) - i \left( \frac{A_o q_{wc} \kappa}{\omega H} \right) \frac{1}{z} \right) dz \\
 a_{12} = a_{21} &= \int_{z_o}^{\delta_{wc}} \left( \ln \left( \frac{z}{z_o} \right) \left( \frac{z-z_o}{z_o} \right) - i \left( \frac{A_o q_{wc} \kappa}{\omega H} \right) \frac{1}{z_o} \right) dz \\
 a_{22} &= \int_{z_o}^{\delta_{wc}} \left( \left( \frac{z-z_o}{z_o} \right)^2 - i \left( \frac{A_o q_{wc} \kappa}{\omega H} \right) \frac{z}{z_o^2} \right) dz \\
 b_1 &= \int_{z_o}^{\delta_{wc}} \ln \left( \frac{z}{z_o} \right) dz U_{w\infty} - i \ln \left( \frac{\delta_{wc}}{z_o} \right) \frac{T_{wi}}{\omega H} \\
 b_2 &= \int_{z_o}^{\delta_{wc}} \left( \frac{z-z_o}{z_o} \right) dz U_{w\infty} - i \left( \frac{\delta_{wc}-z_o}{z_o} \right) \frac{T_{wi}}{\omega H} \\
 T_{wi} &= \left( \frac{A_v}{H} \partial_z U \right)_{z=\delta_{wc}}
 \end{aligned} \tag{4.112}$$

The solution is

$$\begin{Bmatrix} U_{w1} \\ U_{w2} \end{Bmatrix} = \begin{bmatrix} a_{11} & a_{12} \\ a_{21} & a_{22} \end{bmatrix}^{-1} \begin{Bmatrix} \int_{z_o}^{\delta_{wc}} \ln \left( \frac{z}{z_o} \right) dz \\ \int_{z_o}^{\delta_{wc}} \left( \frac{z-z_o}{z_o} \right) dz \end{Bmatrix} U_{w\infty} + \begin{bmatrix} a_{11} & a_{12} \\ a_{21} & a_{22} \end{bmatrix}^{-1} \begin{Bmatrix} -i \ln \left( \frac{\delta_{wc}}{z_o} \right) \\ -i \left( \frac{\delta_{wc}-z_o}{z_o} \right) \end{Bmatrix} \frac{T_{wi}}{\omega H} \tag{4.113}$$

Or in symbolic form

$$\begin{aligned}
 U_{w1} &= A_{11}U_{w\infty} + A_{12}\left(\frac{T_{wi}}{\omega h}\right) \\
 U_{w2} &= A_{21}U_{w\infty} + A_{22}\left(\frac{T_{wi}}{\omega h}\right)
 \end{aligned}
 \tag{4.114}$$

where the complex stress amplitude  $T_{wi}$  at the interface between the lower and central regions remains to be determined as does the constant,  $U_{w3}$ , in the central region solution. The two constants,  $T_{wi}$  and  $U_{w3}$ , must be determined such that the velocity and its vertical gradient are continuous at the interface between the two boundary layer regions by the solution of

$$\begin{aligned}
 &\left(A_{12}\ln\left(\frac{\delta_{wc}}{z_o}\right) + A_{22}\left(\frac{\delta_{wc} - z_o}{z_o}\right)\right)\left(\frac{T_{wi}}{\omega h}\right) - U_{w3} \\
 &= U_{w\infty} - (A_{11}U_{w\infty})\ln\left(\frac{\delta_{wc}}{z_o}\right) - (A_{21}U_{w\infty})\left(\frac{\delta_{wc} - z_o}{z_o}\right) \\
 &\left(\frac{A_{12}}{\delta_{wc}} + \frac{A_{22}}{z_o}\right)\left(\frac{T_{wi}}{\omega h}\right) + \frac{\beta}{\delta_{wc}}U_{w3} = -\left(\frac{A_{11}}{\delta_{wc}} + \frac{A_{21}}{z_o}\right)U_{w\infty}
 \end{aligned}
 \tag{4.115}$$

The solution provides the interface stress in terms of the inviscid wave velocity amplitude and in turn allows  $U_{w1}$  and  $U_{w2}$  to be expressed in terms of the inviscid wave velocity amplitude. The maximum wave bed stress can then be determined by

$$\tau_{wbm} = A_o q_{wc} \kappa |U_{w1} + U_{w2}|
 \tag{4.116}$$

Note that in the absence of currents

$$q_{wc} = \frac{B_1^{1/3}}{2^{1/4}} \tau_{wbm}^{1/2}
 \tag{4.117}$$

with (4.116) becoming

$$\begin{aligned}
 \tau_{wbm} &= \frac{\kappa^2}{\sqrt{2}} |U_{w1} + U_{w2}|^2 = c_{bw} |U_{w\infty}|^2 \\
 c_{bw} &= \frac{\kappa^2}{\sqrt{2}} \frac{|U_{w1} + U_{w2}|^2}{|U_{w\infty}|^2}
 \end{aligned}
 \tag{4.118}$$

The solution for the current velocity is

$$u_c = \frac{\tau_{cb}}{A_o q_{wc} \mathcal{K}} \ln \left( \frac{z}{z_o} \right) \quad (4.119)$$

in the lower region,

$$u_c = \frac{\tau_{cb}}{A_o q_{wc} \mathcal{K}} \left( \frac{z}{\delta_{wc}} + \ln \left( \frac{\delta_{wc}}{z_o} \right) - 1 \right) \quad (4.120)$$

in the central region, and

$$u_c = \frac{\tau_{cb}}{A_o q_{wc} \mathcal{K}} \left( \frac{q_{wc}}{q_c} \right) \ln \left( \frac{z}{z_e} \right) \quad (4.121)$$

$$\frac{z_e e}{\delta_{wc}} = \frac{q_{wc}}{q_c} \left( \frac{z_o e}{\delta_{wc}} \right)^{\frac{q_c}{q_{wc}}}$$

in the upper region. To enforce the integral constraint, the current profile is integrated over the three regions to give

$$\frac{\tau_{cb}}{A_o q_{wc} \mathcal{K}} \int_{z_o}^{\delta_{wc}} \ln \left( \frac{z}{z_o} \right) dz = \frac{\tau_{cb}}{A_o q_{wc} \mathcal{K}} \left( \delta_{wc} \ln \left( \frac{\delta_{wc}}{z_o} \right) - (\delta_{wc} - z_o) \right) \quad (4.122)$$

$$\begin{aligned} & \frac{\tau_{cb}}{A_o q_{wc} \mathcal{K}} \int_{\delta_{wc}}^{\delta_{wc} \frac{q_{wc}}{q_c}} \left( \frac{z}{\delta_{wc}} + \ln \left( \frac{\delta_{wc}}{z_o} \right) - 1 \right) dz \\ &= \frac{\tau_{cb}}{A_o q_{wc} \mathcal{K}} \delta_{wc} \left( \frac{1}{2} \left( \frac{q_{wc}}{q_c} \right)^2 - \left( \frac{q_{wc}}{q_c} \right) + \left( \frac{q_{wc}}{q_c} - 1 \right) \ln \left( \frac{\delta_{wc}}{z_o} \right) + \frac{1}{2} \right) \end{aligned} \quad (4.123)$$

$$\begin{aligned} & \frac{\tau_{cb}}{A_o q_{wc} k} \left( \frac{q_{wc}}{q_c} \right) \int_{\delta_{wc} \frac{q_{wc}}{q_c}}^{m\Delta} \ln \left( \frac{z}{z_e} \right) dz \\ &= \frac{\tau_{cb}}{A_o q_{wc} k} \left( \frac{q_{wc}}{q_c} \right) m\Delta \left( \ln \left( \frac{m\Delta}{z_e} \right) - 1 \right) \\ & - \frac{\tau_{cb}}{A_o q_{wc} k} \left( \frac{q_{wc}}{q_c} \right)^2 \delta_{wc} \left( \ln \left( \frac{\delta_{wc} q_{wc}}{z_e q_c} \right) - 1 \right) \end{aligned} \quad (4.124)$$

with the general integral constraint being

$$\begin{aligned}
 & (m\Delta - z_o) \left( \sum_{k=1}^m u_{ck} \right) & (4.125) \\
 & = \frac{\tau_{cb}}{A_o q_{wc} \kappa} \left( \delta_{wc} \ln \left( \frac{\delta_{wc}}{z_o} \right) - (\delta_{wc} - z_o) \right) \\
 & + \frac{\tau_{cb}}{A_o q_{wc} \kappa} \delta_{wc} \left( \frac{1}{2} \left( \frac{q_{wc}}{q_c} \right)^2 - \left( \frac{q_{wc}}{q_c} \right) + \left( \frac{q_{wc}}{q_c} - 1 \right) \ln \left( \frac{\delta_{wc}}{z_o} \right) + \frac{1}{2} \right) \\
 & + \frac{\tau_{cb}}{A_o q_{wc} \kappa} \left( \frac{q_{wc}}{q_c} \right) m\Delta \left( \ln \left( \frac{m\Delta}{z_e} \right) - 1 \right) \\
 & - \frac{\tau_{cb}}{A_o q_{wc} \kappa} \left( \frac{q_{wc}}{q_c} \right)^2 \delta_{wc} \left( \ln \left( \frac{\delta_{wc} q_{wc}}{z_e q_c} \right) - 1 \right)
 \end{aligned}$$

For the thickness of the wave-current layer exceeding the lower hydrodynamic grid layer. When the wave-current boundary remains inside the bottom layer of the hydrodynamic grid, (4.125) reduces to

$$A_o \kappa q_c u_{c1} = \frac{\tau_{cb}}{(\Delta - z_o)} \left\{ \begin{array}{l} \frac{3}{2} \left( \frac{q_{wc}}{q_c} \right) \delta_{wc} - (\delta_{wc} + \Delta) - \frac{q_c}{q_{wc}} \left( \frac{\delta_{wc}}{2} - z_o \right) \\ + \delta_{wc} \ln \left( \frac{\delta_{wc}}{z_o} \right) + \Delta \ln \left( \frac{\Delta}{z_e} \right) - \left( \frac{q_{wc}}{q_c} \right) \delta_{wc} \ln \left( \frac{\delta_{wc} q_{wc}}{z_e q_c} \right) \end{array} \right\} \quad (4.126)$$

Introducing (4.100) into (4.126) gives

$$\begin{aligned}
 \tau_{cb} & = c_{bc} |u_{c1}| u_{c1} & (4.127) \\
 c_{bc} & = \frac{\kappa^2 (\Delta - z_o)^2}{\left( \Delta \left( \ln \left( \frac{\Delta}{z_e} \right) - 1 \right) + \frac{\delta_{wc}}{2} \left( \frac{q_{wc}}{q_c} - \frac{q_c}{q_{wc}} \right) + z_o \right)^2}
 \end{aligned}$$

an expression for the current stress and bottom current friction coefficient.

## 4.5 Stratified Wave, Current, and Sediment Boundary Layers

Currently under development.

## 5. Sediment Bed Mass Conservation, Armoring and Consolidation

The general conservation of mass for bed sediment has the form

$$\partial_t (S^i B)_k = -\delta(k, k_t) J_{SB}^i + \alpha_A \delta(k, k_t) J_{PA}^i - \alpha_A \delta(k, k_t - 1) J_{PA}^i \quad (5.1)$$

where  $S$  is the mass concentration of per total volume of a bed layer  $k$ ,  $B$  is the layer thickness,  $J_{SB}$  is the net sediment mass flux, mass per unit area and unit time, positive from the bed to the water column,  $\alpha_A$  is an armoring parameter (1 for armoring, 0 otherwise), and  $J_{PA}$  is the parent to armoring layer flux when the top or surface layer of the bed,  $k_t$ , acts to simulate armoring. The superscript  $i$  denotes the  $i$ th sediment size-type class. The sediment concentration can also be defined by

$$S^i = \frac{F^i \rho_s^i}{1 + \varepsilon} \quad (5.2)$$

where  $F$  is the sediment volume fraction,  $\rho_s$  is the sediment particle density, and  $\varepsilon$  is the void ratio. The sediment volume fraction is defined by

$$F_k^i = \left( \sum_i \left( \frac{S^i B}{\rho_s^i} \right)_k \right)^{-1} \left( \frac{S^i B}{\rho_s^i} \right)_k \quad (5.3)$$

Assuming that the sediment particles are incompressible (5.1) can be alternately expressed by

$$\partial_t \left( \frac{F^i B}{1 + \varepsilon} \right)_k = -\delta(k, k_t) \frac{J_{SB}^i}{\rho_s^i} + \alpha_A \delta(k, k_t) \frac{J_{PA}^i}{\rho_s^i} - \alpha_A \delta(k, k_t - 1) \frac{J_{PA}^i}{\rho_s^i} \quad (5.4)$$

Summing (5.4) over the sediment size classes gives

$$\partial_t \left( \frac{B}{1 + \varepsilon} \right)_k = -\delta(k, k_t) \sum_i \frac{J_{SB}^i}{\rho_s^i} + \alpha_A \delta(k, k_t) \sum_i \frac{J_{PA}^i}{\rho_s^i} - \alpha_A \delta(k, k_t - 1) \sum_i \frac{J_{PA}^i}{\rho_s^i} \quad (5.5)$$

The conservation of water volume in a bed layer is given by

$$\begin{aligned}
 \partial_t \left( \frac{\varepsilon B}{1 + \varepsilon} \right)_k &= q_{w:k-} - q_{w:k+} \\
 -\delta(k, k_t) &\left( \sum_i \left( \varepsilon_{kt}^i \max \left( \frac{J_{SB}^i}{\rho_s^i}, 0 \right) \right) + \sum_i \left( \varepsilon_{dep}^i \min \left( \frac{J_{SB}^i}{\rho_s^i}, 0 \right) \right) \right) \\
 +\alpha_A &\left( \frac{\delta(k, k_t)}{-\delta(k, k_t - 1)} \right) \left( \sum_i \left( \varepsilon_{kt-1}^i \max \left( \frac{J_{PA}^i}{\rho_s^i}, 0 \right) \right) + \sum_i \left( \varepsilon_{kt}^i \min \left( \frac{J_{PA}^i}{\rho_s^i}, 0 \right) \right) \right)
 \end{aligned} \tag{5.6}$$

Where  $\varepsilon$  without the  $i$  superscript is the bulk void ratio of the bed layer, and  $\varepsilon$ 's with superscripts  $i$  denote sediment class void ratios required by the mixed material consolidation formulation to be subsequently discussed. Equations (5.5) and (5.6) combine to give

$$\begin{aligned}
 \partial_t B_k &= q_{w:k-} - q_{w:k+} \\
 -\delta(k, k_t) &\left( \sum_i \left( (1 + \varepsilon_{kt}^i) \max \left( \frac{J_{SB}^i}{\rho_s^i}, 0 \right) \right) + \sum_i \left( (1 + \varepsilon_{dep}^i) \min \left( \frac{J_{SB}^i}{\rho_s^i}, 0 \right) \right) \right) \\
 +\alpha_A \delta(k, k_t) &\left( \sum_i \left( (1 + \varepsilon_{kt-1}^i) \max \left( \frac{J_{PA}^i}{\rho_s^i}, 0 \right) \right) + \sum_i \left( (1 + \varepsilon_{kt}^i) \min \left( \frac{J_{PA}^i}{\rho_s^i}, 0 \right) \right) \right) \\
 -\alpha_A \delta(k, k_t - 1) &\left( \sum_i \left( (1 + \varepsilon_{kt-1}^i) \max \left( \frac{J_{PA}^i}{\rho_s^i}, 0 \right) \right) + \sum_i \left( (1 + \varepsilon_{kt}^i) \min \left( \frac{J_{PA}^i}{\rho_s^i}, 0 \right) \right) \right)
 \end{aligned} \tag{5.7}$$

The solution procedure for the bed uses a fractional step approach. The first step involves deposition and resuspension while the second step involves pore water flow and consolidation.

## 5.1 Deposition, Resuspension, and Armoring

The discrete deposition and resuspension step for the sediment class  $i$  mass conservation equation (5.1) is

$$(S^i B)_k^* = (S^i B)_k^n - \theta \delta(k, k_t) J_{SB}^i + \theta \alpha_A \delta(k, k_t) J_{PA}^i - \theta \alpha_A \delta(k, k_t - 1) J_{PA}^i \tag{5.8}$$

Or

$$\left( \frac{F^i B}{1 + \varepsilon} \right)_k^* = \left( \frac{F^i B}{1 + \varepsilon} \right)_k^n = -\theta \delta(k, k_t) \frac{J_{SB}^i}{\rho_s^i} + \theta \alpha_A \delta(k, k_t) \frac{J_{PA}^i}{\rho_s^i} - \theta \alpha_A \delta(k, k_t - 1) \frac{J_{PA}^i}{\rho_s^i} \tag{5.9}$$

The corresponding discrete forms of (5.5), (5.6) and (5.7) are

$$\begin{aligned} \left(\frac{B}{1+\varepsilon}\right)_k^* &= \left(\frac{B}{1+\varepsilon}\right)_k^n = -\theta\delta(k, k_t) \sum_i \frac{J_{SB}^i}{\rho_s^i} + \theta\alpha_A \delta(k, k_t) \sum_i \frac{J_{PA}^i}{\rho_s^i} \\ &\quad - \theta\alpha_A \delta(k, k_t - 1) \sum_i \frac{J_{PA}^i}{\rho_s^i} \end{aligned} \quad (5.10)$$

$$\begin{aligned} \left(\frac{\varepsilon B}{1+\varepsilon}\right)_k^* &= \left(\frac{\varepsilon B}{1+\varepsilon}\right)_k^n - \theta\delta(k, k_t) \sum_i \left( \varepsilon_{kt}^i \max\left(\frac{J_{SB}^i}{\rho_s^i}, 0\right) + \varepsilon_{dep}^i \min\left(\frac{J_{SB}^i}{\rho_s^i}, 0\right) \right) \\ &\quad + \theta\alpha_A (\delta(k, k_t) - \delta(k, k_t - 1)) \sum_i \left( \varepsilon_{kt-1}^i \max\left(\frac{J_{PA}^i}{\rho_s^i}, 0\right) + \varepsilon_{kt}^i \min\left(\frac{J_{PA}^i}{\rho_s^i}, 0\right) \right) \end{aligned} \quad (5.11)$$

$$\begin{aligned} B_k^* &= B_k^n \\ &\quad - \theta\delta(k, k_t) \sum_i \left( (1 + \varepsilon_{kt}^i) \max\left(\frac{J_{SB}^i}{\rho_s^i}, 0\right) + (1 + \varepsilon_{dep}^i) \min\left(\frac{J_{SB}^i}{\rho_s^i}, 0\right) \right) \\ &\quad + \theta\alpha_A \delta(k, k_t) \sum_i \left( (1 + \varepsilon_{kt-1}^i) \max\left(\frac{J_{PA}^i}{\rho_s^i}, 0\right) + (1 + \varepsilon_{kt}^i) \min\left(\frac{J_{PA}^i}{\rho_s^i}, 0\right) \right) \\ &\quad - \theta\alpha_A \delta(k, k_t - 1) \sum_i \left( (1 + \varepsilon_{kt-1}^i) \max\left(\frac{J_{PA}^i}{\rho_s^i}, 0\right) + (1 + \varepsilon_{kt}^i) \min\left(\frac{J_{PA}^i}{\rho_s^i}, 0\right) \right) \end{aligned} \quad (5.12)$$

When the armoring option is inactive, the deposition and resuspension step operates only on the top layer of the bed with (5.8) solved for the new top layer sediment mass per unit area

$$(S^i B)_{kt}^* = (S^i B)_{kt}^n - \theta J_{SB}^i \quad (5.13)$$

using a known sediment depositional or resuspension flux. If the flux in (5.13) is positive, representing resuspension, it is limited over the time step by

$$J_{SB}^i = \min\left(J_{SBR}^i, \theta^{-1} (S^i B)_{kt}^n\right) \quad (5.14)$$

where the subscript *SBR* represents the predicted resuspension flux. Following the solution of (5.13) for each sediment class, equations (5.12) is solved for the new top layer thickness and (5.10) is solved for the new top layer void ratio.

When the noncohesive sediment armoring option is active, equation (5.8) is applied to the top two layers of the bed

$$(S^i B)_{kt}^* = (S^i B)_{kt}^n - \theta J_{SB}^i + \theta J_{PA}^i \quad (5.15a)$$

$$(S^i B)_{kt-1}^* = (S^i B)_{kt-1}^n - \theta J_{PA}^i \quad (5.15b)$$

with the flux limiter (5.14) being applied to (5.15a) for resuspension flux from the top layer. Two options exist for determining the parent to active layer flux. One option is to require that the total mass of sediment in the surface, active layer remains constant during the deposition-resuspension step. The total parent to active layer flux is then given by (5.10) as

$$\sum_i \frac{J_{PA}^i}{\rho_s^i} = \sum_i \frac{J_{SB}^i}{\rho_s^i} \quad (5.16)$$

The class fluxes can then be assigned by

$$\frac{J_{PA}^i}{\rho_s^i} = F_{kt-1}^i \max\left(\sum_i \frac{J_{SB}^i}{\rho_s^i}, 0\right) + F_{kt}^i \min\left(\sum_i \frac{J_{SB}^i}{\rho_s^i}, 0\right) \quad (5.17)$$

allowing (5.15) to be updated. Equation (5.10) and (5.12) are then solved for the new thicknesses and void ratios of the parent and active layer. Another option is to require that the thickness of the active layer to be time invariant during the deposition and resuspension step. Equation (5.12) reduces to

$$\begin{aligned} & \sum_i \left( (1 + \varepsilon_{kt-1}^i) \max\left(\frac{J_{PA}^i}{\rho_s^i}, 0\right) \right) + \sum_i \left( (1 + \varepsilon_{kt}^i) \min\left(\frac{J_{PA}^i}{\rho_s^i}, 0\right) \right) \\ & = \sum_i \left( (1 + \varepsilon_{kt}^i) \max\left(\frac{J_{SB}^i}{\rho_s^i}, 0\right) + (1 + \varepsilon_{dep}^i) \min\left(\frac{J_{SB}^i}{\rho_s^i}, 0\right) \right) \end{aligned} \quad (5.18)$$

The sediment class fluxes can be assigned by

$$\begin{aligned} \frac{J_{PA}^i}{\rho_s^i} &= \frac{F_{kt-1}^i}{(1 + \varepsilon_{kt-1}^i)} \max(Q_{SW}, 0) + \frac{F_{kt}^i}{(1 + \varepsilon_{kt}^i)} \min(Q_{SW}, 0) \\ Q_{SW} &= \sum_i \left( (1 + \varepsilon_{kt}^i) \max\left(\frac{J_{SB}^i}{\rho_s^i}, 0\right) + (1 + \varepsilon_{dep}^i) \min\left(\frac{J_{SB}^i}{\rho_s^i}, 0\right) \right) \end{aligned} \quad (5.19)$$

allowing solution of equations (5.15), (5.10), and (5.12).

## 5.2 Consolidation of Homogeneous Sediment Beds

This section discusses options for representing consolidation of sediment beds containing either cohesive sediment or a mixture of noncohesive sediments defined by multiple size

classes. Mixed cohesive and noncohesive bed consolidation is discussed in the subsequent section. For the second, consolidation half step, the sediment mass per unit area and the sediment volume per unit area remain constant, with (5.1) and (5.5) giving

$$(S^i B)_k^{n+1} = (S^i B)_k^* \quad (5.20)$$

$$\left(\frac{B}{1+\varepsilon}\right)_k^{n+1} = \left(\frac{B}{1+\varepsilon}\right)_k^* \quad (5.21)$$

The second half step for the water volume conservation equation (5.6) is

$$\left(\frac{\varepsilon B}{1+\varepsilon}\right)_k^{n+1} = \left(\frac{\varepsilon B}{1+\varepsilon}\right)_k^* + \theta(q_{w:k-} - q_{w:k+}) \quad (5.22)$$

Equations (5.21) and (5.22) can be combined to give

$$B_k^{n+1} = B_k^* + \theta(q_{w:k-} - q_{w:k+}) \quad (5.23)$$

an equation for the layer thickness, and

$$\varepsilon_k^{n+1} = \varepsilon_k^* + \theta \left(\frac{1+\varepsilon}{B}\right)_k^{n+1} (q_{w:k-} - q_{w:k+}) \quad (5.24)$$

an equation for the void ratio. The EFDC model includes four options for consolidation and pore water flow.

The first option is a constant porosity bed, with (5.24) giving

$$q_{w:k-} = q_{w:k+} = q_{GW} \quad (5.25)$$

which indicates that the pore water specific discharge is equal to a specified groundwater specific discharge at the bottom of the lowest bed layer. The second option is a simple consolidation model based on relaxation of the vertical void ratio profile to a specified profile given by

$$\varepsilon = \varepsilon_m + (\varepsilon_o - \varepsilon_m) \exp(-\alpha_c (t - t_o)) \quad (5.26)$$

where  $\alpha_c$  is a consolidation rate coefficient, and  $\varepsilon_m$  is an ultimate minimum void ratio, which can be dependent on the vertical position in the bed. Evaluating (5.26) at two successive time levels gives

$$\varepsilon^n - \varepsilon_m = (\varepsilon_o - \varepsilon_m) \exp(-\alpha_c (n\theta - t_o)) \quad (5.27)$$

$$\varepsilon^{n+1} - \varepsilon_m = (\varepsilon_o - \varepsilon_m) \exp(-\alpha_c (n\theta + \theta - t_o)) \quad (5.28)$$

Taking their ratio gives

$$\frac{\varepsilon^{n+1} - \varepsilon_m}{\varepsilon^* - \varepsilon_m} = \exp(-\alpha_c \theta) \quad (5.29)$$

or

$$\varepsilon_k^{n+1} = \varepsilon_m + (\varepsilon_k^* - \varepsilon_m) \exp(-\alpha_c \theta) \quad (5.30)$$

Using the new void ratio given by (5.30), the new bed layer thickness is updated by (5.21). The pore water specific discharges are then given by recursively solving (5.23)

$$q_{w:k+} = q_{w:k-} - \theta^{-1} (B_k^{n+1} - B_k^*) \quad (5.31)$$

From  $k = 1, k_t$  using

$$q_{w:1-} = q_{GW} \quad (5.32)$$

The third option for consolidation and pore water flow is based on finite strain consolidation theory. Use of this option requires the bed layers to be composed of either cohesive or noncohesive sediment, such that a single set of constitutive relationships are used over the entire thickness of the bed. The specific discharges in (5.23) or (5.24) are determined using the Darcy equation

$$q = -\frac{K}{g\rho_w} \partial_z u \quad (5.33)$$

where  $K$  is the hydraulic conductivity and  $u$  is the excess pore pressure defined as the difference between the total pore pressure,  $u_t$ , and the hydrostatic pressure,  $u_h$ .

$$u = u_t - u_h \quad (5.34)$$

The total pore pressure is defined as the difference between the total stress  $\sigma$  and effective stress  $\sigma_e$ .

$$u_t = \sigma - \sigma_e \quad (5.35)$$

The total stress and hydrostatic pressure are given by

$$\sigma = p_b + g \int_z^{z_b} \left( \left( \frac{\varepsilon}{1+\varepsilon} \right) \rho_w + \left( \frac{1}{1+\varepsilon} \right) \sum_i (F^i \rho_s^i) \right) dz \quad (5.36)$$

$$u_h = p_b + g \rho_w (z_b - z) \quad (5.37)$$

where  $p_b$  is the water column pressure at the bed surface  $z_b$ . Solving for the excess pore pressure using (5.34) through (5.37) gives

$$u = g \rho_w \int_z^{z_b} \left( \left( \frac{1}{1+\varepsilon} \right) \left( \frac{\bar{\rho}_s}{\rho_w} - 1 \right) \right) dz - \sigma_e \quad (5.38)$$

where

$$\bar{\rho}_s = \sum_i (F^i \rho_s^i) \quad (5.39)$$

is the average sediment density. The specific discharge (5.33), can alternately be expressed in terms of the effective stress

$$q = \frac{K}{g \rho_w} \partial_z \sigma_e + \left( \frac{\bar{\rho}_s}{\rho_w} - 1 \right) \left( \frac{K}{1+\varepsilon} \right) \quad (5.40)$$

or the void ratio

$$q = \frac{K}{g \rho_w} \left( \frac{\partial \sigma_e}{\partial \varepsilon} \right) \partial_z \varepsilon + \left( \frac{\bar{\rho}_s}{\rho_w} - 1 \right) \left( \frac{K}{1+\varepsilon} \right) \quad (5.41)$$

where  $d\varepsilon/d\sigma_e$  is a coefficient of compressibility. For consistency with the Lagrangian representation of sediment mass conservation, a new vertical coordinate  $\zeta$ , defined by

$$\frac{d\zeta}{dz} = \frac{1}{1+\varepsilon} \quad (5.42)$$

is introduced, with (5.40) and (5.41) becoming

$$q_w = \left( \frac{K}{1+\varepsilon} \right) \partial_\zeta \left( \frac{\sigma_e}{g \rho_w} \right) + \left( \frac{\bar{\rho}_s}{\rho_w} - 1 \right) \left( \frac{K}{1+\varepsilon} \right) \quad (5.43)$$

and

$$q_w = -\lambda \left( \frac{K}{1+\varepsilon} \right) \partial_\zeta \varepsilon + \left( \frac{\bar{\rho}_s}{\rho_w} - 1 \right) \left( \frac{K}{1+\varepsilon} \right) \quad (5.44)$$

where  $\lambda$  is a length scale

$$\lambda = -\frac{1}{g\rho_w} \frac{\partial \sigma_e}{\partial \varepsilon} \quad (5.45)$$

The consistency of (5.43) and (5.44) at bed layer interfaces also requires consideration. The finite difference form of (5.33) in the transformed coordinate, defined by (5.42), at an interface between bed layers can be written as

$$q = -\frac{2}{g\rho_w} \left( \frac{K}{1+\varepsilon} \right)_k \left( \frac{u_i - u_k}{\Delta_k} \right) \quad (5.46)$$

below the interface and

$$q = -\frac{2}{g\rho_w} \left( \frac{K}{1+\varepsilon} \right)_{k+1} \left( \frac{u_{k+1} - u_i}{\Delta_{k+1}} \right) \quad (5.47)$$

above the interface, where

$$\Delta_k = (1+\varepsilon_k) B_k \quad (5.48)$$

is the transformed coordinate thickness of the bed layer. Solving (5.47) for the interface excess pore pressure and inserting the results into (5.46) gives

$$q = -\left( \frac{K}{1+\varepsilon} \right)_{k+1/2} \frac{2}{g\rho_w} \frac{(u_{k+1} - u_k)}{(\Delta_{k+1} + \Delta_k)} \quad (5.49)$$

where

$$(\Delta_{k+1} + \Delta_k) \left( \frac{1+\varepsilon}{K} \right)_{k+1/2} = \Delta_{k+1} \left( \frac{1+\varepsilon}{K} \right)_{k+1} + \Delta_k \left( \frac{1+\varepsilon}{K} \right)_k \quad (5.50)$$

defines the hydraulic conductivity at the bed layer interface between layers  $k$  and  $k+1$ . The discrete form of (5.38) in the transformed coordinate is

$$\begin{aligned} \left(\frac{u}{g\rho_w}\right)_{k+1} - \left(\frac{u}{g\rho_w}\right)_k = & -\left(\left(\left(\frac{\bar{\rho}_s}{\rho_w}-1\right)\frac{\Delta}{2}\right)_{k+1} + \left(\left(\frac{\bar{\rho}_s}{\rho_w}-1\right)\frac{\Delta}{2}\right)_k\right) \\ & -\left(\frac{\sigma_e}{g\rho_w}\right)_{k+1} + \left(\frac{\sigma_e}{g\rho_w}\right)_k \end{aligned} \quad (5.51)$$

which after introduction into (5.49) gives

$$\begin{aligned} q = & \left(\frac{K}{1+\varepsilon}\right)_{k+1/2} \frac{2}{(\Delta_{k+1} + \Delta_k)} \left(\left(\frac{\sigma_e}{g\rho_w}\right)_{k+1} - \left(\frac{\sigma_e}{g\rho_w}\right)_k\right) \\ & + \left(\frac{K}{1+\varepsilon}\right)_{k+1/2} \left(\frac{\bar{\rho}_s}{\rho_w} - 1\right)_{k+1/2} \end{aligned} \quad (5.52)$$

where

$$\left(\frac{\bar{\rho}_s}{\rho_w} - 1\right)_{k+1/2} = \frac{1}{(\Delta_{k+1} + \Delta_k)} \left(\Delta_{k+1} \left(\frac{\bar{\rho}_s}{\rho_w} - 1\right)_{k+1} + \Delta_k \left(\frac{\bar{\rho}_s}{\rho_w} - 1\right)_k\right) \quad (5.53)$$

In terms of the void ratio, (5.52) is

$$q = -\left(\frac{K}{1+\varepsilon}\right)_{k+1/2} \frac{2\lambda_{k+1/2}}{(\Delta_{k+1} + \Delta_k)} (\varepsilon_{k+1} - \varepsilon_k) + \left(\frac{K}{1+\varepsilon}\right)_{k+1/2} \left(\frac{\bar{\rho}_s}{\rho_w} - 1\right)_{k+1/2} \quad (5.54)$$

where

$$\lambda_{k+1/2} = -\frac{1}{g\rho_w} \left(\frac{\sigma_{e,k+1} - \sigma_{e,k}}{\varepsilon_{k+1} - \varepsilon_k}\right) \quad (5.55)$$

The effective stress and hydraulic conductivity are functions of the void ratio. For cohesive material

$$\frac{\sigma_e}{\sigma_{eo}} = \exp\left(-\left(\frac{\varepsilon - \varepsilon_o}{\varepsilon_\sigma}\right)\right) \quad (5.56)$$

$$\frac{\partial \sigma_e}{\partial \varepsilon} = -\frac{\sigma_{eo}}{\varepsilon_\sigma} \exp\left(-\left(\frac{\varepsilon - \varepsilon_o}{\varepsilon_\sigma}\right)\right)$$

$$\frac{K}{K_o} = \exp\left(\frac{\varepsilon - \varepsilon_o}{\varepsilon_K}\right) \quad (5.57)$$

are the simplest functional relationships consistent with observational data. Figures 5.1 through 5.4, based on data presented in Cargill (1985) and Palermo *et al.* (1998) confirm these choices. However, they show essentially two regions of behavior, below and above a void ratio of approximately 6. For noncohesive material the linear relationships

$$\frac{\sigma_e}{\sigma_{eo}} = 1 - \left( \frac{\varepsilon - \varepsilon_o}{\varepsilon_\sigma} \right) \quad (5.58)$$

$$\frac{\partial \sigma_e}{\partial \varepsilon} = - \frac{\sigma_{eo}}{\varepsilon_\sigma}$$

$$\frac{K}{K_o} = 1 + \left( \frac{\varepsilon - \varepsilon_o}{\varepsilon_K} \right) \quad (5.59)$$

are appropriate.

Given the unique dependence of the specific discharge on the void ratio, the void ratio form of the consolidation step, (5.24) is selected for the solution, with the thickness of the bed layers then determined by (5.23). The specific discharges at the top and bottom of layer  $k$ , follow from (5.54) and are given by

$$q_{w:k+} = - \left( \frac{2\lambda_{k+}}{\Delta_{k+1} + \Delta_k} \right) \left( \frac{K}{1 + \varepsilon} \right)_{k+} (\varepsilon_{k+1} - \varepsilon_k) + \left( \frac{\bar{\rho}_s}{\rho_w} - 1 \right)_{k+} \left( \frac{K}{1 + \varepsilon} \right)_{k+} \quad (5.60)$$

$$q_{w:k-} = - \left( \frac{2\lambda_{k-}}{\Delta_k + \Delta_{k-1}} \right) \left( \frac{K}{1 + \varepsilon} \right)_{k-} (\varepsilon_k - \varepsilon_{k-1}) + \left( \frac{\bar{\rho}_s}{\rho_w} - 1 \right)_{k-} \left( \frac{K}{1 + \varepsilon} \right)_{k-}$$

For the bottom layer of the bed,

$$q_{w:1-} = q_{gwi} \quad (5.61)$$

where  $q_{gwi}$  is a known specific discharge due to groundwater interaction.

For the top layer of the bed, two alternate formulations are possible. The first formulation assumes that the void ratio at the water column-sediment bed interface is specified by  $\varepsilon_{dep}$ , with (5.60a) modified to

$$q_{w:kt+} = - \left( \frac{2\lambda_{kt+}}{\Delta_{kt}} \right) \left( \frac{K}{1 + \varepsilon} \right)_{kt+} (\varepsilon_{dep} - \varepsilon_k) + \left( \frac{\bar{\rho}_s}{\rho_w} - 1 \right)_{kt+} \left( \frac{K}{1 + \varepsilon} \right)_{kt+} \quad (5.62)$$

The second formulation assumes that the excess pore pressure,  $u$ , at the water column-sediment bed interface is zero with (5.46) giving

$$q_{w:kt+} = \left( \frac{K}{1+\varepsilon} \right)_{Kt} \frac{2}{\Delta_{Kt}} \left( \frac{u}{g\rho_w} \right)_{Kt} \quad (5.63)$$

Using (5.38) the excess pore pressure at the midpoint of the top layer is

$$\frac{u}{g\rho_w} = \left( \frac{\bar{\rho}_s}{\rho_w} - 1 \right) \frac{\Delta}{2} - \frac{\sigma_e}{g\rho_w} \quad (5.64)$$

which combines with (5.63) to give

$$q_{w:kt+} = - \left( \frac{K}{1+\varepsilon} \right)_{Kt} \frac{2}{\Delta_{Kt}} \left( \frac{\sigma_e}{g\rho_w} \right) + \left( \frac{K}{1+\varepsilon} \right)_{Kt} \left( \frac{\bar{\rho}_s}{\rho_w} - 1 \right)_{Kt} \quad (5.65)$$

Equation (5.65) can be expressed in terms of the void ratio at the new time level  $n+1$  by expanding the effective stress at time level  $n+1$  in a Taylor series

$$\sigma_e^{n+1} = \sigma_e^n + (\partial_e \sigma_e)^n (\varepsilon^{n+1} - \varepsilon^*) \quad (5.66)$$

Substituting (5.61) into (5.65) gives

$$q_{w:kt+} = \left( \frac{K}{1+\varepsilon} \right)_{Kt} \frac{2}{\Delta_{Kt}} \lambda^* \varepsilon^{n+1} + \left( \frac{K}{1+\varepsilon} \right)_{Kt} \left( \frac{\bar{\rho}_s}{\rho_w} - 1 \right)_{Kt} - \left( \frac{K}{1+\varepsilon} \right)_{Kt} \frac{2}{\Delta_{Kt}} \left( \frac{\sigma_e^n}{g\rho_w} + \lambda^* \varepsilon^* \right)_{Kt} \quad (5.67)$$

The numerical values of the various parameters in the expressions for the specific discharge indicate that an implicit solution of (5.24) is necessary. This is done in two stages with an intermediate void ratio, denoted by \*\*, determined by substituting the internal specific discharges, written as

$$q_{w:k+} = - \left( \frac{2\lambda_{k+}}{\Delta_{k+1} + \Delta_k} \right)^* \left( \frac{K}{1+\varepsilon} \right)_{k-}^* (\varepsilon_{k+1} - \varepsilon_k)^{**} + \left( \frac{\bar{\rho}_s}{\rho_w} - 1 \right)_{k+} \left( \frac{K}{1+\varepsilon} \right)_{k+}^* \quad (5.68)$$

$$q_{w:k-} = - \left( \frac{2\lambda_{k-}}{\Delta_k + \Delta_{k-1}} \right)^* \left( \frac{K}{1+\varepsilon} \right)_{k-}^* (\varepsilon_k - \varepsilon_{k-1})^{**} + \left( \frac{\bar{\rho}_s}{\rho_w} - 1 \right)_{k-} \left( \frac{K}{1+\varepsilon} \right)_{k-}^*$$

and one of the surface specific discharges corresponding to (5.62)

$$q_{w:kt+} = - \left( \frac{2\lambda}{\Delta} \right)_{kt}^* \left( \frac{K}{1+\varepsilon} \right)_{kt+}^* (\varepsilon_{dep} - \varepsilon_k)^{**} + \left( \frac{\bar{\rho}_s}{\rho_w} - 1 \right)_{kt} \left( \frac{K}{1+\varepsilon} \right)_{kt+}^* \quad (5.69)$$

or (5.67)

$$\begin{aligned}
 q_{w:kt+} = & \left( \frac{K}{1+\varepsilon} \right)_{kt+}^* \left( \frac{2\lambda}{\Delta} \right)_{kt}^* \varepsilon^{**} + \left( \frac{K}{1+\varepsilon} \right)_{kt+}^* \left( \frac{\bar{\rho}_s}{\rho_w} - 1 \right) \\
 & - \left( \frac{K}{1+\varepsilon} \right)_{kt+}^* \left( \frac{2}{\Delta_{kt}} \right) \left( \frac{\sigma_e}{g\rho_w} + \lambda\varepsilon \right)_{kt}^*
 \end{aligned} \tag{5.70}$$

into

$$\varepsilon_k^{**} = \varepsilon_k^* + \frac{\theta}{2} \left( \frac{1+\varepsilon}{B} \right)_k^{**} (q_{w:k-} - q_{w:k+}) \tag{5.71}$$

and solving the resulting tri-diagonal system of equations. The specific discharges are then exactly calculated using (5.68) and (5.69) or (5.70). The new time level thickness of the layers is determined by (5.23) with the void ratios determined from (5.24). The linearized form of this scheme is unconditionally stable.

### 5.3 Consolidation of Mixed Cohesive and Noncohesive Sediment Beds

This section presents a methodology for representing consolidation of sediment beds containing both cohesive and noncohesive sediments. The methodology allows for both cohesive and noncohesive sediment in any bed layer and is based on the following assumptions. First, it is assumed that during the consolidation step, a fraction of the bed pore water volume per unit horizontal area is associated with each sediment type or

$$\left( \frac{\varepsilon B}{1+\varepsilon} \right) = (\psi_{wc} + \psi_{wn}) B \tag{5.72}$$

where the subscripts *wc* and *wn* denote water associated with cohesive and noncohesive sediment, respectively. Likewise the volume of sediment per unit horizontal area can be fractionally partitioned between cohesive and noncohesive

$$\left( \frac{B}{1+\varepsilon} \right) = (\psi_{sc} + \psi_{sn}) B \tag{5.73}$$

Following the Lagrangian formulation of the previous section, the total volume of sediment and the fractional sediment volume in a bed layer remain constant during a consolidation step.

$$\partial_t (B\psi_{sc}) = \partial_t (B\psi_{sn}) = 0 \tag{5.74}$$

Fractional void ratios can also be defined

$$\varepsilon_c = \frac{\psi_{wc}}{\psi_{sc}} \quad (5.75)$$

$$\varepsilon_n = \frac{\psi_{wn}}{\psi_{sn}} \quad (5.76)$$

and using (5.72) and (5.73), the void ratio of the mixture is

$$\varepsilon = \frac{\psi_{sc}\varepsilon_c + \psi_{sn}\varepsilon_n}{\psi_{sc} + \psi_{sn}} \quad (5.77)$$

which is the sediment volume weighted average of the void ratios of the two sediment types.

The second assumption is that during the consolidation time step, the fraction of water associated with noncohesive sediment remains constant, as does the fractional void ratio. This is equivalent to the assuming that the portion of the bed layer associated with noncohesive sediment is incompressible, and that the pore water associated the noncohesive sediment is specified by  $\varepsilon_n$ .

Consistent with the preceding assumptions, the thickness of the bed layer can be divided into cohesive and noncohesive fractions,  $B_c$  and  $B_n$ , respectively.

$$\begin{aligned} B_c &= (\psi_{wc} + \psi_{sc})B = (1 + \varepsilon_c)\psi_{sc}B \\ B_n &= (\psi_{wn} + \psi_{sn})B = (1 + \varepsilon_n)\psi_{sn}B \end{aligned} \quad (5.78)$$

The hydraulic conductivity of the layer can be expressed by

$$K = \frac{(B_c + B_n)}{\left(\frac{B_c}{K_c} + \frac{B_n}{K_n}\right)} \quad (5.79)$$

which is equivalent to an infinite number of alternating infinitesimal cohesive and noncohesive sublayers of proportional thickness comprising the mixed bed layer. Equation (5.79) can be written as

$$\frac{K}{(1 + \varepsilon)} = \frac{1}{\left(f_{sc} \frac{(1 + \varepsilon_c)}{K_c} + f_{sn} \frac{(1 + \varepsilon_n)}{K_n}\right)} \quad (5.80)$$

where

$$f_{sc} = \frac{\psi_{sc}}{(\psi_{sc} + \psi_{sn})} \quad (5.81)$$

$$f_{sn} = \frac{\psi_{sn}}{(\psi_{sc} + \psi_{sn})}$$

are the time invariant total cohesive and noncohesive sediment fractions in the bed layer. Likewise, (5.77) can be write as

$$\varepsilon = f_{sc} \varepsilon_c + f_{sn} \varepsilon_n \quad (5.82)$$

The final assumption for the mixed material consolidation formulation is that changes in effective stress are due entirely to changes in the cohesive void ratio. Under this assumption, the specific discharge given by (5.54) can be written as

$$q = -\left(\frac{K}{1+\varepsilon}\right)_{k+1/2} \frac{2\lambda_{k+1/2}}{(\Delta_{k+1} + \Delta_k)} \left( (f_{sc} \varepsilon_c)_{k+1} - (f_{sc} \varepsilon_c)_k \right) + \left(\frac{K}{1+\varepsilon}\right)_{k+1/2} \left( \frac{\bar{\rho}_s}{\rho_w} - 1 \right)_{k+1/2} \quad (5.83)$$

with (5.55) becoming

$$\lambda_{k+1/2} = -\frac{1}{g\rho_w} \left( \frac{\sigma_{e,k+1} - \sigma_{e,k}}{(f_{sc} \varepsilon_c)_{k+1} - (f_{sc} \varepsilon_c)_k} \right) \quad (5.84)$$

The other layer interface quantities in (5.83) remain defined by (5.50) and (5.53). When the depositional void ratio is specified for the surface layer, (5.62) is modified to

$$q_{w:kt+} = -\left(\frac{2\lambda_{kt+}}{\Delta_{kt+}}\right) \left(\frac{K}{1+\varepsilon}\right)_{kt+} \left( (\varepsilon_c)_{dep} - (\varepsilon_c)_k \right) + \left(\frac{\bar{\rho}_s}{\rho_w} - 1\right)_{kt+} \left(\frac{K}{1+\varepsilon}\right)_{kt+} \quad (5.85)$$

When the zero excess pore pressure boundary condition at the bed surface is used, (5.67) becomes

$$q_{w:kt+} = \left(\frac{K}{1+\varepsilon}\right)_{Kt} \frac{2}{\Delta_{Kt}} \left( \lambda^* f_{sc} \varepsilon_c^{n+1} \right)_{Kt} + \left(\frac{K}{1+\varepsilon}\right)_{Kt} \left( \frac{\bar{\rho}_s}{\rho_w} - 1 \right)_{Kt} - \left(\frac{K}{1+\varepsilon}\right)_{Kt} \frac{2}{\Delta_{Kt}} \left( \frac{\sigma_e^n}{g\rho_w} + \lambda^* f_{sc} \varepsilon_c^* \right)_{Kt} \quad (5.86)$$

Equation (5.71) for updating the void ratio is modified using (5.82) to give

$$(f_{sc}\epsilon_c)^{**}_k = (f_{sc}\epsilon_c)^*_k + \frac{\theta}{2} \left( \frac{1+\epsilon}{B} \right)^{**}_k (q_{w:k-} - q_{w:k+}) \quad (5.87)$$

Thus the mixed bed layer consolidation formulation essentially solves of the space and time evolution of  $f_{sc}\epsilon_c$  with the continuum constitutive relationship for  $\lambda$  given by

$$\lambda = -\frac{1}{f_{sc}} \frac{\partial}{\partial \epsilon} \left( \frac{\sigma}{g\rho_w} \right) \quad (5.88)$$

The formulation has the desirable characteristic of reducing to the well established cohesive formulation in the absence of noncohesive material. The solution for  $f_{sc}\epsilon_c$  proceeds by introducing (5.83) and (5.85) or (5.86) into (5.87) and solving the resulting tri-diagonal system of equations. The new specific discharges are then directly calculated using (5.83) and (5.85) or (5.86) and used to update the layer thickness using (5.23)

$$B_k^{n+1} = B_k^* + \theta (q_{w:k-} - q_{w:k+}) \quad (5.23)$$

Equation (5.21) is then used to solve for the void ratio

$$\left( \frac{B}{1+\epsilon} \right)^{n+1}_k = \left( \frac{B}{1+\epsilon} \right)^*_k \quad (5.21)$$

Followed by the solution of (5.82) for the cohesive void ratio

$$\epsilon_c = \frac{\epsilon - f_{sn}\epsilon_n}{f_{sc}} \quad (5.82)$$

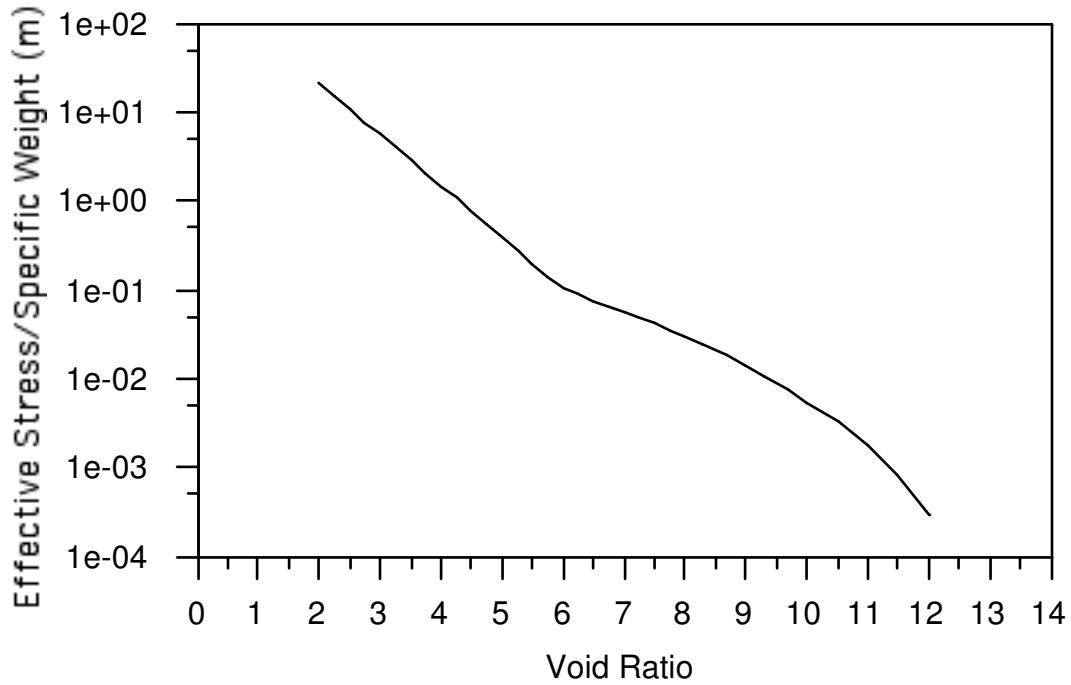


Figure 5.1. Specific Weight Normalized Effective Stress Versus Void Ratio.

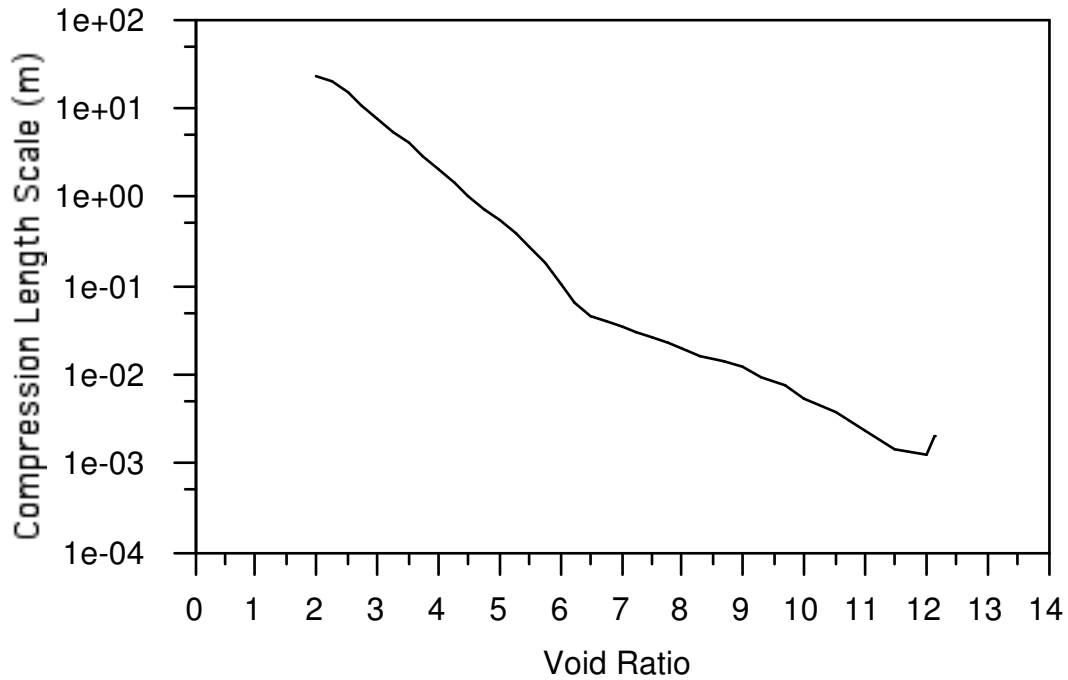


Figure 5.2. Compress Length Scale,  $(g\rho_w)^{-1}(d\sigma_e/d\varepsilon)$ , Versus Void Ratio.

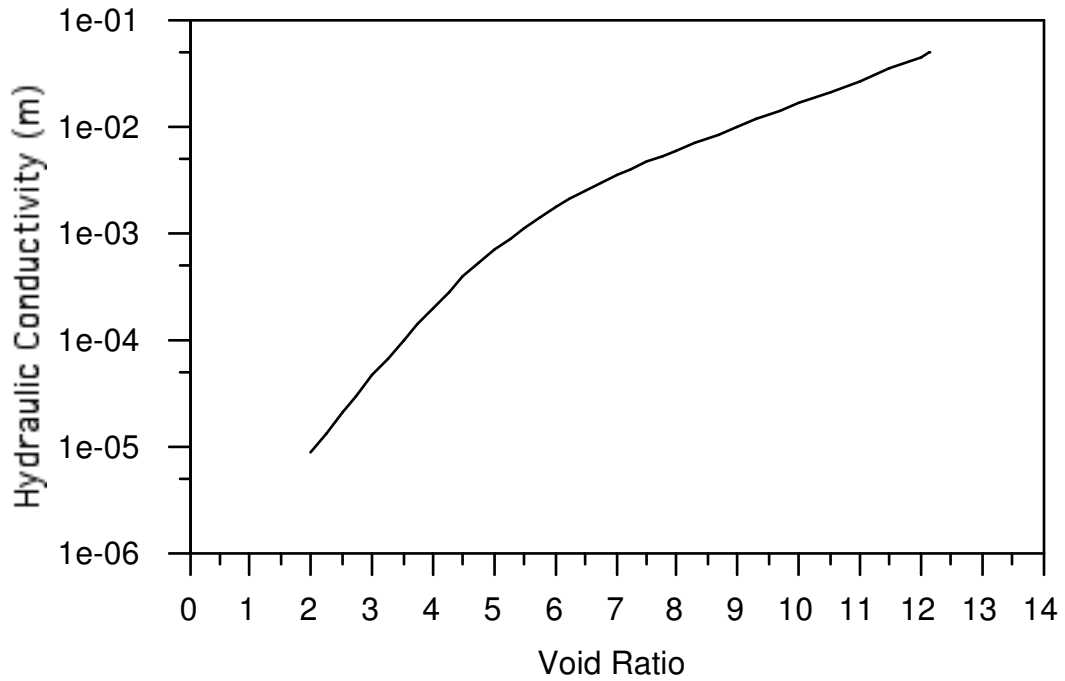


Figure 5.3. Hydraulic Conductivity Versus Void Ratio.

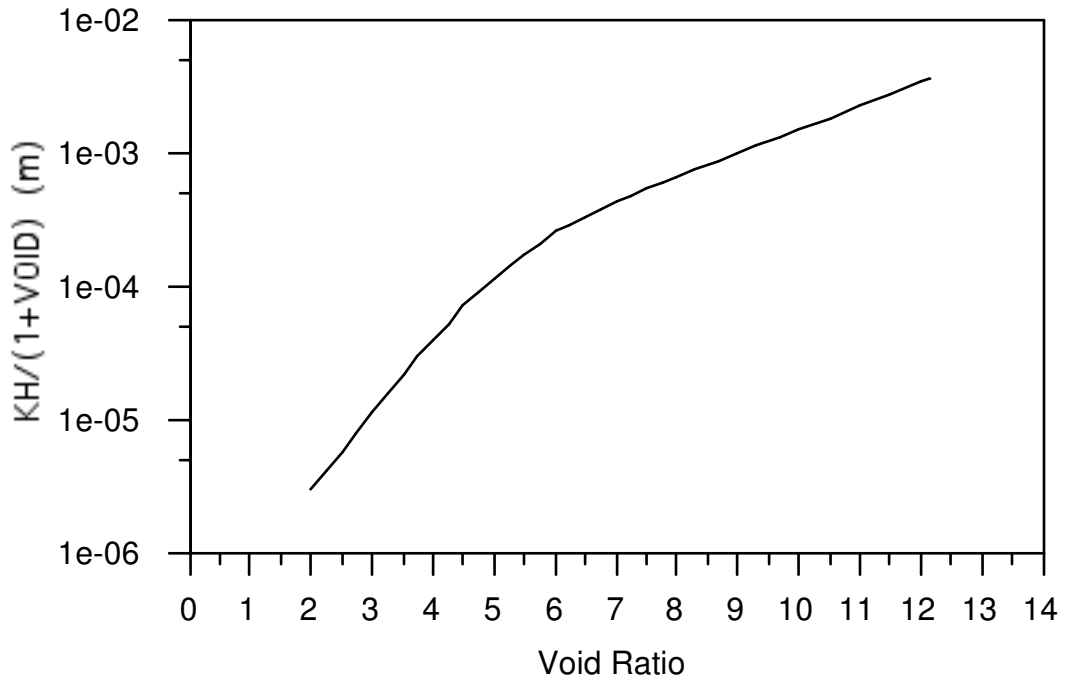


Figure 5.4. Hydraulic Conductivity/(1 + Void Ratio) Versus Void Ratio

## 6. Noncohesive Sediment Settling, Deposition and Resuspension

Noncohesive inorganic sediments settle as discrete particles, with hindered settling and multiphase interactions becoming important in regions of high sediment concentration near the bed. At low concentrations, the settling velocity for the  $j$ th noncohesive sediment class corresponds to the settling velocity of a discrete particle:

$$w_{sj} = w_{soj} \quad (6.1)$$

Useful expressions for the discrete particle settling velocity which depends on the sediment density, effective grain diameter, and fluid kinematic viscosity, provide by van Rijn (1984b) are:

$$\frac{w_{soj}}{\sqrt{g' d_j}} = \begin{cases} \frac{R_{dj}}{18} & : d \leq 100\mu m \\ \frac{10}{R_{dj}} \left( \sqrt{1 + 0.01 R_{dj}^2} - 1 \right) & : 100\mu m < d_j \leq 1000\mu m \\ 1.1 & : d_j > 1000\mu m \end{cases} \quad (6.2)$$

where

$$g' = g \left( \frac{\rho_{sj}}{\rho_w} - 1 \right) \quad (6.3)$$

is the reduced gravitational acceleration and

$$R_{dj} = \frac{d_j \sqrt{g' d_j}}{\nu} \quad (6.4)$$

is a the sediment grain densimetric Reynolds number.

At higher concentrations and hindering settling conditions, the settling velocity is less than the discrete velocity and can be expressed in the form

$$w_{sj} = \left( 1 - \sum_i \frac{S_i}{\rho_{si}} \right)^n w_{soj} \quad (6.5)$$

where  $\rho_s$  is the sediment particle density with values of  $n$  ranging from 2 (Cao *et al.*, 1996) to 4 (Van Rijn, 1984). The expression (6.2) is approximated to within 5 per cent by

$$w_{sj} = \left( 1 - n \sum_i \frac{S_i}{\rho_{si}} \right) w_{soj} \quad (6.6)$$

for total sediment concentrations up to 200,000 mg/liter. For total sediment concentrations less than 25,000 mg/liter, neglect of the hindered settling correction results in less than a 5 per cent error in the settling velocity that is well within the range of uncertainty in parameters used to estimate the discrete particle settling velocity.

Noncohesive sediment is transported as bedload and suspended load. The initiation of both modes of transport begins with erosion or resuspension of sediment from the bed when the bed stress,  $\tau_b$ , exceeds a critical stress referred to as the Shield's stress,  $\tau_{cs}$ . The Shield's stress depends upon the density and diameter of the sediment particles and the kinematic viscosity of the fluid and can be expressed in empirical dimensionless relationships of the form:

$$\theta_{csj} = \frac{\tau_{csj}}{g' d_j} = \frac{u_{*csj}^2}{g' d_j} = f(R_{dj}) \quad (6.7)$$

Useful numerical expressions of the relationship (6.5), provided by van Rijn (1984b), are:

$$\theta_{csj} = \begin{cases} 0.24(R_{dj}^{2/3})^{-1} & : R_{dj}^{2/3} < 4 \\ 0.14(R_{dj}^{2/3})^{-0.64} & : 4 \leq R_{dj}^{2/3} < 10 \\ 0.04(R_{dj}^{2/3})^{-0.1} & : 10 \leq R_{dj}^{2/3} < 20 \\ 0.013(R_{dj}^{2/3})^{0.29} & : 20 \leq R_{dj}^{2/3} < 150 \\ 0.055 & : R_{dj}^{2/3} \geq 150 \end{cases} \quad (6.8)$$

A number of approaches have been used to distinguish whether a particular sediment size class is transported as bedload or suspended load under specific local flow conditions characterized by the bed stress or bed shear velocity:

$$u_* = \sqrt{\tau_b} \quad (6.9)$$

The approach proposed by van Rijn (1984a) is adopted in the EFDC model and is as follows. When the bed velocity is less than the critical shear velocity

$$u_{*csj} = \sqrt{\tau_{csj}} = \sqrt{g' d_j \theta_{csj}} \quad (6.10)$$

no erosion or resuspension takes place and there is no bedload transport. Sediment in suspension under this condition will deposit to the bed as will be subsequently discussed.

When the bed shear velocity exceeds the critical shear velocity but remains less than the settling velocity,

$$u_{*csj} < u_* < w_{soj} \quad (6.11)$$

sediment will be eroded from the bed and transported as bedload. Sediment in suspension under this condition will deposit to the bed. When the bed shear velocity exceeds both the critical shear velocity and the settling velocity, bedload transport ceases and the eroded or resuspended sediment will be transported as suspended load. These various transport modes are further illustrated by reference to Figure 1, which shows dimensional forms of the settling velocity relationship (6.2) and the critical Shield's shear velocity (6.10), determined using (6.8) for sediment with a specific gravity of 2.65. For grain diameters less than approximately 1.3E-4 m (130  $\mu$ m) the settling velocity is less than the critical shear velocity and sediment resuspend from the bed when the bed shear velocity exceeds the critical shear velocity will be transported entirely as suspended load. For grain diameters greater than 1.3E-4 m, eroded sediment be transported by bedload in the region corresponding to (6.11) and then as suspended load when the bed shear velocity exceeds the settling velocity.

In the EFDC model, the preceding set of rules are used to determine the mode of transport of multiple size classes of noncohesive sediment. Bedload transport is determined using a general bedload transport rate formula:

$$\frac{q_B}{\rho_s d \sqrt{g' d}} = \Phi(\theta, \theta_{cs}) \quad (6.12)$$

where  $q_B$  is the bedload transport rate (mass per unit time per unit width) in the direction of the near bottom horizontal flow velocity vector. The function  $\Phi$  depends on the Shield's parameter

$$\theta = \frac{\tau_b}{g' d_j} = \frac{u_*^2}{g' d_j} \quad (6.13)$$

and the critical Shield's parameter defined by (6.7) and (6.8). A number of bedload transport formulas explicitly incorporate the settling velocity. However, since both the critical Shield's parameter and the settling velocity are unique functions of the sediment grain densimetric Reynolds number, the settling velocity can also be expressed as a function of the critical Shield's parameter with (6.12) remaining an appropriate representation.

A number of bedload formulations developed for riverine prediction (Ackers and White, 1973; Laursen, 1958; Yang, 1973; Yang and Molinas, 1982) do not readily conform to (1) and were not incorporated as options in the EFDC model. Two widely used bedload formulations which do conform to (6.12) are the Meyer-Peter and Muller (1948) and

Bagnold (1956) formulas and their derivatives (Raudkivi, 1967; Neilson, 1992; Reid and Frostick, 1994) which have the general form

$$\Phi(\theta, \theta_{cs}) = \phi(\theta - \theta_{cs})^\alpha \left( \sqrt{\theta} - \gamma \sqrt{\theta_{cs}} \right)^\beta \quad (6.14)$$

where

$$\phi = \phi(\theta_{cs}) \quad \text{or} \quad \phi(R_d) \quad (6.15)$$

The Meyer-Peter and Muller formulations are typified by

$$\Phi = \phi(\theta - \theta_{cs})^{3/2} \quad (6.16)$$

while Bagnold formulations are typified by

$$\Phi = \phi(\theta - \theta_{cs}) \left( \sqrt{\theta} - \gamma \sqrt{\theta_{cs}} \right) \quad (6.17)$$

with Bagnold's original formula having  $\gamma$  equal to zero. The Meyer-Peter and Muller formulation has been extended to heterogeneous beds by Suzuki *et al.* (1998), while Bagnold's formula has been similarly extended by van Niekerk *et al.* (1992). The bedload formulation by van Rijn (1984a) having the form

$$\begin{aligned} \Phi &= \phi(\theta - \theta_{cs})^{2.1} \\ \phi &= \frac{0.053}{R_d^{1/5} \theta_{cs}^{2.1}} \end{aligned} \quad (6.18)$$

has been incorporated into the CH3D-SED model and modified for heterogeneous beds by Spasojevic and Holly (1994). Equation (6.18) can be implemented in the EFDC model with an appropriately specified  $\phi$ . A modified formulation of the Einstein bedload function (Einstein, 1950) which conforms to (6.12) and (6.14) has been presented by Rahmeyer (1999) and will be later incorporated into the EFDC model.

The procedure for coupling bedload transport with the sediment bed in the EFDC model is as follows. First, the magnitude of the bedload mass flux per unit width is calculated according to (6.12) at horizontal model cell centers, denoted by the subscript  $c$ . The cell center flux is then transformed into cell center vector components using

$$\begin{aligned} q_{bcx} &= \frac{u}{\sqrt{u^2 + v^2}} q_{bc} \\ q_{bcy} &= \frac{v}{\sqrt{u^2 + v^2}} q_{bc} \end{aligned} \quad (6.19)$$

where  $u$  and  $v$  are the cell center horizontal velocities near the bed. Cell face mass fluxes are determined by down wind projection of the cell center fluxes

$$\begin{aligned} q_{bfx} &= (q_{bcx})_{upwind} \\ q_{bfy} &= (q_{bcy})_{upwind} \end{aligned} \quad (6.20)$$

where the subscript *upwind* denotes the cell center upwind of the  $x$  normal and  $y$  normal cell faces. The net removal or accumulation rate of sediment material from the deposited bed underlying a water cell is then given by:

$$m_x m_y J_b = (m_y q_{bfx})_e - (m_y q_{bfx})_w + (m_x q_{bfy})_n - (m_x q_{bfy})_s \quad (6.21)$$

where  $J_b$  is the net removal rate (gm/m<sup>2</sup>-sec) from the bed,  $m_x$  and  $m_y$  are  $x$  and  $y$  dimensions of the cell, and the compass direction subscripts define the four cell faces. The implementation of (6.19) through (6.21) in the EFDC code includes logic to limit the out fluxes (6.20) over a time step, such that the time integrated mass flux from the bed does not exceed bed sediment available for erosion or resuspension.

Under conditions when the bed shear velocity exceeds the settling velocity and critical Shield's shear velocity, noncohesive sediment will be resuspended and transported as suspended load. When the bed shear velocity falls below both the settling velocity and the critical Shield's shear velocity, suspended sediment will deposit to the bed. A consistent formulation of these processes can be developed using the concept of a near bed equilibrium sediment concentration. Under steady, uniform flow and sediment loading conditions, an equilibrium distribution of sediment in the water column tends to be established, with the resuspension and deposition fluxes canceling each other. Using a number of simplifying assumptions, the equilibrium sediment concentration distribution in the water column can be expressed analytically in terms of the near bed reference or equilibrium concentration, the settling velocity and the vertical turbulent diffusivity. For unsteady or spatially varying flow conditions, the water column sediment concentration distribution varies in space and time in response to sediment load variations, changes in hydrodynamic transport, and associated nonzero fluxes across the water column-sediment bed interface. An increase or decrease in the bed stress and the intensity of vertical turbulent mixing will result in net erosion or deposition, respectively, at a particular location or time.

To illustrate how an appropriate suspended noncohesive sediment bed flux boundary condition can be established, consider the approximation to the sediment transport equation (3.1) for nearly uniform horizontal conditions

$$\partial_t (HS) = \partial_z \left( \frac{K_v}{H} \partial_z S + w_s S \right) \quad (6.22)$$

Integrating (6.22) over the depth of the bottom hydrodynamic model layer gives

$$\partial_t (\Delta H \bar{S}) = J_0 - J_\Delta \quad (6.23)$$

where the over bar denotes the mean over the dimensionless layer thickness,  $\Delta$ . Subtracting (6.23) from (6.22) gives

$$\partial_t (HS') = \partial_z \left( \frac{K_v}{H} \partial_z S + w_s S \right) - \left( \frac{J_0 - J_\Delta}{\Delta} \right) \quad (6.24)$$

Assuming that the rate of change of the deviation of the sediment concentration from the mean is small

$$\partial_t (HS') \ll \partial_t (H \bar{S}) \quad (6.25)$$

allows (6.24) to be approximated by

$$\partial_z \left( \frac{K_v}{H} \partial_z S + w_s S \right) = \left( \frac{J_0 - J_\Delta}{\Delta} \right) \quad (6.26)$$

Integrating (6.26) once gives

$$\frac{K_v}{H} \partial_z S + w_s S = (J_0 - J_\Delta) \frac{z}{\Delta} - J_0 \quad (6.27)$$

Very near the bed, (6.27) can be approximated by

$$\frac{K_v}{H} \partial_z S + w_s S = -J_0 \quad (6.28)$$

Neglecting stratification effects and using the results of Chapter 4, the near bed diffusivity is approximately

$$\frac{K_v}{H} = K_o q \frac{l}{H} \cong u_* \kappa z \quad (6.29)$$

Introducing (6.29) into (6.28) gives

$$\partial_z S + \frac{R}{z} S = -\frac{R}{z} \frac{J_0}{w_s} \quad (6.30)$$

where

$$R = \frac{w_s}{u_* K} \quad (6.31)$$

is the Rouse parameter. The solution of (6.30) is

$$S = -\frac{J_o}{w_s} + \frac{C}{z^R} \quad (6.32)$$

The constant of integration is evaluated using

$$S = S_{eq} \quad : \quad z = z_{eq} \quad \text{and} \quad J_o = 0 \quad (6.33)$$

which sets the near bed sediment concentration to an equilibrium value, defined just above the bed under no net flux condition. Using (6.33), equation (6.32) becomes

$$S = \left( \frac{z_{eq}}{z} \right)^R S_{eq} - \frac{J_o}{w_s} \quad (6.34)$$

For non-equilibrium conditions, the net flux is given by evaluating (6.34) at the equilibrium level

$$J_o = w_s (S_{eq} - S_{ne}) \quad (6.35)$$

where  $S_{ne}$  is the actual concentration at the reference equilibrium level. Equation (6.35) clearly indicates that when the near bed sediment concentration is less than the equilibrium value a net flux from the bed into the water column occurs. Likewise when the concentration exceeds equilibrium, a net flux to the bed occurs. For this case when  $S_{ne}$  is greater than  $S_{eq}$

$$J_o = -w_s S_{ne} \left( 1 - \frac{S_{eq}}{S_{ne}} \right) \quad (6.35b)$$

and the term inside the ( ) can be considered as the deposition factor which does not exceed unity.

For the relationship (6.35) to be useful in a numerical model, the bed flux must be expressed in terms of the model layer mean concentration. For a three-dimensional application, (6.34) can be integrated over the bottom model layer to give

$$J_o = w_s (\bar{S}_{eq} - \bar{S}) \quad (6.36)$$

where

$$\bar{S}_{eq} = \frac{\ln(\Delta z_{eq}^{-1})}{(\Delta z_{eq}^{-1} - 1)} S_{eq} : R = 1 \quad (6.37)$$

$$\bar{S}_{eq} = \frac{\left( (\Delta z_{eq}^{-1})^{1-R} - 1 \right)}{(1-R)(\Delta z_{eq}^{-1} - 1)} S_{eq} : R \neq 1$$

defines an equivalent layer mean equilibrium concentration in terms of the near bed equilibrium concentration. The corresponding quantities in the numerical solution bottom boundary condition (3.6) are

$$w_r S_r = w_s \bar{S}_{eq} \quad (6.38)$$

$$P_d w_s = w_s$$

If the dimensionless equilibrium elevation,  $z_{eq}$  exceeds the dimensionless layer thickness, (6.19) can be modified to

$$\bar{S}_{eq} = \frac{\ln(M \Delta z_{eq}^{-1})}{(M \Delta z_{eq}^{-1} - 1)} S_{eq} : R = 1 \quad (6.39)$$

$$\bar{S}_{eq} = \frac{\left( (M \Delta z_{eq}^{-1})^{1-R} - 1 \right)}{(1-R)(M \Delta z_{eq}^{-1} - 1)} S_{eq} : R \neq 1$$

where the over bars in (6.36) and (6.38) implying an average of the first  $M$  layers above the bed.

For two-dimensional, depth averaged model application, a number of additional considerations are necessary. For depth average modeling, the equivalent of (6.27) is

$$\frac{K_v}{H} \partial_z S + w_s S = -J_o (1-z) \quad (6.40)$$

Neglecting stratification effects and using the results of Chapter 4, the diffusivity is

$$\frac{K_v}{H} = K_o q \frac{l}{H} \cong u_* \kappa z (1-z)^\lambda \quad (6.41)$$

Introducing (6.41) into (6.40) gives

$$\partial_z S + \frac{R}{z(1-z)^\lambda} S = -\frac{R(1-z)^{1-\lambda}}{z} \frac{J_o}{w_s} \quad (6.42)$$

A close form solution of (6.42) is possible for  $\lambda$  equal to zero. Although the resulting diffusivity is not as reasonable as the choice of  $\lambda$  equal to one, the resulting vertical distribution of sediment is much more sensitive to the near bed diffusivity distribution than the distribution in the upper portions of the water column. For  $\lambda$  equal to zero, the solution of (6.42) is

$$S = -\left(1 - \frac{Rz}{(1+R)}\right) \frac{J_o}{w_s} + \frac{C}{z^R} \quad (6.43)$$

Evaluating the constant of integration using (6.43) gives

$$S = \left(\frac{z_{eq}}{z}\right)^R S_{eq} - \left(1 - \frac{Rz}{(1+R)}\right) \frac{J_o}{w_s} \quad (6.44)$$

For non-equilibrium conditions, the net flux is given by evaluating (6.44) at the equilibrium level

$$J_o = w_s \left( \frac{(1+R)}{1+R(1-z_{eq})} \right) (S_{eq} - S_{ne}) \quad (6.45)$$

where  $S_{ne}$  is the actual concentration at the reference equilibrium level. Since  $z_{eq}$  is on the order of the sediment grain diameter divided by the depth of the water column, (6.45) is essentially equivalent (6.35). To obtain an expression for the bed flux in terms of the depth average sediment concentration, (6.44) is integrated over the depth to give

$$J_o = w_s \left( \frac{2(1+R)}{2+R(1-z_{eq})} \right) (\bar{S}_{eq} - \bar{S}) \quad (6.46)$$

where

$$\begin{aligned} \bar{S}_{eq} &= \frac{\ln(z_{eq}^{-1})}{(z_{eq}^{-1} - 1)} S_{eq} : R = 1 \\ \bar{S}_{eq} &= \frac{(z_{eq}^{R-1} - 1)}{(1-R)(z_{eq}^{-1} - 1)} S_{eq} : R \neq 1 \end{aligned} \quad (6.47)$$

The corresponding quantities in the numerical solution bottom boundary condition (3.6) are

$$w_r S_r = w_s \left( \frac{2(1+R)}{2+R(1-z_{eq})} \right) \bar{S}_{eq} \quad (6.48)$$

$$P_d w_s = \left( \frac{2(1+R)}{2+R(1-z_{eq})} \right) w_s$$

When multiple sediment size classes are simulated, the equilibrium concentrations given by (6.37), (6.39), and (6.47) are adjusted by multiplying by their respective sediment volume fractions in the surface layer of the bed.

The specification of the water column-bed flux of noncohesive sediment has been reduced to specification of the near bed equilibrium concentration and its corresponding reference distance above the bed. Garcia and Parker (1991) evaluated seven relationships, derived by combinations of analysis and experiment correlation, for determining the near bed equilibrium concentration as well as proposing a new relationship. All of the relationships essential specify the equilibrium concentration in terms of hydrodynamic and sediment physical parameters

$$S_{eq} = S_{eq}(d, \rho_s, \rho_w, w_s, u_*, \nu) \quad (6.49)$$

including the sediment particle diameter, the sediment and water densities, the sediment settling velocity, the bed shear velocity, and the kinematic molecular viscosity of water. Garcia and Parker concluded that the representations of Smith and McLean (1977) and Van Rijn (1984b) as well as their own proposed representation perform acceptably when tested against experimental and field observations.

Smith and McLean's formula for the equilibrium concentration is

$$S_{eq} = \rho_s \frac{0.65 \gamma_o T}{1 + \gamma_o T} \quad (6.50)$$

where  $\gamma_o$  is a constant equal to 2.4E-3 and  $T$  is given by

$$T = \frac{\tau_b - \tau_{cs}}{\tau_{cs}} = \frac{u_*^2 - u_{*cs}^2}{u_{*cs}^2} \quad (6.51)$$

where  $\tau_b$  is the bed stress and  $\tau_{cs}$  is the critical Shields stress. The use of Smith and McLean's formulation requires that the critical Shields stress be specified for each sediment size class. Van Rijn's formula is

$$S_{eq} = 0.015 \rho_s \frac{d}{z_{eq}} T^{3/2} R_d^{-1/5} \quad (6.52)$$

where  $z_{eq}^*$  ( $= Hz_{eq}$ ) is the dimensional reference height and  $R_d$  is a sediment grain Reynolds number. When van Rijn's formula is select for use in EFDC, the critical Shields stress is internally calculated using relationships from van Rijn (1984b). van Rijn suggested setting the dimensional reference height to three grain diameters. In the EFDC model, the user specifies the reference height as a multiple of the largest noncohesive sediment size class diameter.

Garcia and Parker's general formula for multiple sediment size classes is

$$S_{jeq} = \rho_s \frac{A(\lambda Z_j)^5}{(1 + 3.33A(\lambda Z)^5)} \quad (6.53)$$

$$Z_j = \frac{u_*}{w_{sj}} R_{dj}^{3/5} F_H \quad (6.54)$$

$$F_H = \left( \frac{d_j}{d_{50}} \right)^{1/5} \quad (6.55)$$

$$\lambda = 1 + \frac{\sigma_\phi}{\sigma_{\phi_o}} (\lambda_o - 1) \quad (6.56)$$

where  $A$  is a constant equal to  $1.3E-7$ ,  $d_{50}$  is the median grain diameter based on all sediment classes,  $\lambda$  is a straining factor,  $F_H$  is a hiding factor and  $\sigma_\phi$  is the standard deviation of the sedimentological phi scale of sediment size distribution. Garcia and Parker's formulation is unique in that it can account for armoring effects when multiple sediment classes are simulated. For simulation of a single noncohesive size class, the straining factor and the hiding factor are set to one. The EFDC model has the option to simulate armoring with Garcia and Parker's formulation. For armoring simulation, the current surface layer of the sediment bed is restricted to a thickness equal to the dimensional reference height.

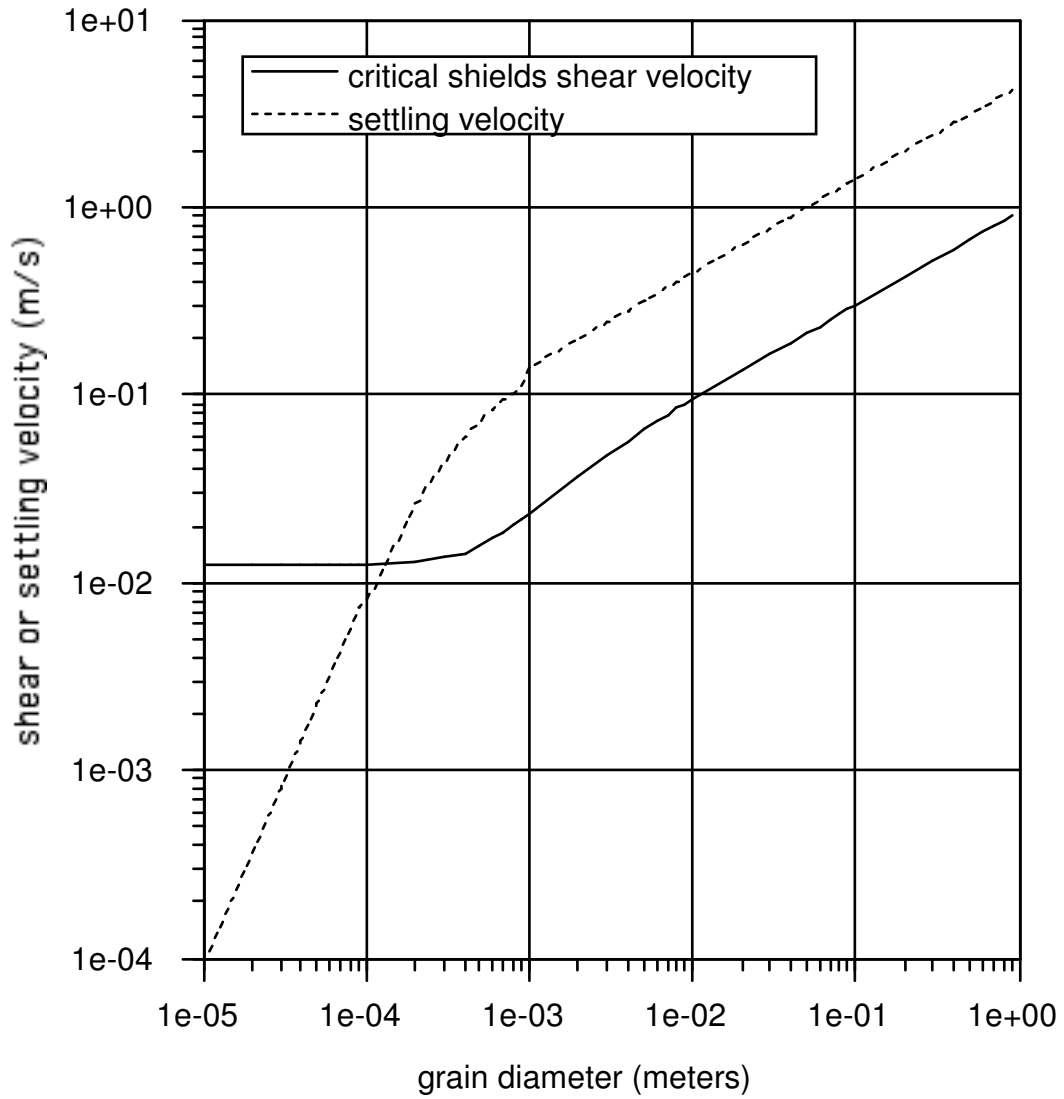


Figure 6.1. Critical Shield's shear velocity and settling velocity as a function of sediment grain size.

## 7. Cohesive Sediment Settling, Deposition and Resuspension

The settling of cohesive inorganic sediment and organic particulate material is an extremely complex process. Inherent in the process of gravitational settling is the process of flocculation, where individual cohesive sediment particles and particulate organic particles aggregate to form larger groupings or flocs having settling characteristics significantly different from those of the component particles (Burban et al., 1989; 1990; Gibbs, 1985; Mehta *et al.*, 1989). Floc formation is dependent upon the type and concentration of the suspended material, the ionic characteristics of the environment, and the fluid shear and turbulence intensity of the flow environment. Progress has been made in first principles mathematical modeling of floc formation or aggregation, and disaggregation by intense flow shear (Lick and Lick, 1988; Tsai *et al.*, 1987). However, the computational intensity of such approaches precludes direct simulation of flocculation in operational cohesive sediment transport models for the immediate future.

An alternative approach, which has met with reasonable success, is the parameterization of the settling velocity of flocs in terms of cohesive and organic material fundamental particle size,  $d$ ; concentration,  $S$ ; and flow characteristics such as vertical shear of the horizontal velocity,  $du/dz$ , shear stress,  $A_v du/dz$ , or turbulence intensity in the water column or near the sediment bed,  $q$ . This has allowed semi-empirical expressions having the functional form

$$W_{se} = W_{se} \left( d, S, \frac{du}{dz}, q \right) \quad (7.1)$$

to be developed to represent the effective settling velocity. A widely used empirical expression, first incorporated into a numerical by Ariathurai and Krone (1976), relates the effective settling velocity to the sediment concentration:

$$w_s = w_{s0} \left( \frac{S}{S_0} \right)^\alpha \quad (7.2)$$

with the 0 superscript denoting reference values. Depending upon the reference concentration and the value of  $\alpha$ , this equation predicts either increasing or decreasing settling velocity as the sediment concentration increases. Equation (7.2) with user defined base settling velocity, concentration and exponent is an option in the EFDC model. Hwang and Mehta (1989) proposed

$$w_s = \frac{aS^n}{(S^2 + b^2)^m} \quad (7.3)$$

based on observations of settling at six sites in Lake Okeechobee. This equation has a general parabolic shape with the settling velocity decreasing with decreasing

concentration at low concentrations and decreasing with increasing concentration at high concentration. Least squares analysis for the parameters,  $a$ ,  $m$ , and  $n$ , in (7.3) was shown to agree well with observational data. Equation (7.3) does not have a dependence on flow characteristics, but is based on data from an energetic field condition having both currents and high frequency surface waves. A generalized form of (7.3) can be selected as an option in the EFDC model.

Ziegler and Nisbet (1994, 1995) proposed a formulation to express the effective settling as a function of the floc diameter,  $d_f$

$$w_s = ad_f^b \quad (7.4)$$

with the floc diameter given by:

$$d_f = \left( \frac{\alpha_f}{S\sqrt{\tau_{xz}^2 + \tau_{yz}^2}} \right)^{1/2} \quad (7.5)$$

where  $S$  is the sediment concentration,  $\alpha_f$  is an experimentally determined constant and  $\tau_{xz}$  and  $\tau_{yz}$  are the  $x$  and  $y$  components of the turbulent shear stresses at a given position in the water column. Other quantities in (7.4) have been experimentally determined to fit the relationships:

$$a = B_1 \left( S\sqrt{\tau_{xz}^2 + \tau_{yz}^2} \right)^{-0.85} \quad (7.6)$$

$$b = -0.8 - 0.5 \log \left( S\sqrt{\tau_{xz}^2 + \tau_{yz}^2} - B_2 \right) \quad (7.7)$$

where  $B_1$  and  $B_2$  are experimental constants. This formulation is also an option in the EFDC model.

A final settling option in EFDC is based on that proposed by Shrestha and Orlob (1996). The formulation in EFDC has the form

$$w_s = S^\alpha \exp(-4.21 + 0.147G) \quad (7.8)$$

$$\alpha = 0.11 + 0.039G$$

where

$$G = \sqrt{(\partial_z u)^2 + (\partial_z v)^2} \quad (7.9)$$

is the magnitude of the vertical shear of the horizontal velocity. It is noted that all of these formulations are based on specific dimensional units for input parameters and

predicted settling velocities and that appropriate unit conversion are made internally in their implementation in the EFDC model.

Water column-sediment bed exchange of cohesive sediments and organic solids is controlled by the near bed flow environment and the geomechanics of the deposited bed. Net deposition to the bed occurs as the flow-induced bed surface stress decreases. The most widely used expression for the depositional flux is:

$$J_o^d = \begin{cases} -w_s S_d \left( \frac{\tau_{cd} - \tau_b}{\tau_{cd}} \right) = -w_s T_d S_d & : \tau_b \leq \tau_{cd} \\ 0 & : \tau_b \geq \tau_{cd} \end{cases} \quad (7.10)$$

where  $\tau_b$  is the stress exerted by the flow on the bed,  $\tau_{cd}$  is a critical stress for deposition which depends on sediment material and floc physiochemical properties (Mehta *et al.*, 1989) and  $S_d$  is the near bed depositing sediment concentration. The critical deposition stress is generally determined from laboratory or *in situ* field observations and values ranging from 0.06 to 1.1 N/m<sup>2</sup> have been reported in the literature. Given this wide range of reported values, in the absence of site specific data the depositional stress is generally treated as a calibration parameter. The depositional stress is an input parameter in the EFDC model.

Since the near bed depositing sediment concentration in (7.10) is not directly calculated, the procedures of Chapter 5 can be applied to relate the near bed depositional concentration to the bottom layer or depth averaged concentration. Using (6.14) the near bed concentration during times of deposition can be determined in terms of the bottom layer concentration for three-dimensional model applications. Inserting (7.10) into (6.14) and evaluating the constant at a near bed depositional level gives

$$S = \left( T_d + (1 - T_d) \frac{z_d^R}{z^R} \right) S_d \quad (7.11)$$

Integrating (7.11) over the bottom layer gives

$$S_d = \left( T_d + \frac{\ln(\Delta z_d^{-1})}{(\Delta z_d^{-1} - 1)} (1 - T_d) \right)^{-1} \bar{S} : R = 1 \quad (7.12)$$

$$S_d = \left( T_d + \frac{\left( (\Delta z_{eq}^{-1})^{1-R} - 1 \right)}{(1 - R)(\Delta z_d^{-1} - 1)} (1 - T_d) \right)^{-1} \bar{S} : R \neq 1$$

The corresponding quantities in the numerical solution bottom boundary condition (3.6) are

$$\begin{aligned}
 P_d w_s &= \left( T_d + \frac{\ln(\Delta z_d^{-1})}{(\Delta z_d^{-1} - 1)} (1 - T_d) \right)^{-1} w_s : R = 1 \\
 P_d w_s &= \left( T_d + \frac{\left( (\Delta z_{eq}^{-1})^{1-R} - 1 \right)}{(1-R)(\Delta z_d^{-1} - 1)} (1 - T_d) \right)^{-1} w_s : R \neq 1
 \end{aligned} \tag{7.13}$$

For depth averaged model application, (7.10) is combined with (6.25) and the constant of integration is evaluated at a near bed depositional level to give

$$S = \left( 1 - \frac{Rz}{(1+R)} \right) T_d S_d + \left( 1 - \left( 1 - \frac{Rz_d}{(1+R)} \right) T_d \right) S_d \frac{z_d^R}{z^R} \tag{7.14}$$

Integrating (7.14) over the depth gives

$$\begin{aligned}
 S_d &= \left( \left( \frac{2+R(1-z_d)}{2(1+R)} \right) T_d + \frac{\ln(z_d^{-1})}{(z_d^{-1} - 1)} \left( 1 - \left( \frac{1+R(1-z_d)}{(1+R)} \right) T_d \right) \right)^{-1} \bar{S} : R = 1 \\
 S_d &= \left( \left( \frac{2+R(1-z_d)}{2(1+R)} \right) T_d + \frac{(z_d^{R-1} - 1)}{(1-R)(z_d^{-1} - 1)} \left( 1 - \left( 1 - \frac{Rz_d}{(1+R)} \right) T_d \right) \right)^{-1} \bar{S} : R \neq 1
 \end{aligned} \tag{7.15}$$

The corresponding quantities in the numerical solution bottom boundary condition (3.6) are

$$\begin{aligned}
 P_d w_s &= \left( \left( \frac{2+R(1-z_d)}{2(1+R)} \right) T_d + \frac{\ln(z_d^{-1})}{(z_d^{-1} - 1)} \left( 1 - \left( \frac{1+R(1-z_d)}{(1+R)} \right) T_d \right) \right)^{-1} w_s : R = 1 \\
 P_d w_s &= \left( \left( \frac{2+R(1-z_d)}{2(1+R)} \right) T_d + \frac{(z_d^{R-1} - 1)}{(1-R)(z_d^{-1} - 1)} \left( 1 - \left( 1 - \frac{Rz_d}{(1+R)} \right) T_d \right) \right)^{-1} w_s : R \neq 1
 \end{aligned} \tag{7.16}$$

It is noted that the assumptions used to arrive at the relationships, (7.12) and (7.15) are more tenuous for cohesive sediment than the similar relationships for noncohesive sediment. The settling velocity for cohesive sediment is highly concentration dependent and the use of a constant settling velocity to arrive at (7.12) and (7.15) is questionable. The specification of an appropriate reference level for cohesive sediment is difficult. One

possibility is to relate the reference level to the floc diameter using (7.5). An alternative is to set the reference level to a laminar sublayer thickness

$$z_d = \frac{\nu(S)}{Hu_*} \quad (7.17)$$

where  $\nu(S)$  is a sediment concentration dependent kinematic viscosity and the water depth is included to non-dimensionalize the reference level. A number of investigators, including Mehta and Jiang (1990) have presented experimental results indicating that at high sediment concentrations, cohesive sediment-water mixtures behave as high viscosity fluids. Mehta and Jain's results indicate that a sediment concentration of 10,000 mg/L results in a viscosity ten time that of pure water and that the viscosity increases logarithmically with increasing mixture density. Use of the relationships (7.12) and (7.16) is optional in the EFDC model. When they are used, the reference height is set using (7.17) with the viscosity determined using Mehta and Jain's experimental relationship between viscosity and sediment concentration. To more fully address the deposition prediction problem, a nested sediment, current and wave boundary layer model based on the near bed closure presented in Chapter 4 is under development.

Cohesive bed erosion occurs in two distinct modes, mass erosion and surface erosion. Mass erosion occurs rapidly when the bed stress exerted by the flow exceeds the depth varying shear strength,  $\tau_s$ , of the bed at a depth,  $H_{me}$ , below the bed surface. Surface erosion occurs gradually when the flow-exerted bed stress is less than the bed shear strength near the surface but greater than a critical erosion or resuspension stress,  $\tau_{ce}$ , which is dependent on the shear strength and density of the bed. A typical scenario under conditions of accelerating flow and increasing bed stress would involve first the occurrence of gradual surface erosion, followed by a rapid interval of mass erosion, followed by another interval of surface erosion. Alternately, if the bed is well consolidated with a sufficiently high shear strength profile, only gradual surface erosion would occur. Transport into the water column by mass or bulk erosion can be expressed in the form

$$J_o^r = w_r S_r = \frac{m_{me} (\tau_s \leq \tau_b)}{T_{me}} \quad (7.18)$$

where  $J_o$  is the erosion flux, the product  $w_r S_r$  represents the numerical boundary condition (3.6),  $m_{me}$  is the dry sediment mass per unit area of the bed having a shear strength,  $\tau_s$ , less than the flow-induced bed stress,  $\tau_b$ , and  $T_{me}$  is a somewhat arbitrary time scale for the bulk mass transfer. The time scale can be taken as the numerical model integration time step (Shrestha and Orlob, 1996). Observations by Hwang and Mehta (1989) have indicated that the maximum rate of mass erosion is on the order of 0.6 gm/s-m<sup>2</sup> which provides a means of estimating the transfer time scale in (4.10). The shear strength of the cohesive sediment bed is generally agreed to be a linear function of the bed bulk density (Mehta *et al.*, 1982; Villaret and Paulic, 1986; Hwang and Mehta, 1989).

$$\tau_s = a_s \rho_b + b_s \quad (7.19)$$

For the shear strength in  $\text{N/m}^2$  and the bulk density in  $\text{gm/cm}^3$ , Hwang and Mehta (1989) give  $a_s$  and  $b_s$  values of 9.808 and -9.934 for bulk density greater than  $1.065 \text{ gm/cm}^3$ . The EFDC model currently implements Hwang and Mehta's relationship, but can be readily modified to incorporate other functional relationships.

Surface erosion is generally represented by relationships of the form

$$J_o^r = w_r S_r = \frac{dm_e}{dt} \left( \frac{\tau_b - \tau_{ce}}{\tau_{ce}} \right)^\alpha \quad : \quad \tau_b \geq \tau_{ce} \quad (7.20)$$

or

$$J_o^r = w_r S_r = \frac{dm_e}{dt} \exp \left( -\beta \left( \frac{\tau_b - \tau_{ce}}{\tau_{ce}} \right)^\gamma \right) \quad : \quad \tau_b \geq \tau_{ce} \quad (7.21)$$

where  $dm_e/dt$  is the surface erosion rate per unit surface area of the bed and  $\tau_{ce}$  is the critical stress for surface erosion or resuspension. The critical erosion rate and stress and the parameters  $\alpha$ ,  $\beta$ , and  $\gamma$  are generally determined from laboratory or *in situ* field experimental observations. Equation (7.20) is more appropriate for consolidated beds, while (7.21) is appropriate for soft partially consolidated beds. The base erosion rate and the critical stress for erosion depend upon the type of sediment, the bed water content, total salt content, ionic species in the water, pH and temperature (Mehta *et al.*, 1989) and can be measured in laboratory and sea bed flumes.

The critical erosion stress is related to but generally less than the shear strength of the bed, which in turn depends upon the sediment type and the state of consolidation of the bed. Experimentally determined relationships between the critical surface erosion stress and the dry density of the bed of the form

$$\tau_{ce} = c \rho_s^d \quad (7.22)$$

have been presented (Mehta *et al.*, 1989). Hwang and Mehta (1989) proposed the relationship

$$\tau_{ce} = a (\rho_b - \rho_l)^b + c \quad (7.23)$$

between the critical surface erosion stress and the bed bulk density with  $a$ ,  $b$ ,  $c$ , and  $\rho_l$  equal to 0.883, 0.2, 0.05, and  $1.065$ , respectively for the stress in  $\text{N/m}^2$  and the bulk density in  $\text{gm/cm}^3$ . Considering the relationship between dry and bulk density

$$\rho_d = \rho_s \frac{(\rho_b - \rho_w)}{(\rho_s - \rho_w)} \quad (7.24)$$

equations (7.22) and (7.23) are consistent. The EFDC model allow for a user defined constant critical stress for surface erosion or the use of (7.23). Alternate predictive expression can be readily incorporated into the model.

Surface erosion rates ranging from 0.005 to 0.1 gm/s-m<sup>2</sup> have been reported in the literature, and it is generally accepted that the surface erosion rate decreases with increasing bulk density. Based on experimental observations, Hwang and Mehta (1989) proposed the relationship

$$\log_{10} \left( \frac{dm_e}{dt} \right) = 0.23 \exp \left( \frac{0.198}{\rho_b - 1.0023} \right) \quad (7.25)$$

for the erosion rate in mg/hr-cm<sup>2</sup> and the bulk density in gm/cm<sup>3</sup>. The EFDC model allows for a user defined constant surface erosion rate or predicts the rate using (7.25). Alternate predictive expression can be readily incorporated into the model. The use of bulk density functions to predict bed strength and erosion rates in turn requires the prediction of time and depth in bed variations in bulk density which is related to the water and sediment density and the bed void ratio by

$$\rho_b = \left( \frac{\varepsilon}{1 + \varepsilon} \right) \rho_w + \left( \frac{1}{1 + \varepsilon} \right) \rho_s \quad (7.26)$$

Selection of the bulk density dependent formulations in the EFDC model requires implementation of a bed consolidation simulation to predict the bed void ratio as discussed in the following chapter.

## 8. Sorptive Contaminant Transport

The transport of a sorptive contaminant in the water column is governed by transport equations for the contaminant dissolved in the water phase, for the contaminant sorbed to material effectively dissolved in the water phase, and for the contaminant sorbed to suspended particles. For the portion of the contaminant dissolved directly in the water phase

$$\begin{aligned}
 & \partial_t (m_x m_y H C_w) + \partial_x (m_y H u C_w) + \partial_y (m_x H v C_w) + \partial_z (m_x m_y w C_w) \\
 &= \partial_z \left( m_x m_y \frac{A_b}{H} \partial_z C_w \right) + m_x m_y H \left( \sum_i (K_{dS}^i S^i \chi_S^i) + \sum_j (K_{dD}^j D^j \chi_D^j) \right) \\
 & \quad - m_x m_y H \left( \begin{aligned} & \sum_i (K_{aS}^i S^i) \left( \psi_w \frac{C_w}{\phi} \right) (\hat{\chi}_S^i - \chi_S^i) \\ & + \sum_j (K_{aD}^j D^j) \left( \psi_w \frac{C_w}{\phi} \right) (\hat{\chi}_D^j - \chi_D^j) + \gamma C_w \end{aligned} \right)
 \end{aligned} \tag{8.1}$$

where  $C_w$  is the mass of water dissolved contaminant per unit total volume,  $\chi_S$  is the mass of contaminant sorbed to sediment class  $i$  per mass of sediment,  $\chi_D$  is the mass of contaminant sorbed to dissolved material  $j$  per unit mass of dissolved material,  $\phi$  is the porosity,  $\psi_w$  is the fraction of the water dissolved contaminant available for sorption,  $K_a$  is the adsorption rate,  $K_d$  is the desorption rate, and  $\gamma$  is a net linearized decay rate coefficient. The sorption kinetics are based on the Langmuir isotherm (Chapra, 1997) with  $\hat{\chi}$  denoting the saturation sorbed mass per carrier mass. The sediment and dissolved material concentrations,  $S$  and  $D$  are defined as mass per unit total volume. The transport equation for the portion of material sorbed to a dissolved constituent  $D$  is,

$$\begin{aligned}
 & \partial_t (m_x m_y H D^j \chi_D^j) + \partial_x (m_y H u D^j \chi_D^j) + \partial_y (m_x H v D^j \chi_D^j) + \partial_z (m_x m_y w D^j \chi_D^j) \\
 &= \partial_z \left( m_x m_y \frac{A_b}{H} \partial_z (D^j \chi_D^j) \right) + m_x m_y H (K_{sD}^j D^j) \left( \psi_w \frac{C_w}{\phi} \right) (\hat{\chi}_D^j - \chi_D^j) \\
 & \quad - m_x m_y H (K_{dD}^j + \gamma) (D^j \chi_D^j)
 \end{aligned} \tag{8.2}$$

The transport equation for the portion of material sorbed to a suspended constituent  $S$  is,

$$\begin{aligned}
 & \partial_t (m_x m_y H S^i \chi_S^i) + \partial_x (m_y H u S^i \chi_S^i) + \partial_y (m_x H v S^i \chi_S^i) + \partial_z (m_x m_y w S^i \chi_S^i) \\
 & \quad + \partial_z (m_x m_y w_s^i S^i \chi_S^i) = \partial_z \left( m_x m_y \frac{A_b}{H} \partial_z (S^i \chi_S^i) \right) \\
 & \quad + m_x m_y H (K_{aS}^i S^i) \left( \psi_w \frac{C_w}{\phi} \right) (\hat{\chi}_S^i - \chi_S^i) - m_x m_y H (K_{dS}^i + \gamma) (S^i \chi_S^i)
 \end{aligned} \tag{8.3}$$

Introducing sorbed concentrations defining sorbed mass per unit total volume

$$C_D^j = D^j \chi_D^j \quad (8.4)$$

$$C_S^i = S^i \chi_S^i \quad (8.5)$$

Allows equations (8.1) through (8.3) to be written as

$$\begin{aligned} & \partial_t (m_x m_y H C_w) + \partial_x (m_y H u C_w) + \partial_y (m_x H v C_w) + \partial_z (m_x m_y w C_w) \\ & = \partial_z \left( m_x m_y \frac{A_b}{H} \partial_z C_w \right) + m_x m_y H \left( \sum_i (K_{dS}^i C_S^i) + \sum_j (K_{dD}^j C_D^j) \right) \\ & \quad - m_x m_y H \left( \begin{aligned} & \sum_i (K_{aS}^i S^i) \left( \psi_w \frac{C_w}{\phi} \right) (\hat{\chi}_S^i - \chi_S^i) \\ & + \sum_j (K_{dD}^j D^j) \left( \psi_w \frac{C_w}{\phi} \right) (\hat{\chi}_D^j - \chi_D^j) + \gamma C_w \end{aligned} \right) \end{aligned} \quad (8.6)$$

$$\begin{aligned} & \partial_t (m_x m_y H C_D^j) + \partial_x (m_y H u C_D^j) + \partial_y (m_x H v C_D^j) + \partial_z (m_x m_y w C_D^j) \\ & = \partial_z \left( m_x m_y \frac{A_b}{H} \partial_z C_D^j \right) + m_x m_y H (K_{sD}^j D^j) \left( \psi_w \frac{C_w}{\phi} \right) (\hat{\chi}_D^j - \chi_D^j) \\ & \quad - m_x m_y H (K_{dD}^j + \gamma) C_D^j \end{aligned} \quad (8.7)$$

$$\begin{aligned} & \partial_t (m_x m_y H C_S^i) + \partial_x (m_y H u C_S^i) + \partial_y (m_x H v C_S^i) + \partial_z (m_x m_y w C_S^i) \\ & \quad + \partial_z (m_x m_y w_S^i C_S^i) = \partial_z \left( m_x m_y \frac{A_b}{H} \partial_z C_S^i \right) \\ & \quad + m_x m_y H (K_{aS}^i S^i) \left( \psi_w \frac{C_w}{\phi} \right) (\hat{\chi}_S^i - \chi_S^i) - m_x m_y H (K_{dS}^i + \gamma) C_S^i \end{aligned} \quad (8.8)$$

The EFDC sorbed contaminant transport formulation currently employees equilibrium partitioning with the adsorption and desorption terms in (8.7) and (8.8) balancing

$$(K_{sD}^j D^j) \left( \psi_w \frac{C_w}{\phi} \right) (\hat{\chi}_D^j - \chi_D^j) = K_{dD}^j C_D^j \quad (8.9)$$

$$(K_{aS}^i S^i) \left( \psi_w \frac{C_w}{\phi} \right) (\hat{\chi}_S^i - \chi_S^i) = K_{dS}^i C_S^i \quad (8.10)$$

Solving (8.9) and (8.10) for the sorbed to water phase concentration ratios gives

$$\frac{C_D^j}{C_w} = \frac{f_D^j}{f_w} = P_D^j \frac{D^j}{\phi}$$

$$P_D^j = P_{Do}^j \left( 1 + P_{Do}^j \left( \frac{C_w}{\hat{\chi}_D^j \phi} \right) \right)^{-1} \quad (8.11)$$

$$P_{Do}^j = \frac{\psi_w K_{aD}^j \hat{\chi}_D^j}{K_{dD}^j}$$

$$\frac{C_S^i}{C_w} = \frac{f_S^i}{f_w} = P_S^i \frac{S^i}{\phi}$$

$$P_S^i = P_{So}^i \left( 1 + P_{So}^i \left( \frac{C_w}{\hat{\chi}_S^i \phi} \right) \right)^{-1} \quad (8.12)$$

$$P_{So}^i = \frac{\psi_w K_{aS}^i \hat{\chi}_S^i}{K_{dS}^i}$$

where  $P$  denotes the partition coefficient, and  $P_o$  is its linear equilibrium value. For linear equilibrium partitioning,  $P$  is set to  $P_o$ , which in effect approximates  $( )^{-1}$  terms in (8.11) and (8.12) by unity. Requiring the mass fractions to sum to unity

$$f_w + \sum_i f_S^i + \sum_j f_D^j = 1 \quad (8.13)$$

gives

$$f_w = \frac{C_w}{C} = \frac{\phi}{\phi + \sum_i P_S^i S^i + \sum_j P_D^j D^j}$$

$$f_D^j = \frac{C_D^j}{C} = \frac{P_D^j D^j}{\phi + \sum_i P_S^i S^i + \sum_j P_D^j D^j} \quad (8.14)$$

$$f_S^i = \frac{C_S^i}{C} = \frac{P_S^i S^i}{\phi + \sum_i P_S^i S^i + \sum_j P_D^j D^j}$$

The dissolved concentrations can be alternately expressed by mass per unit volume of the water phase

$$\begin{aligned}
 C_{w:w} &= \frac{C_w}{\phi} \\
 C_{D:w}^j &= \frac{C_D^j}{\phi} \\
 D_{:w}^j &= \frac{D^j}{\phi}
 \end{aligned}
 \tag{8.15}$$

with (8.14) becoming

$$\begin{aligned}
 \frac{C_{w:w}}{C} &= \frac{1}{\phi + \sum_i P_S^i S^i + \sum_j P_D^j \phi D_{:w}^j} \\
 \frac{C_{D:w}^j}{C} &= \frac{P_D^j D_{:w}^j}{\phi + \sum_i P_S^i S^i + \sum_j P_D^j \phi D_{:w}^j} \\
 \frac{C_S^i}{C} &= \frac{P_S^i S^i}{\phi + \sum_i P_S^i S^i + \sum_j P_D^j \phi D_{:w}^j}
 \end{aligned}
 \tag{8.16}$$

which is a generalization of Chapra's (1997) formulation for sorption to dissolved and particulate organic carbon.

Adding equations (8.6), (8.7), and (8.8), using the equilibrium partitioning relationships (8.9) and (8.10) gives

$$\begin{aligned}
 \partial_t (m_x m_y H C) + \frac{1}{m_x m_y} \partial_x (m_y H u C) + \frac{1}{m_x m_y} \partial_y (m_x H v C) + \partial_z (m_x m_y w C) \\
 - \partial_z \left( m_x m_y \sum_i w_S^i f_S^i C \right) = \partial_z \left( m_x m_y \frac{A_b}{H} \partial_z C \right) - m_x m_y H \gamma C
 \end{aligned}
 \tag{8.17}$$

the equation for the total concentration,  $C$ . The boundary condition at the water column-sediment bed interface,  $z = 0$ , is

$$\begin{aligned}
 & -\frac{A_b}{H} \partial_z C - \sum_i w_s^i f_s^i C \\
 = & \sum_i \left( \left( \max(J_{SBS}^i \mathcal{X}_S^i, 0) + \varepsilon \max\left(\frac{J_{SBS}^i}{\rho_S^i}, 0\right) \right) \left( \frac{C_w + \sum_j C_D^j}{\phi} \right) \right)_{SB} \\
 & + \sum_i \left( \left( \min(J_{SBS}^i \mathcal{X}_S^i, 0) + \varepsilon_{dep} \min\left(\frac{J_{SBS}^i}{\rho_S^i}, 0\right) \right) \left( \frac{C_w + \sum_j C_D^j}{\phi_{dep}} \right) \right)_{WC} \\
 & + \sum_i \left( \left( \varepsilon \max\left(\frac{J_{SBB}^i}{\rho_S^i}, 0\right) \right) \left( \frac{C_w + \sum_j C_D^j}{\phi} \right) \right)_{SB} \\
 & + \sum_i \left( \left( \varepsilon_{dep} \min\left(\frac{J_{SBB}^i}{\rho_S^i}, 0\right) \right) \left( \frac{C_w + \sum_j C_D^j}{\phi_{dep}} \right) \right)_{WC} \\
 & + \left( \max(q_w, 0) \left( \frac{C_w + \sum_j C_D^j}{\phi} \right) \right)_{SB} + \left( \min(q_w, 0) \left( \frac{C_w + \sum_j C_D^j}{\phi_{dep}} \right) \right)_{WC} \\
 & - q_{dif} \left( \left( \frac{C_w + \sum_j C_D^j}{\phi_{dep}} \right)_{WC} - \left( \frac{C_w + \sum_j C_D^j}{\phi} \right)_{SB} \right)
 \end{aligned} \tag{8.18}$$

where  $J_{SBS}$  and  $J_{SBB}$  are the suspended load and bedload sediment fluxes between the sediment bed and the water column, defined as positive from the bed,  $\rho_s$  is the sediment density,  $q_w$  is the water specific discharge due to bed consolidation and groundwater interaction, defined as positive from the bed, and  $q_{dif}$  is a diffusion velocity incorporating the effects of molecular diffusion, hydrodynamic dispersion, and biological induced mixing. The subscript *SB* denotes conditions in the top layer of the sediment bed, while the subscript *WC* denotes condition in the water column immediately above the bed, with the exception that the specific discharge and diffusion velocity are defined at the water column-bed interface. The subscript, *dep*, is used to denote the void ratio and porosity of newly depositing sediment. Equation (8.16) indicates that contaminant flux between the bed and water column includes, a flux of suspended sediment sorbed material; fluxes of water dissolved and sorbed to water dissolved material due to the specific discharge of water associated with consolidation and ground water interaction and water entrainment and expulsion associated with both suspended and bedload sediment deposition and resuspension; and a flux of water dissolved and sorbed to water dissolved material due to diffusion like processes. Transport of bedload sediment sorbed material is represented by direct transport between horizontally adjacent top bed layers and is included in the

contaminant mass conservation equations for the sediment bed. The boundary condition at the water free surface is

$$-\frac{A_b}{H} \partial_z C - \sum_i w_s^i f_s^i C = 0 \quad : \quad z = 1 \quad (8.19)$$

Using the relationship between the porosity and void ratio

$$\phi = \frac{\varepsilon}{1 + \varepsilon} \quad (8.20)$$

and (8.5) allows (8.18) to be written as

$$\begin{aligned} & -\frac{A_b}{H} \partial_z C - \sum_i w_s^i f_s^i C \\ &= \sum_i \left( \left( \max \left( J_{SBS}^i \frac{C_S^i}{S^i}, 0 \right) + (1 + \varepsilon) \max \left( \frac{J_{SBS}^i}{\rho_S^i}, 0 \right) \right) \left( C_w + \sum_j C_D^j \right) \right)_{SB} \\ &+ \sum_i \left( \left( \min \left( J_{SBS}^i \frac{C_S^i}{S^i}, 0 \right) + (1 + \varepsilon_{dep}) \min \left( \frac{J_{SBS}^i}{\rho_S^i}, 0 \right) \right) \left( C_w + \sum_j C_D^j \right) \right)_{WC} \\ &+ \sum_i \left( \left( (1 + \varepsilon) \max \left( \frac{J_{SBB}^i}{\rho_S^i}, 0 \right) \right) \left( C_w + \sum_j C_D^j \right) \right)_{SB} \\ &+ \sum_i \left( \left( (1 + \varepsilon_{dep}) \min \left( \frac{J_{SBB}^i}{\rho_S^i}, 0 \right) \right) \left( C_w + \sum_j C_D^j \right) \right)_{WC} \\ &+ \left( (\max(q_w, 0) + q_{dif}) \frac{1}{\phi} \left( C_w + \sum_j C_D^j \right) \right)_{SB} \\ &+ \left( (\min(q_w, 0) - q_{dif}) \frac{1}{\phi} \left( C_w + \sum_j C_D^j \right) \right)_{WC} \end{aligned} \quad (8.21)$$

The sediment concentration can be expressed in terms of the sediment density and void ratio by

$$S^i = \frac{F^i \rho_s^i}{1 + \varepsilon} \quad (8.22)$$

where  $F^i$  is the fraction of the total sediment volume occupied by each sediment class

$$F^i = \left( \sum_i \left( \frac{S^i}{\rho_s^i} \right) \right)^{-1} \left( \frac{S^i}{\rho_s^i} \right) \quad (8.23)$$

Introducing (8.14) and (8.22) into (8.21) gives the final form of the bottom boundary condition

$$\begin{aligned} & -\frac{A_b}{H} \partial_z C - \sum_i w_s^i f_s^i C \\ & = \sum_i \left( \max \left( \frac{J_{SBS}^i f_s^i}{S^i}, 0 \right) C + \max \left( \frac{F^i J_{SBS}^i}{S^i}, 0 \right) \left( f_w + \sum_j f_D^j \right) C \right)_{SB} \\ & + \sum_i \left( \min \left( \frac{J_{SBS}^i f_s^i}{S^i}, 0 \right) C + \min \left( \frac{F_{dep}^i J_{SBS}^i}{S_{dep}^i}, 0 \right) \left( f_w + \sum_j f_D^j \right) C \right)_{WC} \\ & + \sum_i \left( \left( (1 + \varepsilon) \max \left( \frac{J_{SBB}^i}{\rho_s^i}, 0 \right) \right) \left( C_w + \sum_j C_D^j \right) \right)_{SB} \\ & + \sum_i \left( \left( (1 + \varepsilon_{dep}) \min \left( \frac{J_{SBB}^i}{\rho_s^i}, 0 \right) \right) \left( C_w + \sum_j C_D^j \right) \right)_{WC} \\ & + \left( \left( \max(q_w, 0) + q_{dif} \right) \frac{1}{\phi} \left( f_w + \sum_j f_D^j \right) C \right)_{SB} \\ & + \left( \left( \min(q_w, 0) - q_{dif} \right) \frac{1}{\phi} \left( f_w + \sum_j f_D^j \right) C \right)_{WC} \end{aligned} \quad (8.24)$$

Note that the form of the bed flux associated with bedload transport remains unmodified since a sediment concentration in the water column cannot be readily defined for sediment being transported as bedload.

The transport equation (8.17) for the total contaminant concentration in the water column is solved using a fractional step procedure which sequentially treats advection; settling, deposition, and resuspension; pore water advection and diffusion; and reactions. The fractional phase distribution of the contaminant is recalculated between the advection, settling, deposition and resuspension, and pore water advection and diffusion steps using (8.14). The advection step is

$$(HC)^{n+1/4} - (HC)^n + \frac{\theta}{m_x m_y} \partial_x (m_y H u C) + \frac{\theta}{m_x m_y} \partial_y (m_x H v C) + \theta \partial_z (w C) = 0 \quad (8.25)$$

with the vertical boundary conditions

$$wC = 0 \quad : \quad z = 0, 1 \quad (8.26)$$

The fractional time level in (8.25) and subsequent equations is used to denote an intermediate result in the fractional step procedure. The spatially discrete form of (8.25) is solved using one of the standard high order, flux limited, advective transport solvers in the EFDC model.

The settling, deposition, and resuspension step is

$$(HC)^{n+1/2} - (HC)^{n+1/4} = \theta \partial_z \left( \sum_i w_s^i f_s^i C \right) \quad (8.27)$$

with the boundary conditions

$$\begin{aligned} & -\sum_i w_s^i f_s^i C = \\ & \sum_i \left( \max \left( \frac{J_{SBS}^i f_s^i}{S^i}, 0 \right) C + \max \left( \frac{F^i J_{SBS}^i}{S^i}, 0 \right) \left( f_w + \sum_j f_D^j \right) C \right)_{SB} \\ & + \sum_i \left( \min \left( \frac{J_{SBS}^i f_s^i}{S^i}, 0 \right) C + \min \left( \frac{F_{dep}^i J_{SBS}^i}{S_{dep}^i}, 0 \right) \left( f_w + \sum_j f_D^j \right) C \right)_{WC} \\ & + \sum_i \left( \left( (1 + \varepsilon) \max \left( \frac{J_{SBB}^i}{\rho_s^i}, 0 \right) \right) \left( C_w + \sum_j C_D^j \right) \right)_{SB} \\ & + \sum_i \left( \left( (1 + \varepsilon_{dep}) \min \left( \frac{J_{SBB}^i}{\rho_s^i}, 0 \right) \right) \left( C_w + \sum_j C_D^j \right) \right)_{WC} \quad : \quad z = 0 \end{aligned} \quad (8.28)$$

$$w_s^i f_s^i C = 0 \quad : \quad z = 1 \quad (8.29)$$

Integrating (8.27) over a water column layer and using upwind differencing for the settling gives,

$$\begin{aligned} \Delta_k (HC)_k^{n+1/2} - \Delta_k (HC)_k^{n+1/4} &= \theta \sum_i \left( \frac{(w_s^i S^i)_{k+}}{H} \left( \frac{f_s^i}{S^i} \right)_{k+1} \right)^{n+1/2} (HC)_{k+1}^{n+1/2} \\ & - \theta \sum_i \left( \frac{(w_s^i S^i)_{k-}}{H} \left( \frac{f_s^i}{S^i} \right)_k \right)^{n+1/2} (HC)_k^{n+1/2} \end{aligned} \quad (8.30)$$

for a layer not adjacent to the bed, and,

$$\begin{aligned}
 \Delta_1 (HC)_1^{n+1/2} - \Delta_1 (HC)_1^{n+1/4} &= \theta \sum_i \left( (w_s^i S^i)_{1+} \left( \frac{f_s^i}{S^i} \right)_2 \right)^{n+1/2} C_2^{n+1/2} \\
 + \theta \sum_i \left( \max \left( \frac{J_{SBS}^i f_s^i}{S^i}, 0 \right) + \max \left( \frac{J_{SBS}^i F^i}{S^i}, 0 \right) \left( f_w + \sum_j f_D^j \right) \right)_{sb}^{n+1/2} C_{sb}^{n+1/2} \\
 + \theta \sum_i \left( \min \left( \frac{J_{SBS}^i f_s^i}{S^i}, 0 \right) + \min \left( \frac{J_{SBS}^i F^i}{S^i}, 0 \right) \left( f_w + \sum_j f_D^j \right) \right)_{1}^{n+1/2} C_1^{n+1/2} \\
 + \theta \sum_i \left( (1 + \varepsilon) \max \left( \frac{J_{SBB}^i}{\rho_s^i}, 0 \right) \left( f_w + \sum_j f_D^j \right) \right)_{sb}^{n+1/2} C_{sb}^{n+1/2} \\
 + \theta \sum_i \left( (1 + \varepsilon) \min \left( \frac{J_{SBB}^i}{\rho_s^i}, 0 \right) \left( f_w + \sum_j f_D^j \right) \right)_{1}^{n+1/2} C_1^{n+1/2}
 \end{aligned} \tag{8.31}$$

for the first layer adjacent to the bed. Note that (8.31) is also the appropriate form for single layer or depth average application. Since the sediment settling flux is zero at the top of the free surface adjacent layer, (8.27) is integrated downward from the top layer to the bottom layer. The bottom layer equation (8.31) is solved simultaneously with a corresponding equation for the top layer of the sediment bed. The settling fluxes,  $w_s S$ , and water column-sediment bed fluxes,  $J_{SB}$ , in (8.30) and (8.31) are known from the preceding solution for sediment settling, deposition and resuspension. Terms containing the sediment sorbed fraction divided by the sediment concentration in (8.30) and (8.31) are given by

$$\frac{f_s^i}{S^i} = \frac{P_s^i}{\phi + \sum_i P_s^i S^i + \sum_j P_D^j D^j} \tag{8.32}$$

The diffusion step is given by

$$(HC)^{n+3/4} - (HC)^{n+1/2} = \theta \partial_z \left( \frac{A_b}{H} \partial_z C \right) \tag{8.33}$$

with boundary conditions

$$\begin{aligned}
 -\frac{A_b}{H} \partial_z C &= \left( (\max(q_w, 0) + q_{dif}) \frac{1}{\phi} \left( f_w + \sum_j f_D^j \right) C \right)_{SB} \\
 + \left( (\min(q_w, 0) - q_{dif}) \frac{1}{\phi_{dep}} \left( f_w + \sum_j f_D^j \right) C \right)_{WC} &: z = 0
 \end{aligned} \tag{8.34}$$

$$-\frac{A_b}{H} \partial_z C = 0 \quad : \quad z=1 \quad (8.35)$$

For the first layer adjacent to the bed

$$\begin{aligned} (HC)_1^{n+3/4} - (HC)_1^{n+1/2} &= \frac{\theta}{\Delta_1} \left( \frac{A_b}{H} \partial_z C \right)_{1+}^{n+3/4} \\ &+ \frac{\theta}{\Delta_1} (\max(q_w, 0) + q_{dif}) \left( \left( f_w + \sum_j f_D^j \right) \frac{1}{\phi} \right)_{SB}^{n+1/2} C_{SB}^{n+3/4} \\ &+ \frac{\theta}{\Delta_1} (\min(q_w, 0) - q_{dif}) \left( \left( f_w + \sum_j f_D^j \right) \frac{1}{\phi_{dep}} \right)_1^{n+1/2} C_1^{n+1/2} \end{aligned} \quad (8.36)$$

It is noted that the bed concentrations are advanced to the  $n+3/4$  intermediate time level before the advance of the water column concentrations. While for layers not adjacent to the bed,

$$(HC)_k^{n+3/4} - (HC)_k^{n+1/2} = \frac{\theta}{\Delta_1} \left( \frac{A_b}{H} \partial_z C \right)_{k+}^{n+3/4} - \frac{\theta}{\Delta_1} \left( \frac{A_b}{H} \partial_z C \right)_{k-}^{n+3/4} \quad (8.37)$$

The solution is completed by

$$(HC)_k^{n+1} - (HC)_k^{n+3/4} = -\theta\gamma(HC)_k^{n+1} \quad (8.38)$$

an implicit reaction step.

Contaminant transport in the sediment bed is represented using the discrete layer formulation developed for bed geomechanical processes. The conservation of mass for the total contaminant concentration in a layer of the sediment bed is given by

$$\begin{aligned}
 & \partial_t (BC)_k = -\gamma(BC)_k \\
 & -\delta(k, kt) \sum_i \left( \max \left( \frac{J_{SBS}^i f_S^i}{BS^i}, 0 \right) + \max \left( \frac{J_{SBS}^i F^i}{BS^i}, 0 \right) \left( f_w + \sum_j f_D^j \right) \right) (BC)_{kt} \\
 & -\delta(k, kt) \sum_i \left( \min \left( \frac{J_{SBS}^i f_S^i}{S^i}, 0 \right) C + \min \left( \frac{J_{SBS}^i F_{dep}^i}{S_{dep}^i}, 0 \right) \left( f_w + \sum_j f_D^j \right) C \right)_{WC} \\
 & -\delta(k, kt) \sum_i \left( (J_{SBB}^i \chi_{SBL}^i, 0) \right) \\
 & -\delta(k, kt) \sum_i \left( (1 + \varepsilon) \max \left( \frac{J_{SBB}^i}{B \rho_S^i}, 0 \right) \left( f_w + \sum_j f_D^j \right) \right) (BC)_{kt} \\
 & -\delta(k, kt) \sum_i \left( (1 + \varepsilon_{dep}) \min \left( \frac{J_{SBB}^i}{\rho_S^i}, 0 \right) \left( f_w + \sum_j f_D^j \right) C \right)_{WC} \\
 & -\left( (\max(q_w, 0) + q_{dif})_{k+} - (\min(q_w, 0) - q_{dif})_{k-} \right) \left( \frac{1}{\phi B} \left( f_w + \sum_j f_D^j \right) \right) (BC)_k \\
 & -\delta(k, kt) (\min(q_w, 0) - q_{dif})_{kt+} \left( \frac{1}{\phi} \left( f_w + \sum_j f_D^j \right) C \right)_{WC} \\
 & -(1 - \delta(k, kt)) (\min(q_w, 0) - q_{dif})_{k+} \left( \frac{1}{\phi B} \left( f_w + \sum_j f_D^j \right) \right)_{k+1} (BC)_{k+1} \\
 & + (\max(q_w, 0) + q_{dif})_{k-} \left( \frac{1}{\phi B} \left( f_w + \sum_j f_D^j \right) \right)_{k-1} (BC)_{k-1}
 \end{aligned} \tag{8.39}$$

where

$$\delta(k, kt) = \begin{cases} 0 & : k = kt \\ 1 & : k \neq kt \end{cases} \tag{8.40}$$

is used to distinguish processes specific to the top, water column adjacent layer of the bed,  $kt$ . Advective fluxes associated with pore water advection in (8.40) are represented in upwind form. In the sediment bed, the actual computational variables for sediment, contaminant, and dissolved material are their concentrations times the thickness of the bed layer. Consistent with this formulation, the fractional phase components in the bed are defined by

$$\begin{aligned}
 (f_w)_k &= \left( \frac{BC_w}{BC} \right)_k = \left( \frac{B\phi}{B\phi + \sum_i P_S^i BS^i + \sum_j P_D^j BD^j} \right)_k \\
 (f_D^j)_k &= \left( \frac{BC_D^j}{BC} \right)_k = \left( \frac{P_D^j BD^j}{B\phi + \sum_i P_S^i BS^i + \sum_j P_D^j BD^j} \right)_k \\
 (f_S^i)_k &= \left( \frac{BC_S^i}{BC} \right)_k = \left( \frac{P_S^i BS^i}{B\phi + \sum_i P_S^i BS^i + \sum_j P_D^j BD^j} \right)_k
 \end{aligned} \tag{8.41}$$

The contaminant fluxes associated bedload sediment transport are determined as follows. The net sediment flux from the bedload transport equation

$$m_x m_y J_{SBB}^i = \partial_x (m_y Q_{SBLx}^i) + \partial_x (m_x Q_{SBLy}^i) \tag{8.42}$$

is used to evaluate the flux associated with pore water entrainment and expulsion in (8.25) and (8.40). The transport equation for material sorbed to the bedload is

$$\partial_x (m_y Q_{SBLx}^i \chi_{SBL}^i) + \partial_x (m_x Q_{SBLy}^i \chi_{SBL}^i) = m_x m_y J_{SBB}^i \chi_{SBL}^i \tag{8.43}$$

Since the contaminant mass per sediment mass in the transport divergence corresponds to conditions in the top layer of the sediment bed, (8.43) can be written as

$$\partial_x \left( m_y Q_{SBLx}^i \frac{f_S^i}{S^i} C \right) + \partial_x \left( m_x Q_{SBLy}^i \frac{f_S^i}{S^i} C \right) = m_x m_y J_{SBB}^i \chi_{SBL}^i \tag{8.44}$$

and solved using an upwind approximation

$$\begin{aligned}
 & m_x m_y J_{SBB}^i \chi_{SBL}^i = \\
 & \max (m_y Q_{SBLx}^i)_E \left( \frac{f_S^i}{S^i} C \right)_C + \min (m_y Q_{SBLx}^i)_E \left( \frac{f_S^i}{S^i} C \right)_E \\
 & - \max (m_y Q_{SBLx}^i)_W \left( \frac{f_S^i}{S^i} C \right)_W - \min (m_y Q_{SBLx}^i)_W \left( \frac{f_S^i}{S^i} C \right)_C \\
 & + \max (m_x Q_{SBLy}^i)_N \left( \frac{f_S^i}{S^i} C \right)_C + \min (m_x Q_{SBLy}^i)_N \left( \frac{f_S^i}{S^i} C \right)_N \\
 & - \max (m_x Q_{SBLy}^i)_S \left( \frac{f_S^i}{S^i} C \right)_S - \min (m_x Q_{SBLy}^i)_S \left( \frac{f_S^i}{S^i} C \right)_C
 \end{aligned} \tag{8.45}$$

to evaluate the transport of bedload sorbed material between horizontally adjacent top layers of the sediment bed.

Equation (8.39) is solved using a fractional step procedure consistent with that used for the water column transport. Equation (8.41) is used to update the fractional distribution in the bed between the settling, deposition, and resuspension step and the pore water advection and diffusion step. The settling, deposition and resuspension step applies only to the top layer of the bed and is

$$\begin{aligned}
 & (BC)_{kt}^{n+1/2} - (BC)_{kt}^n = \\
 & -\theta \sum_i \left( \max \left( \frac{J_{SBS}^i f_S^i}{BS^i}, 0 \right) + \max \left( \frac{J_{SBS}^i F^i}{BS^i}, 0 \right) \left( f_w + \sum_j f_D^j \right) \right)_{kt}^{n+1/2} (BC)_{kt}^{n+1/2} \\
 & -\theta \sum_i \left( \min \left( \frac{J_{SBS}^i f_S^i}{S^i}, 0 \right) C + \min \left( \frac{J_{SBS}^i F_{dep}^i}{S_{dep}^i}, 0 \right) \left( f_w + \sum_j f_D^j \right) C \right)_{WC}^{n+1/2} \\
 & -\theta \sum_i \left( (J_{SBB}^i \chi_{SBL}^i, 0) \right) \\
 & -\theta \sum_i \left( (1 + \varepsilon) \max \left( \frac{J_{SBB}^i}{B \rho_S^i}, 0 \right) \left( f_w + \sum_j f_D^j \right) \right)_{kt}^{n+1/2} (BC)_{kt}^{n+1/2} \\
 & -\theta \sum_i \left( (1 + \varepsilon_{dep}) \min \left( \frac{J_{SBB}^i}{\rho_S^i}, 0 \right) \left( f_w + \sum_j f_D^j \right) C \right)_{WC}^{n+1/2}
 \end{aligned} \tag{8.46}$$

This equation is solved simultaneously with equation (8.31) for the bottom layer of the water column. The solution is represented by

$$\begin{bmatrix} a_{11} & a_{12} \\ a_{21} & a_{22} \end{bmatrix} \begin{Bmatrix} (BC)_{kt}^{n+1/2} \\ (HC)_1^{n+1/2} \end{Bmatrix} = \begin{Bmatrix} (BC)_{kt}^n - \theta \sum_{i=ib} (J_{SB}^i \chi_{SBL}^i)^{n+1/2} \\ \Delta_1 (HC)_1^{n+1/4} + \theta \sum_i \left( (w_S^i S^i)_{1+} \left( \frac{f_S^i}{S^i} \right)_2 \right)^{n+1/2} C_2^{n+1/2} \end{Bmatrix} \tag{8.47}$$

where the coefficients are given by

$$\begin{aligned}
 a_{11} &= 1 + \theta \sum_i \left( \max \left( \frac{J_{SBS}^i f_S^i}{BS^i}, 0 \right) + \max \left( \frac{J_{SBS}^i F^i}{BS^i}, 0 \right) \left( f_w + \sum_j f_D^j \right) \right)_{kt}^{n+1/2} \\
 &\quad + \theta \sum_i \left( (1 + \varepsilon) \max \left( \frac{J_{SBB}^i}{B \rho_S^i}, 0 \right) \left( f_w + \sum_j f_D^j \right) \right)_{kt}^{n+1/2} \\
 a_{12} &= \frac{\theta}{H} \sum_i \left( \min \left( \frac{J_{SBS}^i f_S^i}{S^i}, 0 \right) + \min \left( \frac{J_{SBS}^i F_{dep}^i}{S_{dep}^i}, 0 \right) \left( f_w + \sum_j f_D^j \right) \right)_1^{n+1/2} \\
 &\quad + \frac{\theta}{H} \sum_i \left( (1 + \varepsilon_{dep}) \min \left( \frac{J_{SBB}^i}{\rho_S^i}, 0 \right) \left( f_w + \sum_j f_D^j \right) \right)_1^{n+1/2} \\
 a_{21} &= -\theta \sum_i \left( \max \left( \frac{J_{SBS}^i f_S^i}{BS^i}, 0 \right) + \max \left( \frac{J_{SBS}^i F^i}{BS^i}, 0 \right) \left( f_w + \sum_j f_D^j \right) \right)_{kt}^{n+1/2} \\
 &\quad - \theta \sum_i \left( (1 + \varepsilon) \max \left( \frac{J_{SBB}^i}{B \rho_S^i}, 0 \right) \left( f_w + \sum_j f_D^j \right) \right)_{kt}^{n+1/2} \\
 a_{22} &= \Delta_1 - \frac{\theta}{H} \sum_i \left( \min \left( \frac{J_{SBS}^i f_S^i}{S^i}, 0 \right) + \min \left( \frac{J_{SBS}^i F^i}{S^i}, 0 \right) \left( f_w + \sum_j f_D^j \right) \right)_1^{n+1/2} \\
 &\quad - \frac{\theta}{H} \sum_i \left( (1 + \varepsilon) \min \left( \frac{J_{SBB}^i}{\rho_S^i}, 0 \right) \left( f_w + \sum_j f_D^j \right) \right)_1^{n+1/2}
 \end{aligned} \tag{8.48}$$

Adding the two equations in (8.47) gives

$$\begin{aligned}
 (BC)_{kt}^{n+1/2} + \Delta_1 (HC)_1^{n+1/2} &= (BC)_{kt}^n + \Delta_1 (HC)_1^{n+1/4} \\
 + \theta \sum_i \left( (w_S^i S^i)_{1+} \left( \frac{f_S^i}{S^i} \right)_2 \right)_{1+}^{n+1/2} C_2^{n+1/2} &- \theta \sum_i (J_{SBS}^i \chi_{SBL}^i)^{n+1/2}
 \end{aligned} \tag{8.49}$$

This equation verifies the consistency of the water column-sediment bed exchange since the source and sinks on the right side include only settling into the top of the water column layer, and transfer of bedload sediment sorbed contaminant between horizontal sediment bed cells.

The pore water advection and diffusion step for the top, water column adjacent, layer is

$$\begin{aligned}
 (BC)_{kt}^{n+3/4} &= (BC)_{kt}^{n+1/2} \\
 -\theta(\max(q_w, 0) + q_{dif})_{kt+} &\left( \frac{1}{\phi B} \left( f_w + \sum_j f_D^j \right) \right)_{kt}^{n+1/2} (BC)_{kt}^{n+3/4} \\
 +\theta(\min(q_w, 0) - q_{dif})_{kt-} &\left( \frac{1}{\phi B} \left( f_w + \sum_j f_D^j \right) \right)_{kt}^{n+1/2} (BC)_{kt}^{n+3/4} \\
 -\theta(\min(q_w, 0) - q_{dif})_{kt+} &\left( \frac{1}{\phi H} \left( f_w + \sum_j f_D^j \right) \right)_1^{n+1/2} (HC)_1^{n+1/2} \\
 +\theta(\max(q_w, 0) + q_{dif})_{kt-} &\left( \frac{1}{\phi B} \left( f_w + \sum_j f_D^j \right) \right)_{kt-1}^{n+1/2} (BC)_{kt-1}^{n+1/2}
 \end{aligned} \tag{8.50}$$

which is an implicit form. Writing (8.36) in the form

$$\begin{aligned}
 \Delta_1 (HC)_1^{n+3/4} &= \Delta_1 (HC)_1^{n+1/2} + \theta \left( \frac{A_b}{H} \partial_z C \right)_{1+}^{n+3/4} \\
 +\theta(\max(q_w, 0) + q_{dif})_{kt+} &\left( \frac{1}{\phi B} \left( f_w + \sum_j f_D^j \right) \right)_{SB}^{n+1/2} (BC)_{kt}^{n+3/4} \\
 +\theta(\min(q_w, 0) - q_{dif})_{kt+} &\left( \frac{1}{\phi H} \left( f_w + \sum_j f_D^j \right) \right)_1^{n+1/2} (HC)_1^{n+1/2}
 \end{aligned} \tag{8.51}$$

and combining with (4.49) gives

$$\begin{aligned}
 (BC)_{kt}^{n+3/4} + \Delta_1 (HC)_1^{n+3/4} &= (BC)_{kt}^{n+1/2} + \Delta_1 (HC)_1^{n+1/2} + \theta \left( \frac{A_b}{H} \partial_z C \right)_{1+}^{n+3/4} \\
 +\theta(\min(q_w, 0) - q_{dif})_{kt-} &\left( \frac{1}{\phi B} \left( f_w + \sum_j f_D^j \right) \right)_{kt}^{n+1/2} (BC)_{kt}^{n+3/4} \\
 +\theta(\max(q_w, 0) + q_{dif})_{kt-} &\left( \frac{1}{\phi B} \left( f_w + \sum_j f_D^j \right) \right)_{kt-1}^{n+1/2} (BC)_{kt-1}^{n+3/4}
 \end{aligned} \tag{8.52}$$

This equation verifies the consistency of the representation of pore water advection and diffusion across water column-sediment bed interface since the source and sink terms on the right side of (8.52) represent fluxes at the top to the water column cell and the bottom of the bed cell.

The pore water diffusion and advection step for the remaining bed layers is given by

$$\begin{aligned}
 (BC)_k^{n+3/4} &= (BC)_k^{n+1/2} \\
 -\theta \left( \min(q_w, 0) - q_{dif} \right)_{k+} &\left( \frac{1}{\phi B} \left( f_w + \sum_j f_D^j \right) \right)_{k+1}^{n+1/2} (BC)_{k+1}^{n+3/4} \\
 -\theta \left( \max(q_w, 0) + q_{dif} \right)_{k+} &\left( \frac{1}{\phi B} \left( f_w + \sum_j f_D^j \right) \right)_k^{n+1/2} (BC)_k^{n+3/4} \\
 +\theta \left( \min(q_w, 0) - q_{dif} \right)_{k-} &\left( \frac{1}{\phi B} \left( f_w + \sum_j f_D^j \right) \right)_k^{n+1/2} (BC)_k^{n+3/4} \\
 +\theta \left( \max(q_w, 0) + q_{dif} \right)_{k-} &\left( \frac{1}{\phi B} \left( f_w + \sum_j f_D^j \right) \right)_{k-1}^{n+1/2} (BC)_{k-1}^{n+3/4}
 \end{aligned} \tag{8.53}$$

For the bottom layer of the bed,  $k = 1$ , the bottom,  $k-$ , specific discharge and diffusion velocity must be specified as well as the total contaminant concentration,  $C_0$ . The corresponding thickness of the unresolved layer,  $k = 0$ , is set to unity without loss of generality. The system of equations represented by (8.49) and (8.52) is implicit and is solved using a tri-diagonal linear equation solver. It is noted that the  $n+3/4$  time level layer thickness is actually the  $n+1$  time level thickness determined by the solution of (8.23). The specific discharges in (8.49) and (8.52) are given by (8.41) and represent those appearing in (8.23) and guarantee mass conservation for the pore water advection.

The bed transport solution is completed by

$$(BC)_k^{n+1} - (BC)_k^{n+3/4} = -\theta \gamma (BC)_k^{n+1} \tag{8.54}$$

an implicit reaction step.

## 9. References

Ackers, P., and W. R. White, 1973: Sediment transport: New approaches and analysis. *J. Hyd. Div. ASCE*, **99**, 2041-2060.

Ariathurai, R., and R. B. Krone, 1976: Finite element model for cohesive sediment transport. *J. Hyd. Div. ASCE*, **102**, 323-338.

Ambrose, R. B., T. A. Wool, and J. L. Martin, 1993: The water quality analysis and simulation program, WASP5: Part A, model documentation version 5.1. U.S. EPA, Athens Environmental Research Laboratory, 210 pp.

Bear, J., 1879: *Hydraulics of groundwater*, McGraw-Hill, New York.

Bagnold, R. A., 1956: The flow of cohesionless grains in fluids. *Phil. Trans. Roy. Soc. Lond.*, Series A, Vol **249**, No. 964, 235-297.

Belleudy, P., 2001: Numerical simulation of sediment mixture deposition, part 1: analysis of flume experiments. *J. Hyd. Res.*, **38**, 417-425.

Belleudy, P., 2001: Numerical simulation of sediment mixture deposition, part 2: a sensitivity analysis. *J. Hyd. Res.*, **39**, 25-31.

Blumberg, A. F., B. Galperin, and D. J. O'Connor, 1992: Modeling vertical structure of open-channel flow. *J. Hyd. Engr.*, **118**, 1119-1134.

Boyer, J. M., S. C. Chapra, C. E. Ruiz, and M. S. Dortch, 1994: RECOVERY, a mathematical model to predict the temporal response of surface water to contaminated sediment. Tech. Rpt. W-94-4, U.S. Army Engineer Waterways Experiment Station, Vicksburg, MS, 61 pp.

Burban, P. Y., W. Lick, and J. Lick, 1989: The flocculation of fine-grained sediments in estuarine waters. *J. Geophys. Res.*, **94**, 8323-8330.

Burban, P. Y., Y. J. Xu, J. McNeil, and W. Lick, 1990: Settling speeds of flocs in fresh and seawater. *J. Geophys. Res.*, **95**, 18,213-18,220.

Cargill, K. W., 1985: Mathematical model of the consolidation and desiccation processes in dredge material. U.S. Army Corps of Engineers, Waterways Experiment Station, Technical Report D-85-4.

Dortch, M., C. Ruiz, T. Gerald, and R. Hall, 1998: Three-dimensional contaminant transport/fate model. *Estuarine and Coastal Modeling, Proceedings of the 5th International Conference*, M. L. Spaulding and A. F. Blumberg, Eds., American Society of Civil Engineers, New York, 75-89.

Einstein, H. A., 1950: The bed load function for sediment transport in open channel flows. *U.S. Dept. Agric. Tech. Bull.*, 1026.

Fredricks, C., and J. M. Hamrick, 1996: The effect of channel geometry on gravitational circulation in partially mixed estuaries. *Buoyancy Effects on Coastal and Estuarine Dynamics*, D. Aubrey and C. Fredricks, Eds., AGU, 283-300.

Galperin, B., L. H. Kantha, S. Hassid, and A. Rosati, 1988: A quasi-equilibrium turbulent energy model for geophysical flows. *J. Atmos. Sci.*, **45**, 55-62.

Garcia, M., and G. Parker, 1991: Entrainment of bed sediment into suspension. *J. Hyd. Engrg.*, **117**, 414-435.

Gibbs, R. J., 1985: Estuarine Floccs: their size, settling velocity and density. *J. Geophys. Res.*, **90**, 3249-3251.

Gibson, R. E., G. L. England, and M. J. L. Hussey, 1967: The theory of one-dimensional consolidation of saturated clays. *Geotechnique*, **17**, 261-273.

Hamrick, J. M., 1992: A three-dimensional environmental fluid dynamics computer code: Theoretical and computational aspects. The College of William and Mary, Virginia Institute of Marine Science, Special Report 317, 63 pp.

Hamrick, J. M., 1994: Linking hydrodynamic and biogeochemical transport models for estuarine and coastal waters. *Estuarine and Coastal Modeling, Proceedings of the 3rd International Conference*, M. L. Spaulding et al, Eds., American Society of Civil Engineers, New York, 591-608.

Hamrick, J. M., and Wm. B. Mills, 2001: Analysis of temperatures in Conowingo Pond as influenced by the Peach Bottom atomic power plant thermal discharge. *Environ. Sci. Policy*, **3**, s197-s209.

Hamrick, J. M., and T. S. Wu, 1997: Computational design and optimization of the EFDC/HEM3D surface water hydrodynamic and eutrophication models. *Next Generation Environmental Models and Computational Methods*. G. Delich and M. F. Wheeler, Eds., Society of Industrial and Applied Mathematics, Philadelphia, 143-156.

Hayter, E. J., and A. J. Mehta, 1983: Modeling fine sediment transport in estuaries. Report EPA-600/3-83-045, U.S. Environmental Protection Agency. Athens, GA.

Hayter, E.J., M. Bergs, R. Gu, S. McCutcheon, S. J. Smith, and H. J. Whiteley, 1998: HSCTM-2D, a finite element model for depth-averaged hydrodynamics, sediment and contaminant transport. Technical Report, U. S. EPA Environmental Research Laboratory, Athens, GA.

- Hwang, K.-N, and A. J. Mehta, 1989: Fine sediment erodibility in Lake Okeechobee. Coastal and Oceanographic Engineering Dept., University of Florida, Report UFL/COEL-89/019, Gainesville, FL.
- Ji, Z.-G., J. H. Hamrick, and J. Pagenkopf, 2002: Sediment and metals modeling in shallow river, *J. Environ. Engrg.*, **128**, 105-119.
- Jin, K. R., J. M. Hamrick, and T. S. Tisdale, 2000: Application of a three-dimensional hydrodynamic model for Lake Okeechobee, *J. Hyd. Engrg.*, **106**, 758-772.
- Jin, K. R., Z. G. Ji, and J. M. Hamrick, 2002: Modeling winter circulation in Lake Okeechobee, Florida. *J. Waterway, Port, Coastal, Ocean Engrg.*, **128**, 114-125.
- Karim, M. F., and F. M. Holley, Jr., 1986: Armoring and sorting simulation in alluvial rivers. *J. Hyd. Engrg.*, **112**, 705-715.
- Kleinhans, M. G., and L. C. Van Rijn, 2002: Stochastic prediction of sediment transport in sand-gravel bed rivers. *J. Hyd. Engrg.*, **128**, 412-425.
- Kuo, A. Y., J. Shen, and J. M. Hamrick, 1996: The effect of acceleration on bottom shear stress in tidal estuaries. *J. Waterway, Port, Coastal, Ocean Engrg.*, **122**, 75-83.
- Laursen, E., 1958: The total sediment load of streams *J. Hyd. Div. ASCE*, **84**, 1-36.
- Letter, J. V., L. C. Roig, B. P. Donnell, Wa. A. Thomas, W. H. McAnally, and S. A. Adamec, 1998: A user's manual for SED2D-WES, a generalized computer program for two-dimensional, vertically averaged sediment transport. Version 4.3 Beta Draft Instructional Report, U. S. Army Corps of Engrs., Wtrwy. Exper. Sta., Vicksburg, MS.
- Le Normant, C., E. Peltier, and C. Teisson, 1998: Three-dimensional modelling of cohesive sediment in estuaries. in *Physics of Estuaries and Coastal Seas*, (J. Dronkers and M. Scheffers, Eds.), Balkema, Rotterdam, pp 65-71.
- Lick, W., and J. Lick, 1988: Aggregation and disaggregation of fine-grained lake sediments. *J Great Lakes Res.*, **14**, 514-523.
- Mehta, A. J., E. J. Hayter, W. R. Parker, R. B. Krone, A. M. Teeter, 1989: Cohesive sediment transport. I: Process description. *J. Hyd. Engrg.*, **115**, 1076-1093.
- Mehta, A. J., T. M. Parchure, J. G. Dixit, and R. Ariathurai, 1982: Resuspension potential of deposited cohesive sediment beds, in *Estuarine Comparisons*, V. S. Kennedy, Ed., Academic Press, New York, 348-362.
- Mehta, A. J., and F. Jiang, 1990: Some field observations on bottom mud motion due to waves. Coastal and Oceanographic Engineering Dept., University of Florida, Gainesville, FL.

- Mellor, G. L., and T. Yamada, 1982: Development of a turbulence closure model for geophysical fluid problems. *Rev. Geophys. Space Phys.*, **20**, 851-875.
- Meyer-Peter, E. and R. Muller, 1948: Formulas for bed-load transport. Proc. Int. Assoc. Hydr. Struct. Res., Report of Second Meeting, Stockholm, 39-64.
- Middleton, G. V., and P. R. Wilcock, 1994: Mechanics in the Earth and Environmental Sciences. Cambridge University Press, Cambridge, UK.
- Moustafa, M. Z., and J. M. Hamrick, 2000: Calibration of the wetland hydrodynamic model to the Everglades nutrient removal project. *Water Quality and Ecosystem Modeling*, **1**, 141-167.
- Nielsen, P., 1992: *Coastal bottom boundary layers and sediment transport*, World Scientific, Singapore.
- Park, K., A. Y. Kuo, J. Shen, and J. M. Hamrick, 1995: A three-dimensional hydrodynamic-eutrophication model (HEM3D): description of water quality and sediment processes submodels. The College of William and Mary, Virginia Institute of Marine Science. Special Report 327, 113 pp.
- Rahmeyer, W. J., 1999: Lecture notes for CEE5560/6560: Sedimentation Engineering, Dept. of Civil and Environmental Engineering, Utah State University, Logan, Utah.
- Rahuel, J. L., F. M. Holly, Jr., J. P. Chollet, P. J. Belleudy, 1990: Modeling riverbed evolution for bedload sediment mixtures. *J. Hyd. Engrg.*, **115**, 1521-1542.
- Raukivi, A. J., 1990: *Loose boundary hydraulics*. 3rd Ed., Pergamon, New York, NY.
- Ried, I., and L. E. Frostick, 1994: Fluvial sediment transport and deposition. in *Sediment Transport and Depositional Processes*, K. Pye, ed., Blackwell, Oxford, UK, 89-155.
- Roberts, J., R. Jepson, D. Gotthard, and W. Lick, 1998: Effects of particle size and bulk density on erosion of quartz particles. *J. Hyd. Engrg.*, **124**, 1261-1267.
- Shen, J., J. D. Boon, and A. Y. Kuo, 1999: A modeling study of a tidal intrusion front and its impact on larval dispersion in the James River estuary, Virginia. *Estuaries*, **22**, 681-692.
- Shen, J. and A.Y. Kuo. 1999: Numerical investigation of an estuarine front and its associated topographic eddy. *J. Waterway, Port, Coastal Ocean Engrg.*, **125**, 127-135.
- Shrestha, P. A., and G. T. Orlob, 1996: Multiphase distribution of cohesive sediments and heavy metals in estuarine systems. *J. Environ. Engrg.*, **122**, 730-740.
- Smagorinsky, J., 1963: General circulation experiments with the primitive equations, Part I: the basic experiment. *Mon. Wea. Rev.*, **91**, 99-152.

- Smith, J. D., and S. R. McLean, 1977: Spatially averaged flow over a wavy bed. *J. Geophys. Res.*, **82**, 1735-1746.
- Smolarkiewicz, P. K., and T. L. Clark, 1986: The multidimensional positive definite advection transport algorithm: further development and applications. *J. Comp. Phys.*, **67**, 396-438.
- Smolarkiewicz, P. K., and W. W. Grabowski, 1990: The multidimensional positive definite advection transport algorithm: non-oscillatory option. *J. Comp. Phys.*, **86**, 355-375.
- Spasojevic, M., and F. M. Holly, Jr., 1990: 2-D bed evolution in natural watercourses-new simulation approach. *J. Hyd. Engrg.*, **116**, 425-443.
- Spasojevic, M., and F. M. Holly, Jr., 1994: Three-dimensional numerical simulation of mobile-bed hydrodynamics. Contract Report HL-94-2, U.S. Army Engineer Waterways Experiment Station, Vicksburg, MS.
- Stark, T. D., 1996: Program documentation and users guide: PSDDF primary consolidation, secondary compression, and desiccation of dredge fill. Instructional Report EL-96-xx, US Army Engineer Waterways Experiment Station, Vicksburg, MS.
- Styles, R. and S. M. Glenn, 2000: Modeling stratified wave and current boundary layers on the continental shelf. *J. Geophys. Res.*, **105**, 24,119-24,139.
- Suzuki, K., H. Yamamoto, and A. Kadota, 1998: Mechanism of bed load fluctuations of sand-gravel mixture in a steep slope channel, Proc. of the 11th Congress of APD IAHR, Yogyakarta, pp.679-688.
- Tetra Tech, 2007a: The Environmental Fluid Dynamics Code Theory and Computation. Volume 1: Hydrodynamics and Mass Transport.
- Tsai, C. H., S. Iacobellis, and W. Lick, 1987: Flocculation of fine-grained lake sediments due to a uniform shear stress. *J Great Lakes Res.*, **13**, 135-146.
- van Niekerk, A., K. R. Vogel, R. L Slingerland, and J. S. Bridge, 1992: Routing of heterogeneous sediments over movable bed: Model development. *J. Hyd. Engrg.*, **118**, 246-262.
- Van Rijn, L. C., 1984a: Sediment transport, Part I: Bed load transport. *J. Hyd. Engrg.*, **110**, 1431-1455.
- Van Rijn, L. C., 1984b: Sediment transport, Part II: Suspended load transport. *J. Hyd. Engrg.*, **110**, 1613-1641.

Villaret, C., and M. Paulic, 1986: Experiments on the erosion of deposited and placed cohesive sediments in an annular flume and a rocking flume. Coastal and Oceanographic Engineering Dept., University of Florida, Report UFL/COEL-86/007, Gainesville, FL.

Vogel, K. R., A. van Niekerk, R. L. Slingerland, and J. S. Bridge, 1992: Routing of heterogeneous sediments over movable bed: Model verification. *J. Hyd. Engrg.*, **118**, 263-279.

Wu, W., S. S. Y. Wang, and Y. Jia, 2000: Nonuniform sediment transport in alluvial rivers. *J. Hyd. Res.*, **38**, 427-434.

Yang, C. T., 1973: Incipient motion and sediment transport. *J. Hyd. Div. ASCE*, **99**, 1679-1704.

Yang, C. T., 1984: Unit stream power equation for gravel. *Journal of Hydraulic Engineering*, **110**, 1783-1797.

Yang, C. T., and A. Molinas, 1982: Sediment transport and unit streams power function. *J. Hyd. Div. ASCE*, **108**, 774-793.

Yang, Z., A. Baptista, and J. Darland, 2000: Numerical modeling of flow characteristics in a rotating annular flume. *Dyn. Atmos. Oceans*, **31**, 271-294.

Ziegler, C. K., and B. Nesbitt, 1994: Fine-grained sediment transport in Pawtuxet River, Rhode Island. *J. Hyd. Engrg.*, **120**, 561-576.

Ziegler, C. K., and B. Nesbitt, 1995: Long-term simulation of fine-grained sediment transport in large reservoir. *J. Hyd. Engrg.*, **121**, 773-781.